Supplemental Beach, Nearshore, and Wave-Current Monitoring Due to the Unanticipated Coastal Response at the Raccoon Island Breakwater Demonstration Project (TE-29)

Gregory W. Stone, Ph.D. [1]
James P. Morgan Distinguished Professor of Coastal Geology

Baozhu Liu, Ph.D. [1]

Qing He, Ph.D. [2]

Xiongping Zhang, Ph.D. [1]

[1]Coastal Studies Institute
336 Howe-Russell Geo-Science Complex
Louisiana State University
Baton Rouge, LA 70803

[2]State Key Laboratory of Estuarine and Coastal Research
East China Normal University
3663 Zhongshan Northern Road
Shanghai, 200062, China

September 2003

Supplemental Beach, Nearshore, and Wave-Current Monitoring Due to the Unanticipated Coastal Response at the Raccoon Island Breakwater Demonstration Project (TE-29)

Gregory W. Stone, Ph.D. [1]
James P. Morgan Distinguished Professor of Coastal Geology

Baozhu Liu, Ph.D. [1]

Qing He, Ph.D. [2]

Xiongping Zhang, Ph.D. [1]

[1]Coastal Studies Institute
336 Howe-Russell Geo-Science Complex
Louisiana State University
Baton Rouge, LA 70803

[2]State Key Laboratory of Estuarine and Coastal Research
East China Normal University
3663 Zhongshan Northern Road
Shanghai, 200062, China

September 2003

SUMMARY

Raccoon Island, located along the western margin of the Isles Dernieres, underwent rapid and persistent sand accumulation post-construction of eight detached breakwaters (TE-29) beginning 1997. The response of the beach and nearshore was extremely unique in that ***Reverse Salients*** were observed and monitored extensively post-construction. Extensive searches in both the scientific and engineering literature did not reveal documentation of similar responses to breakwaters along other coasts. Consequently, the current project was funded in 2000 by the Louisiana Department of Natural Resources (LDNR) to identify and elucidate the mechanism/s involved in sediment accretion at the breakwater site. The project was deemed particularly important in that post-construction monitoring carried out as part of TE-29 revealed that the response of the beach and nearshore to breakwater construction may have been the exception rather than the norm and linked to the presence of a sand body located adjacent to the structures offshore in the Gulf of Mexico. After several months of discussion between scientists in the Coastal Studies Institute at Louisiana State University and engineers/resource managers at LDNR, a number of carefully constructed scientific research questions were formulated to address the unanticipated response of the beach and nearshore to the breakwaters.

In this report we present detailed data sets on the hydrodynamics, sediment transport and bathymetric/topographic change at the site measured over a two year period (2000-2002). The data reveal the importance of the offshore shoal as the primary sand source for the material that was deposited in the gaps, landward and seaward of the breakwaters. A model is presented which describes the evolution of the sand bodies around the structures and detailed sediment budgets are discussed in order to explain their formation. The questions formulated and addressed are as follows: (1) Why did sand accumulation begin preferentially along the western flank of the breakwater array (7, 6, 5, 4 and 3 respectively)? (2) Where is the primary sand source for the sediment that accumulated in the vicinity of the breakwaters within the initial 12-month monitoring period and beyond should the trend continue? (3) What is the volume of sediment that comprises the source and what is the projected longevity and availability to nearshore processes of this source? (4) What are the precise roles of longshore and cross-shore sediment transport at the site? (5) How is the beach west of the structures responding to breakwater construction? (6) Can the design criteria used to construct the breakwaters be refined to maximize sediment accumulation at this and other prospective sites? (7) Are the trends that have been established for the first 12 months of monitoring likely short or longer-term?

Table of Contents

List of Figures

List of Tables

List of Appendices

INTRODUCTION

The Isle Dernieres barrier island chain (Figure 1) is experiencing some of the highest rates of erosion of any coastal region in the world. Between 1887 and 1988 the average annual rate of land loss was 0.28 km^2 yr^{-1} (69.6 ac yr^{-1}), while the average rate of shoreline retreat was 11.09 m yr^{-1} (36.4 ft yr^{-1}) (McBride et al. 1991). This condition has led to the rapid landward migration of the Gulf-facing shoreline and disintegration of the Isle Dernieres, as well as a decrease in the ability of the island chain to protect the adjacent mainland marshes and wetlands from the effects of storm surge, salt water intrusion, an increased tidal prism, and energetic storm waves (McBride and Byrnes 1997; Stone and McBride, 1998; Stone et al., 2003). As part of a comprehensive barrier island restoration plan along the Isle Dernieres, the Raccoon Island Breakwaters Demonstration (TE-29) project was constructed in July 1997, to reduce the rate of shoreline retreat and protect bird habitat. The breakwaters are 91.44 m (300 ft) long and 3.05 m (10 ft) wide at the crown and construction costs approximated $1.4 million.

On July 6 1999, representatives from the Coastal Restoration Division (CRD) and Louisiana State University, Coastal Studies Institute (LSU/CSI), met to discuss preliminary results during the initial 15 months of monitoring. Data from the monitoring effort are presented in Stone et al., 1998a, 1998b, 1998c and Armbruster, 1999. Wave and beach-profile data revealed a unique morphological development of the beach and upper shoreface in response to a series of eight detached segmented breakwaters. The rapid and persistent development of sand bodies in the immediate lee of the breakwaters was ***unanticipated*** when considering our present understanding of these structures. A net increase in volume between the dune and many of the breakwaters was measured and indicated that sediment was delivered to the project site from sources other than the beach and dune. The sediments comprising the upper shoreface deposits appeared to have been supplied from an offshore source through cross-shore transport processes, as opposed to capture of sediments transported from an alongshore source (Stone et al. 1999). The emergence of sand bodies in the immediate lee of the structures suggested that sediment

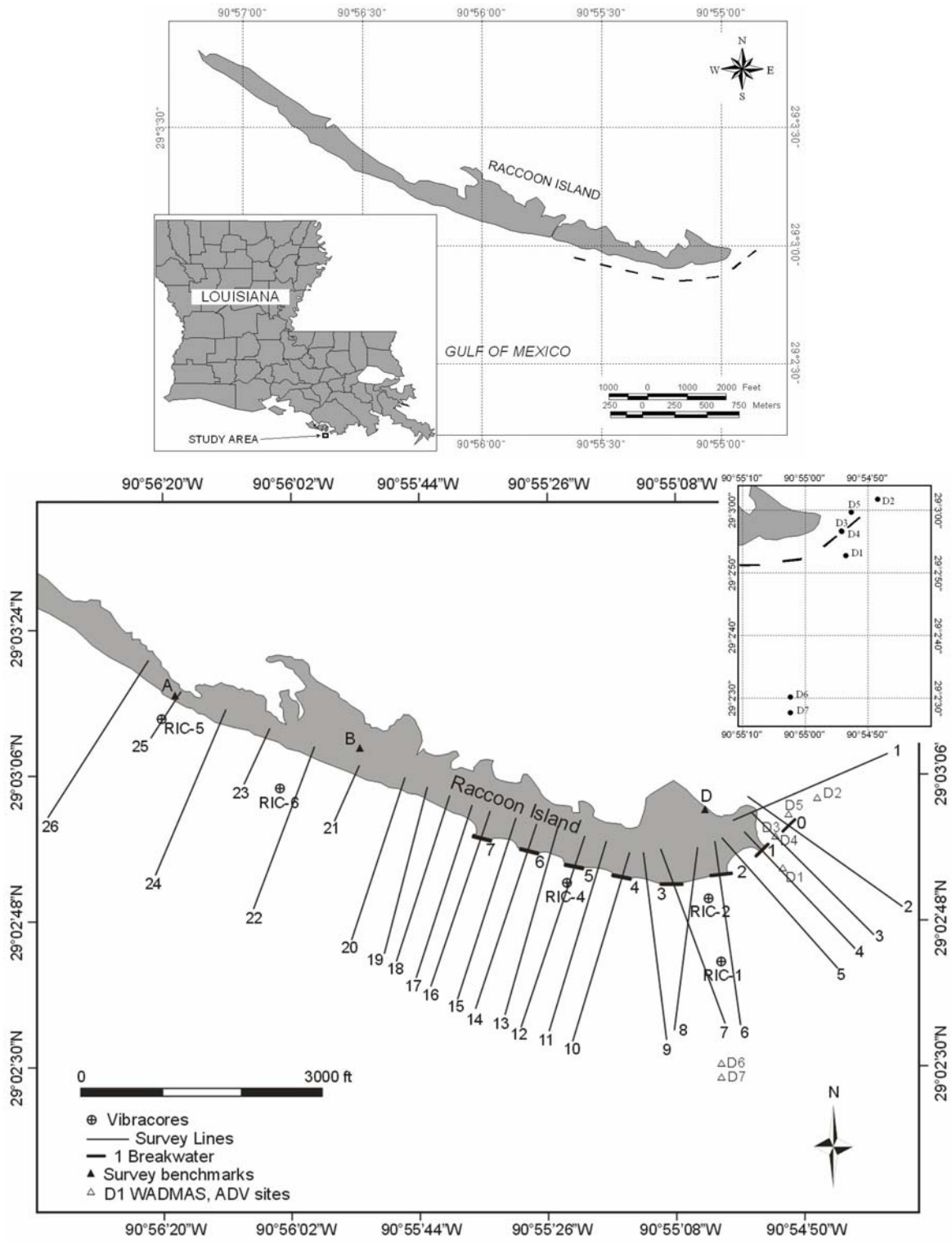

Figure 1. Upper: Study area showing the location of Raccoon Island and the breakwaters along the eastern end of the barrier. Lower: Study area, showing the location of WADMAS, ADV, Sea Gauge, vibracores, and topographic/bathymetric survey lines discussed later in text. Shoreline is based on an aerial photograph taken on 2-6-2002 by the USGS.

was transported through the gaps between breakwaters during periods of onshore sediment transport. The formation of a beach on the seaward side of several breakwaters also provided direct evidence of net onshore sediment transport.

These findings were deemed highly significant with respect to assessing the potential use of segmented breakwaters for coastal protection along Louisiana's barrier islands because they indicate an abundance of sand in the nearshore, previously considered to be a sand-starved system. In addition, present engineering models do not account for the dimensions of the lower shoreface morphology and cross-shore (onshore) transport of sediment (Stone et al., 1999). Consequently, predicting future trends in sedimentation at Raccoon Island is subject to a more comprehensive understanding of: 1) the preferential deposition of sediment along the western breakwaters as opposed to their eastern counterpart; 2) the primary sediment source that was impounded in the vicinity of the breakwaters; 3) the volume of sediment that comprises the source and its projected longevity; 4) sediment transport dynamics; and 5) the precise roles of longshore and cross-shore transport at the project site (Stone et al. 1998c).

At the conclusion of the meeting, the participants agreed that these engineering issues had not been adequately addressed in the current CWPPRA monitoring scheme, but could be through additional data collection and analysis. The Assistant Secretary of DNR requested that LSU/CSI submit a proposal for any supplemental monitoring that would complement the existing efforts previously undertaken by CWPPRA.

OBJECTIVES AND RATIONALE

The unanticipated response of Raccoon Island to the structures and magnitude of sediment accumulation warranted further investigation. Utilizing this restoration technique in other locations, necessitates a greater understanding of the local roles of sediment supply, wave-current interactions on the inner shelf and engineering structures (breakwaters) on coastal response. The CWPPRA monitoring plan addressed most of the

coastal ***response*** issues, but was severely lacking in any coastal ***process*** data collection. The enhanced interest generated from this ***unanticipated*** coastal response from the first two years of monitoring data is unique, having never, to our knowledge, been documented in the coastal scientific or engineering literature (Stone et al., 1999). As defined below, supplemental monitoring was essential to further our understanding of breakwater effects on nearshore sediment processes and was investigated by addressing the following questions:

1. Why did sand accumulation begin preferentially along the western flank of the breakwaters array (breakwaters 7, 6, 5, 4 and 3 respectively)?
2. Where is the primary sand source for the sediment that accumulated in the vicinity of the breakwaters within the initial 15-month monitoring period and beyond should the trend continue?
3. What is the volume of sediment that comprises the source and what is the projected longevity and availability to nearshore processes of this source?
4. What are the precise roles of longshore and cross-shore sediment transport at the site?
5. How is the beach west of the structures responding to breakwater construction?
6. Can the design criteria used to construct the breakwaters be refined to maximize sediment accumulation at this and other prospective sites?
7. Are the trends that have been established for the first 12 months of monitoring likely short or longer-term?

To address these issues, the supplemental monitoring plan was composed of three tasks: (1) wave and current measurement and sediment transport measurements; (2) beach and inner-shelf topographic/bathymetric surveys; and (3) geotechnical determination of nearshore and beach sediments. Wave and current measurements were obtained by deploying instrumentation immediately offshore in shallow water (2-3 m; 6-9 feet). Shorter duration field experiments were conducted involving the use of CSI's WADMAS system which measures directional wave characteristics, 3-dimensional currents, sediment concentrations and current velocities via collocated, vertically stacked optical backscatter sensors and two-dimensional current meters, and micro-scale

bathymetric change through a vertically mounted sonar altimeter. These data were important in addressing the source and transport pathways of sediment in the nearshore under variable wave conditions. The geotechnical properties of sediment on the beach, nearshore and offshore shoal complex were determined from bottom samples obtained through ponar grabs and limited sub-bottom sediments through vibracores taken on the shoal. The methodological approach associated with each of these tasks is summarized below.

METHODS

The above objectives were addressed using observations from a two year study but also included data from the previous monitoring effort (Stone et al., 1998c). The monitoring was conducted using two temporal and spatial scales. Thus, data obtained over a five year period (1997-2002) are presented.

Dynamic and Sedimentary Measurements

Instrumentation and sample collections

A review of a series of field deployments is listed in Table 1. The deployments contained three types of measuring systems, WADMAS, ADV and Sea Gauge. The WADMAS system was a unique multi-sensor package (Figure 2). It consisted of a Paros Scientific digital quartz pressure transducer, a sonar altimeter, and a vertical array of co-located Marsh-McBirney electromagnetic current meters and ANALITE optical backscatter turbidity sensors (OBS). This system was controlled by an electronic data logger and enabled WADMAS to measure water level, directional wave parameters, and seabed elevation, as well as current velocity and suspended sediment concentration at heights of 32, 68, and 108 cm (12.6, 26.8, and 42.5 in) above the seabed. All of the sensors on WADMAS were programmed for burst-mode sampling. Specifically, the sonar altimeter collected one measurement every 15 minutes, while all other sensors sampled for 8.5 minutes per hour at a frequency of 4 Hz. Another component of the deployments was a SonTek downward-looking Acoustic Doppler Velocimeter (ADV)

Table 1. Deployment details of hydrodynamic and sediment research for Raccoon Island breakwater project.

Deploy-ment No.	Monitoring system	Date	Latitude Longitude	Depth (m/ft)	First burst (GMT)	Last burst (GMT)	Comments
D1	Sea Gauge, Pressure: Wave	09/11/00 ~ 10/02/00	29º 2.8788′ N 90º 54.8906′ W	1.6/5.25	12:15:00	15:00:00	
D2	ADV: Currents	12/20/00 ~ 01/26/01	29º 3.02′ N 90º 54.8056′ W	1.2/3.94	18:00:00	10:00:00	
D3	WADMAS: Wave, currents	12/20/00 ~ 01/26/01	29º 2.94438′ N 90º 54.9017′ W	1.2/3.94	18:45:20	10:00:26	
D4	Sea Gauge, Pressure: Wave	12/20/00 ~ 01/26/01	29º 2.94348′ N 90º 54.9013′ W	1.2/3.94	03:00:00		
D5	ADV w/pressure: Currents	09/28/01 ~ 10/31/01	29º 2.994′ N 90º 54.876′ W	1.2/3.94	00:00:00	16:00:00	Instrument failure on 10/06/01 12:00 GMT
D6	WADMAS: Wave, currents, SSC	11/19/01 ~ 12/08/01	29º 2.502′ N 90º 55.038′ W	2.4/7.87	17:00:19	22:00:08	
D7	ADV: SSC	09/16/02 ~ 10/08/02	29º 2.46′ N 90º 55.038′ W	2.4/7.87	17:00:00	19:00:00	T.S. ISIDORE and H LILI

that measured seabed elevation, relative particulate concentration and 3-dimensional currents at an elevation of 20 cm (7.8 in) above the bed, and a pressure sensor to measure water level and wave characteristics (Figure 3). Data were also used from the existing WAVCIS program. WAVCIS is a prototype online Wave-Current-Surge Information System for coastal Louisiana. It provides wave information including wave height, period, direction of propagation, water level, surge, current speed and direction and meteorological conditions on a real time basis around the entire Louisiana coast (Figure 4). WAVCIS involves offshore deployment of instrumentation around the entire state in order to provide real time information on a frequent basis (3 hours or less) describing sea state, current velocity and meteorological conditions. The instrumentation provides information from deep to shallow water off the Louisiana coast in addition to the major bays. Information from each station is transmitted to a base station at Coastal Studies Institute, Louisiana State University where it undergoes quality control, post-processing and archiving in an online database. The information is then made available on the World Wide Web and is accessible to computers with an Internet connection and web browser. A station was built in the nearshore off breakwater 7 but was damaged.

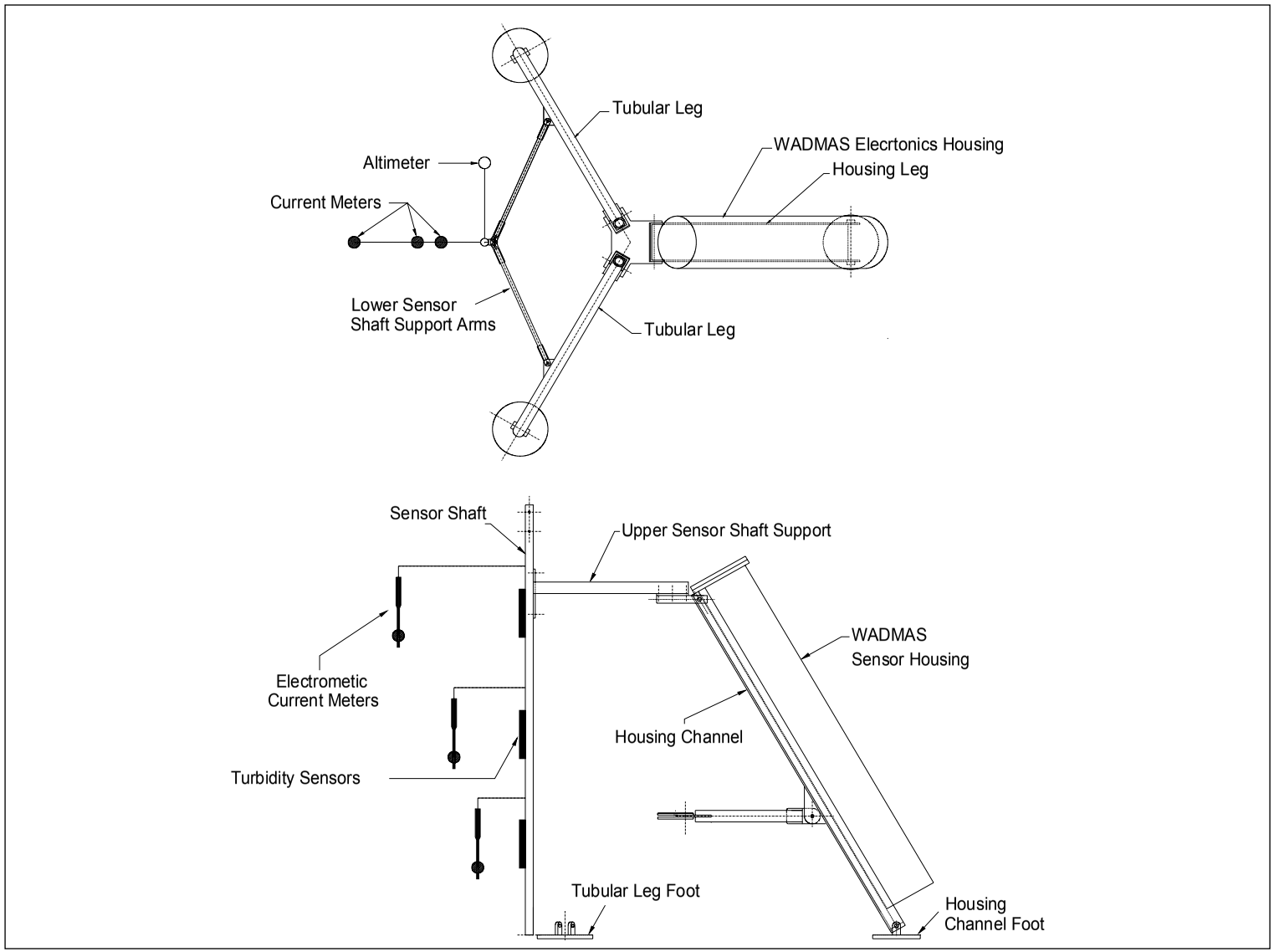

Figure 2. WADMAS sensor platform shown in planform (top) and section (bottom). The array was built by Coastal Studies Institute at LSU and stands ~1.5 m (4.92 ft) high.

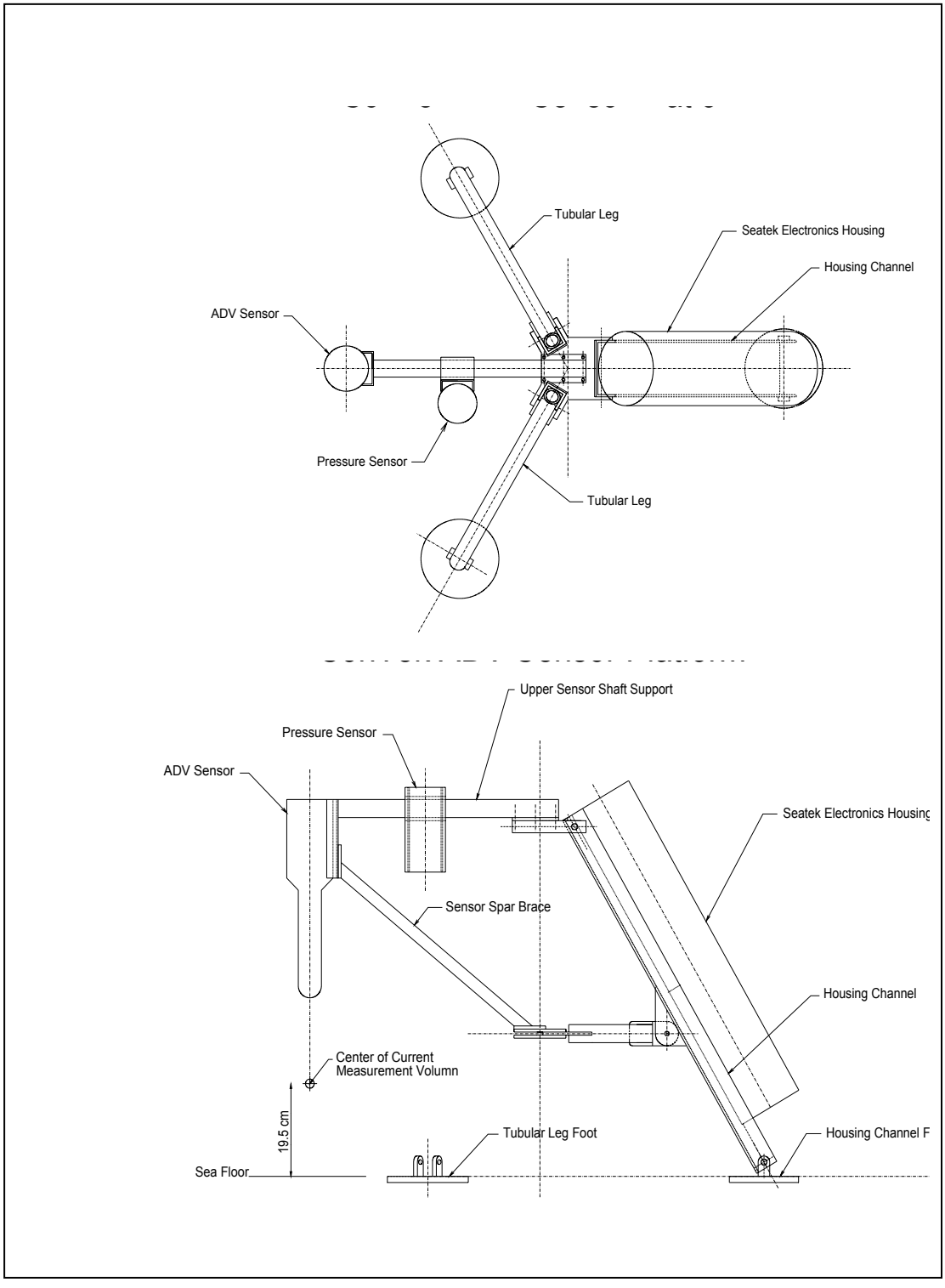

Figure 3. SonTek ADV sensor platform in planform (top) and section (bottom).

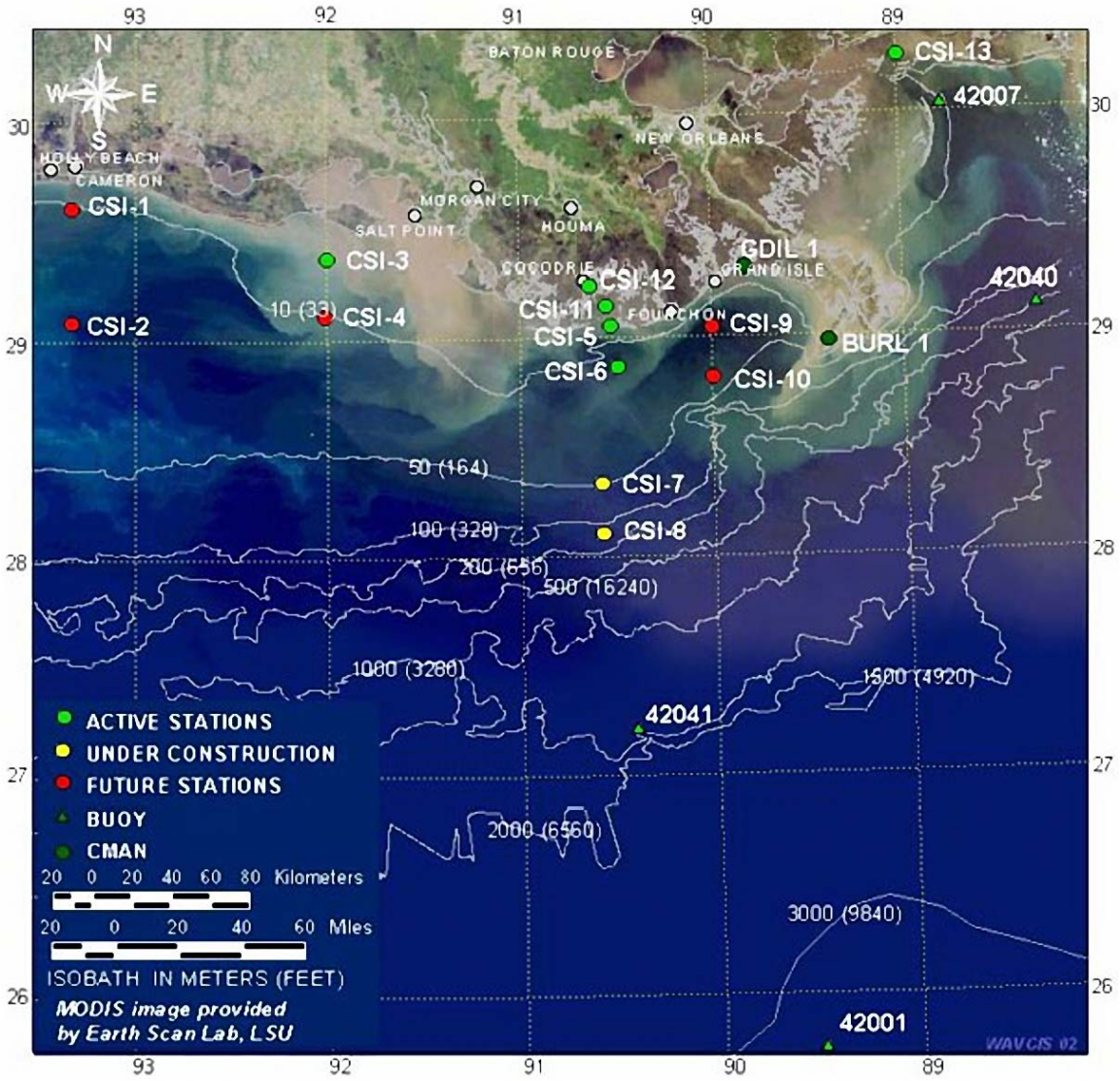

Figure 4. MODIS image showing Wave-Current-Surge Information System (WAVCIS).

The fine scale study area was located at Raccoon Island, south-central Louisiana inner shelf, in water depths of approximately one to two meters (Figure 1). Five deployment sites were chosen so as to understand dynamic and sedimentary environments between, inside and outside of the breakwaters (Figure 1, Table 1). In total, seven deployments were carried out using ADV, WADMAS and Sea gauge pressure systems separately. Sea gauge system (D1) was located at 29°02.979′N, 90°54.829′W, approximately 100 m (328.08 ft) seaward of the center of breakwater 1. The water depth at the offshore location was about 1.6 m (5.25 ft). The ADV system (D2), measuring offshore wave conditions along the eastern part of Raccoon Island, was located at

29°3.029′N, 90°54.806′W at approximately the 1.25 m (4.1 ft) water depth. Deployment #3 WADMAS system (D3) and Sea gauge system (D4) were set between breakwater 0 and breakwater 1, as well as seaward and landward of them at coordinates 29°2.982′N, 90°54.902′W. Dynamic conditions landward were measured by the ADV (D5) approximately half the breakwater-length landward of the center of breakwater 0 for the period September 28 and October 31. Coordinates of the location were 29°02.994′N, 90°54.877′W. Offshore environmental conditions were measured approximately 500 m (1640.42 ft) seaward of the breakwaters by the WADMAS system (D6). Deployment 6 WADMAS system had three current meters with probe 1 at the top of the staff and probe 3 at the bottom. There were two turbidity probes installed on that deployment. Turbidity probe 1 was mounted next to the current meter probe 1 and turbidity probe 2 was mounted to current meter probe 3. Deployment coordinates were 29°02.501′N, 90°55.038′W. The WADMAS was deployed south of the gap between breakwater 2 and breakwater 3. The deployment took place between November 19 and December 8, 2001. The D7 ADV system was deployed south of the gap between breakwater 2 and breakwater 3, very close to the D6 position. The deployment occurred between September 16 and October 8, 2002. Two tropical cyclones made landfall during this short period: TS Isidore and Hurricane Lili.

Data Analysis

Waves

One of the major objectives of the wave monitoring effort is to quantify the influence of the breakwaters on incident wave conditions. This was accomplished by comparing wave conditions measured behind the breakwaters (D5), between the two breakwaters (D4), east end of Raccoon Island (D2) and seaward of the breakwaters (D6) (Figure 1, Table 1). Instrument data were analyzed in the laboratory using various methods. The water level fluctuations were sampled at a frequency of 4 Hz to ensure reliable coverage of high frequency, locally generated wind waves. Spectral analysis of the raw data was based on a standard procedure recommended by the Coastal Engineering Research Center (Earle et al., 1995). Significant wave height (the mean of the highest one-third of the waves), Hs, was calculated as:

$$H_s = 4.0\sqrt{m_o}$$

Where the zero moment, m_0, is computed as:

$$m_o = \sum_{n=1}^{N_b} C_{zz}(f_n) df_n$$

Where C_{zz} (f_n) is the power spectrum density of the nth frequency f_n, and df_n is the bandwidth. The power spectrum densities were calculated using the Welch method of the fast Fourier transformation (Welch, 1967). Peak period is the reciprocal of the frequency, f_p (peak frequency), for which spectral wave energy density is a maximum. It is representative of the higher waves that occurred during the wave record. Peak period *Tp* is given by

$$T_P = \frac{1}{f_p}$$

Currents

Following deployments (Table 1), time series of velocity were de-spiked and were corrected using the most recent calibration results. The compass data were used to rotate the axes to obtain the u and v components, with u defined as positive eastward and v as positive northward. Burst mean averages, $u_c(z)$, were computed. The apparent hydraulic roughness, z_0', was estimated by applying the log-profile method and using the von Karman-Prandtl equation to estimate mean current friction velocity u_{*c} via

$$\frac{u_c(z)}{u_{*c}} = \frac{1}{\kappa}\ln(\frac{z}{z_0'})$$

where $u_c(z)$ is mean current velocity at elevation z and κ is von Karman's constant (0.41). $u_{*}c$ is mean current friction velocity and z_0' is apparent hydraulic roughness. This approach was applied to velocity profiles that satisfied the following criteria: (i) currents

at different elevations exhibited the same direction within ±30°; and (ii) at least three points were required to fall on a log profile with $R^2 \geq 0.98$.

Sediment sensor calibration

Since intensity of the backscattered signal is a function of grain size, the OBS at WADMAS was calibrated for the range of 0 – 6 g/l with a bulk surface sediment sample collected at the study site (Appendix I). The NTU output from the optical sensors is converted to suspended-solids concentration using linear regression equations. Sediment sample grain size distribution and the sample calibration curve from WADMAS are shown in Figures 5 and 6. The linear calibration plot includes the number of samples, correlation coefficient and squared correlation coefficient. While this method would overestimate the suspended sediment concentration if the fines were preferentially suspended, the narrow grain-size distribution and very low (< 6%) silt content afforded a significant degree of confidence in calibration efforts (Figure 5).

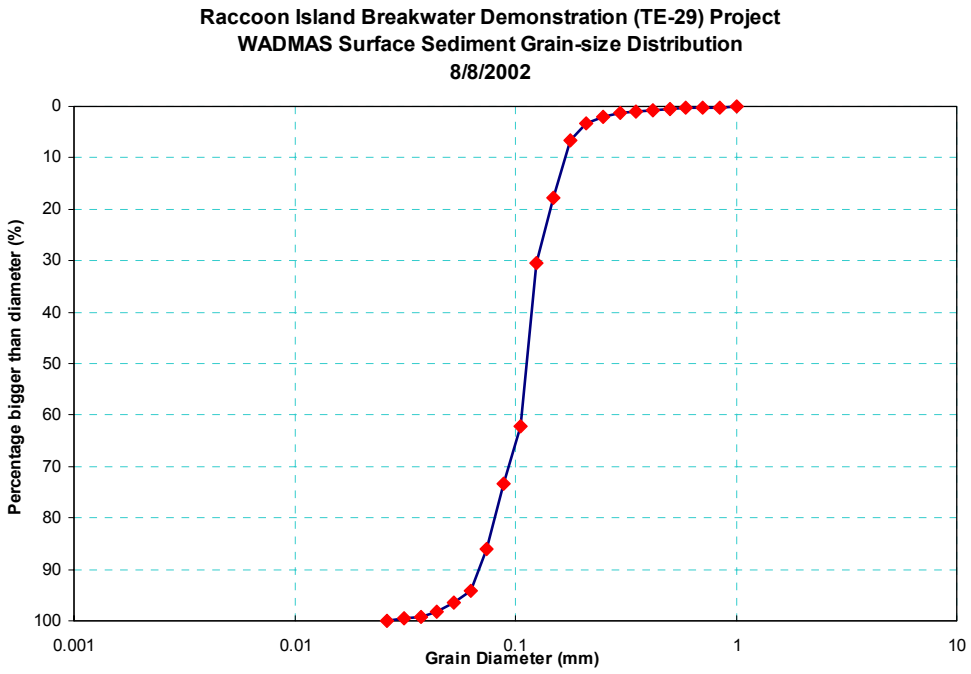

Figure 5. WADMAS surface sediment sample grain size distribution.

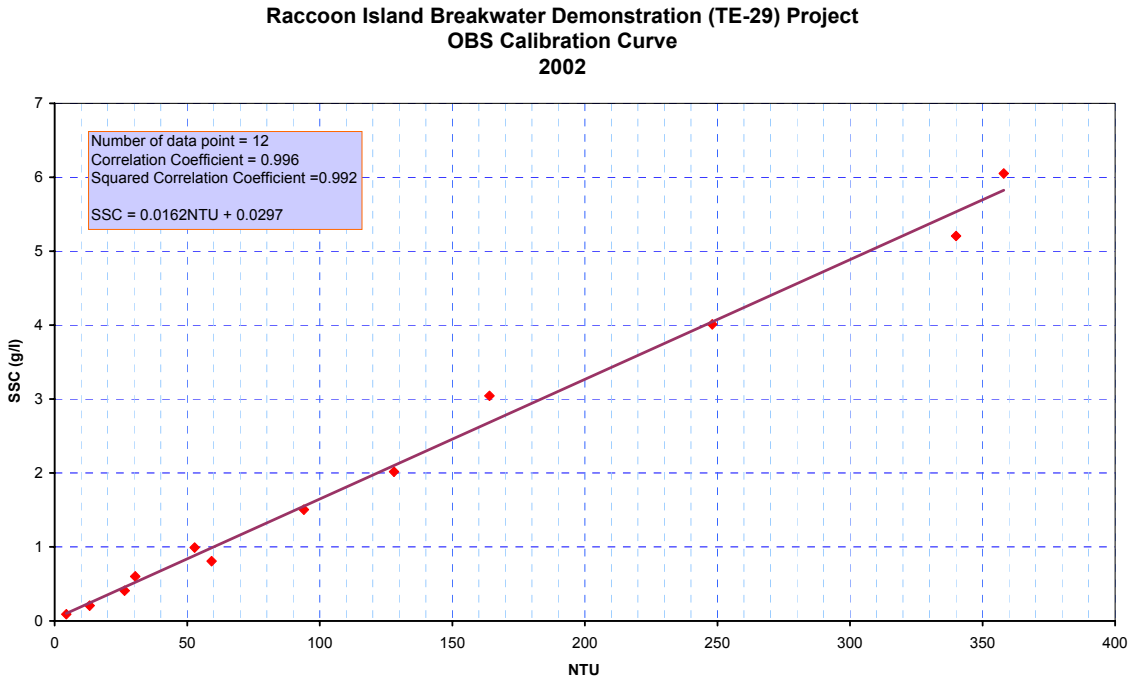

Figure 6. Calibration of near-bottom optical backscatter sensor (OBS) at Raccoon Island, Louisiana, 2002.

Surface sediments

Surface sediment grain-size information was obtained by analyzing samples collected using a grab between September 18 and September 30, 2002. Altogether, 80 surface samples were collected along the 26 topographic/bathymetric survey lines (Figure 1), among which 26 samples were located on the beach, another 26 samples at the end of each survey line, and the remainder along the middle portion of each line. The coordinates for respective samples are presented in Table 2a.

Grain-size analysis for sand samples was conducted using a Gilsonic AutoSiever GA-6, for grain-sizes ranging from 0 Φ (1 mm) to 5.25 Φ (0.026278 mm). Ten of the samples were too fine to be analyzed by sieves, and were subsequently analyzed using a Micrometritics SediGraph 5100. Grain-size classification, typology, and nomenclature were mainly based on the method proposed by Folk and Ward (1957).

Vibracores

Five vibracores were collected during October, 2002, among which three (RIC-1, RIC-2, and RIC-4) were located on the shoal, and two (RIC-5, RIC-6) were located on the nearshore west of the breakwaters (Figure 1, Table 2b).

In the sedimentological laboratory at LSU, all five vibracores were split into two halves from the center, and photographs were taken of each core. One half of the core was preserved for future use, and lithologic logging and grain-size subsampling were conducted on the other half. Sub samples were extracted at an interval of 50 cm (1.64 ft) from each core for routine granulometric analyses as discussed above.

Bathymetry/Topography Surveys

Twenty-six bathymetry/topography survey lines were established in the study area (Figure 1). Surveys were conducted in November 2000, May 2001, November 2001, and May 2002. (After the impacts of Tropical Cyclones Isidore Josephine, Kyle and Lili---September–October 2003---a continuation of this work was funded by LDNR to evaluate quantitatively, the storm impacts at Raccoon Island and post-storm adjustment of the bathymetry and topography of the Gulf-facing barrier). The survey lines extended offshore approximately 610 m (2000 ft) from the dune except at three transects, numbered 21, 23, and 25, which extended only to the maximum water depth where the equipment being used could reach.

Topographic surveys were achieved using a TOPCON Total Station with an HP48GX data logger. The vertical datum used for all surveys was National Geodetic Vertical Datum 1929 (NGVD 29), which was referenced to the survey benchmarks A and B on the island established by DNR (Figure 1). Benchmark A is located at 201689.9141 Northing, 3407040.404 Easting in State Plane Coordinate System 1983, Louisiana South 1702, with an elevation of 4.061806694 ft above NGVD29; while the benchmark B is located at 201049.2115 Northing, 3409349.832 Easting in State Plane Coordinate System

Table 2a. Surface sediment sample locations.

Sample No.	Longitude	Latitude	Sample No.	Longitude	Latitude
1	-90.91187	29.05141	41	-90.92448	29.04893
2	-90.91406	29.05063	42	-90.92537	29.04916
3	-90.91656	29.04964	43	-90.92658	29.04712
4	-90.91215	29.04796	44	-90.92783	29.04492
5	-90.91362	29.04891	45	-90.92802	29.04523
6	-90.91603	29.05050	46	-90.92722	29.04729
7	-90.91242	29.04664	47	-90.92636	29.04934
8	-90.91342	29.04761	48	-90.92704	29.04968
9	-90.91622	29.05019	49	-90.92785	29.04752
10	-90.91282	29.04613	50	-90.92865	29.04541
11	-90.91395	29.04713	51	-90.92798	29.05068
12	-90.91644	29.04950	52	-90.92893	29.04787
13	-90.91358	29.04560	53	-90.92970	29.04583
14	-90.91474	29.04681	54	-90.92852	29.05090
15	-90.91700	29.04903	55	-90.93035	29.04813
16	-90.91644	29.04417	56	-90.92940	29.05110
17	-90.91696	29.04616	57	-90.93073	29.04612
18	-90.91731	29.04867	58	-90.93127	29.05152
19	-90.91760	29.04376	59	-90.93251	29.04978
20	-90.91836	29.04584	60	-90.93495	29.04729
21	-90.91902	29.04778	61	-90.93430	29.04940
22	-90.91811	29.04794	62	-90.93301	29.05212
23	-90.91868	29.04413	63	-90.93476	29.05279
24	-90.91955	29.04348	64	-90.93567	29.05100
25	-90.91973	29.04555	65	-90.93693	29.05345
26	-90.92006	29.04785	66	-90.93741	29.05117
27	-90.92238	29.04370	67	-90.93842	29.04874
28	-90.92173	29.04567	68	-90.94229	29.05127
29	-90.92092	29.04799	69	-90.94091	29.05308
30	-90.92186	29.04836	70	-90.93967	29.05484
31	-90.92266	29.04602	71	-90.93817	29.05401
32	-90.92343	29.04403	72	-90.93899	29.05303
33	-90.92443	29.04410	73	-90.93270	29.04767
34	-90.92360	29.04635	74	-90.93649	29.04896
35	-90.92273	29.04843	75	-90.94023	29.05122
36	-90.92368	29.04887	76	-90.91525	29.04509
37	-90.92445	29.04656	77	-90.92098	29.04384
38	-90.92527	29.04436	78	-90.91217	29.04967
39	-90.92599	29.04445	79	-90.91359	29.04977
40	-90.92527	29.04675	80	-90.91629	29.04730

Table 2b. Vibrocore locations.

Core ID	Longitude	Latitude
RIC-1	-90.91710	29.04480
RIC-2	-90.91758	29.04697
RIC-4	-90.92310	29.04753
RIC-5	-90.93888	29.05317
RIC-6	-90.93427	29.05080

1983, Louisiana South 1702, with an elevation of 2.721003028 ft above NGVD29. The data were later converted to North America Vertical Datum 1988 (NAVD 88), using the computer program "corpscon" developed and maintained by the US Army Corps Engineers.

During the survey, for each setup the TOPCON Total Station was oriented to the north using a compass. Bathymetry/topography surveys were divided into two parts for each line: from dune to the maximum water depth where the rod person could safely reach. Survey points were obtained at approximately 3.5 m (about 12 ft) intervals and at significant points where distinct breaks in slope were observed. Where water depth exceeding wading, a sled was used.

The sled was designed and built by the CSI field support group and is shown in Figure 7. Six prisms/reflectors were placed on a mast at an approximate elevation of 6.6 m (21.65 ft) so that the Total Station would have the ability to receive reflected signals even if the sled made a turn. During surveys, the sled was towed by a boat at the lowest possible speed so that the Total Station could ping at the reflectors continuously and maximize the data density as much as possible. This made it possible for the survey to extend from shallow water offshore to approximately 610 m (2000 ft) from the beach.

Topographic/bathymetric survey data were analyzed to quantify the morphological development of the study area during the monitoring period. Data were downloaded to a PC and processed to obtain X, Y, and Z values of each survey point, among which X and Y are in the State Plane Coordinates System, Louisiana South 1983,

Figure 7. Sled used in bathymetric surveys in the Raccoon Island area. Six reflectors were placed on top of the mast that stands on the sled. The height from the bottom to the reflectors is 6.6 m (21.65 ft).

Z in NGVD 29 and then transformed to NAVD 88. Profile data from each transect were plotted and compared to those of previous surveys. Sediment volume changes at each transect were calculated by using the Beach Morphology Analysis Package (USACE version 2.0), as well as Goldensoftware Surfer 8.0 to quantify deposition and erosion and volumes. ArcGIS software was used to generate the maps of bathymetry/topography of each survey, and comparisons between two surveys.

HYDRODYNAMICS

Introduction

The inner shelf of the northern Gulf of Mexico, and specifically Louisiana, is unique in comparison with most locations that have been studied, in that it is exposed to a much lower mean level of hydrodynamic energy (Pepper and Stone, 2002). It has an average significant wave height (Hs) of approximately 1.0 ± 0.2 m (3.28 ± 0.66 ft) and a mean peak period of 4.5 – 6.0 s. The monthly mean significant wave heights in winter are 0.2 – 0.6 m (0.66 – 1.97 ft) higher than that of the rest of the year. The predominant wave direction is from the southeastern quadrant (Stone and Xu, 1996). Despite the dominant low wave energy, winter storms and tropical cyclones influence sea state significantly (Stone et al., 2003). Hurricanes have played a critical role in the transgressive evolution of Louisiana's barrier islands. Some estimates suggest that storms may account for up to 90% of long-term (10^2 years) shoreline erosion (Stone et al., 1997). Tides in the study area are diurnal, with a tropic range of approximately 0.4 m (1.31 ft), resulting in only weak tidal currents (Wright et al., 1997; Stone, 2000; Pepper and Stone, 2002).

An overall summary of the hydrodynamic parameters measured offshore Raccoon Island is shown in Table 1. The high-frequency sampling scheme allows an examination of wave properties including significant wave height, peak wave period and wave energy distribution with respect to frequency.

Waves

Sea Gauge (D1, 9/2000 & D4, 12/2000)

Waves along Raccoon Island are significantly influenced in winter by pre-frontal conditions when strong southerly winds rapidly develop sea state. As shown in Figures 8 and 9, a number of fronts moved through the area during respective deployments. Significant wave heights measured at offshore site D1 ranged from 0.06 m to 0.81 m (0.20 – 2.66 ft) with an average of 0.34 m (1.12 ft) (Figure 8). Similar wave heights were observed in the gap between breakwaters 0 and 1 (D4) and ranged from 0.02 m to 0.59 m (0.07 – 1.94 ft) with an average of 0.19 m (0.62 ft).

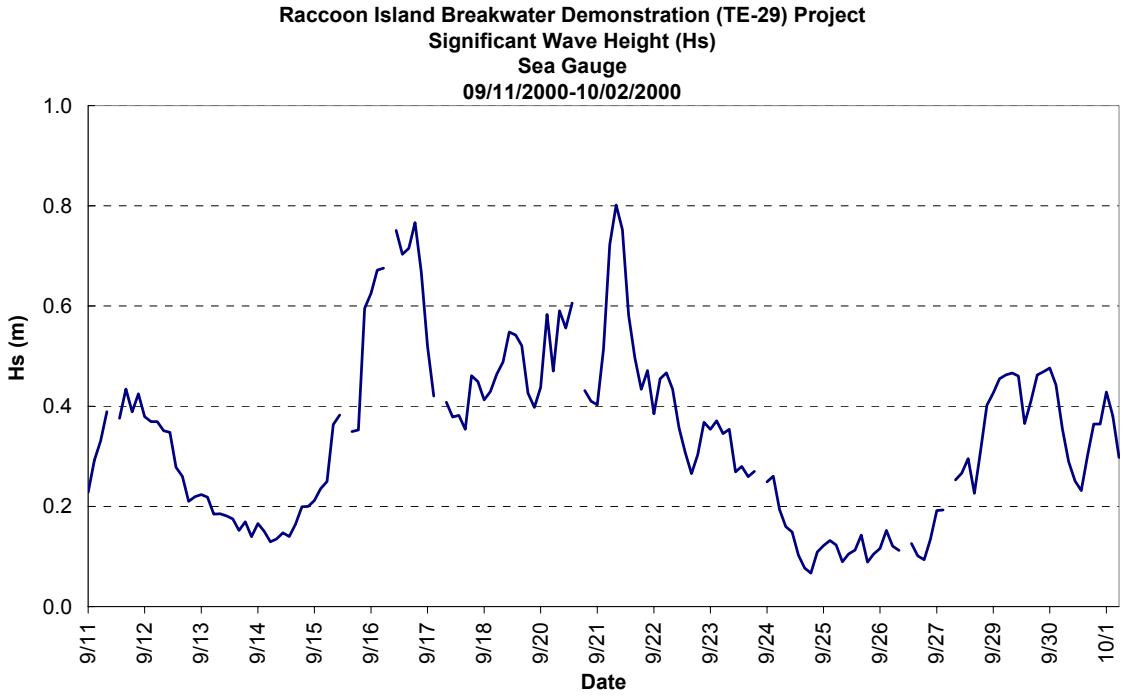

Figure 8. Time series of significant wave height (Hs) at deployment #1 (D1)

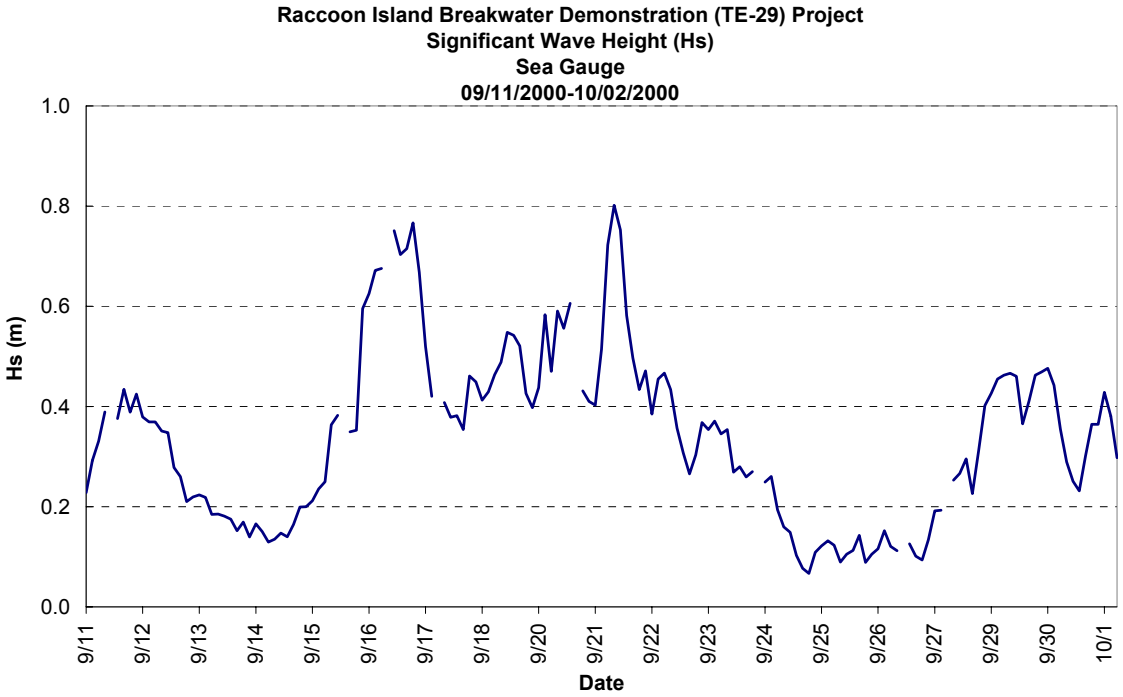

Figure 9. Time series of significant wave height (Hs) at deployment #4 (D4)

Peak wave period, also referred to as dominant wave period or period of maximum wave energy, is defined as the wave period corresponding to the center frequency of the frequency band with the maximum non-directional spectral density. The D1 average peak wave period is 6.5 s measured seaward of the breakwater 1, and at D4, is 6.3 s (Figures 10, 11). Although there are insignificant differences in peak wave period for D1 and D4, both locations respond to storms in a similar manner, i.e. a significant increase in low frequency waves in which wave period ranges from 10–12 s. Given the respective depths at which both sensors were deployed 1.6 m (5.25 ft) and 1.2 m (3.94 ft) respectively, waves were breaking at these sites during peak energy events. Waves were in the lower frequency band during some storms where wave periods (Figures 10 and 11) approached 10–12 s. Thus the energy dissipation mechanism likely switched from breaking when high steep waves were generated to bottom frictional dissipation during this longer swell wave dominated period.

WADMAS (D3, 12/2000 & D6, 11/2001)

Figures 12 and 13 show significant wave height and peak wave period, respectively, at D3 landward of breakwaters 0 and 1. Three peaks in wave height are particularly evident, associated with three cold fronts, respectively. Significant wave heights during these storms were several times the mean fair-weather height and appeared equally as energetic as those measured seaward of the breakwaters---approximately 0.7 m (2.3 ft) in the lee of the structures. Trends in peak wave period were not especially clear from the time series, although peak period appears to have fluctuated in a similar manner during the pre-frontal storms with longest waves during maximum wave height. The persistent relatively high wave energy levels measured behind both breakwaters is an important finding for future design. Figure 14 shows significant wave height at D2 measured by the ADV approximately half the breakwater-length landward of the center of breakwater 0. Significant wave height ranged from 0.01 m to 0.39 m (0.03 to 1.28 ft) with an average of 0.06 m (0.20 ft). Figure 15 shows peak wave period ranged from 3 s to 10 s with an average of 6 s.

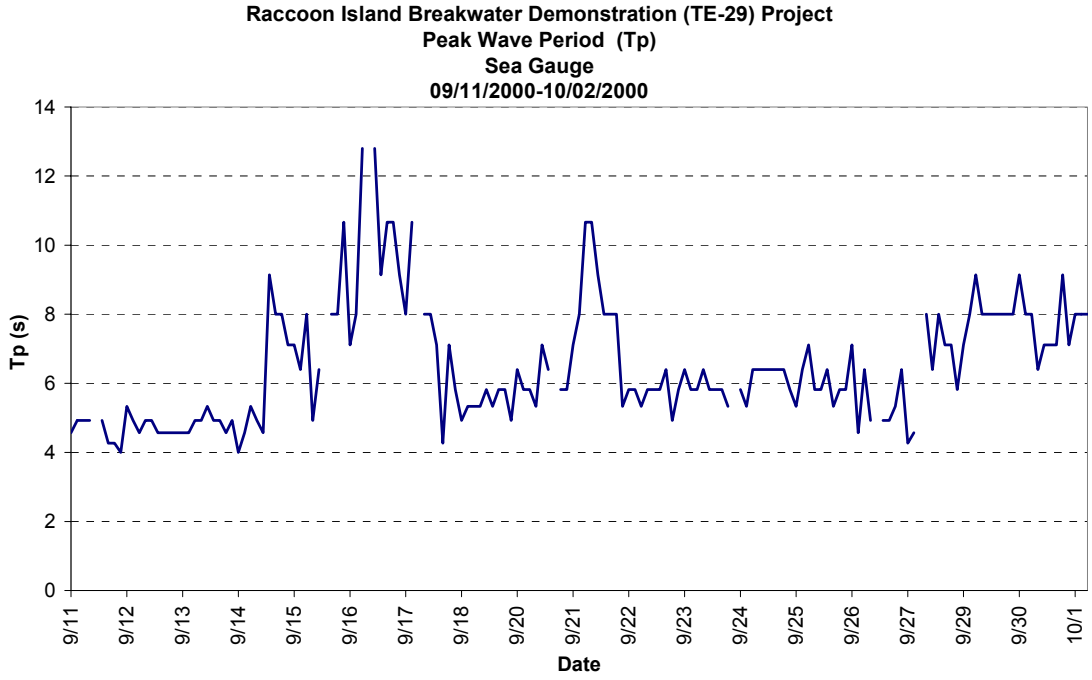

Figure 10. Peak wave period at deployment #1 (D1)

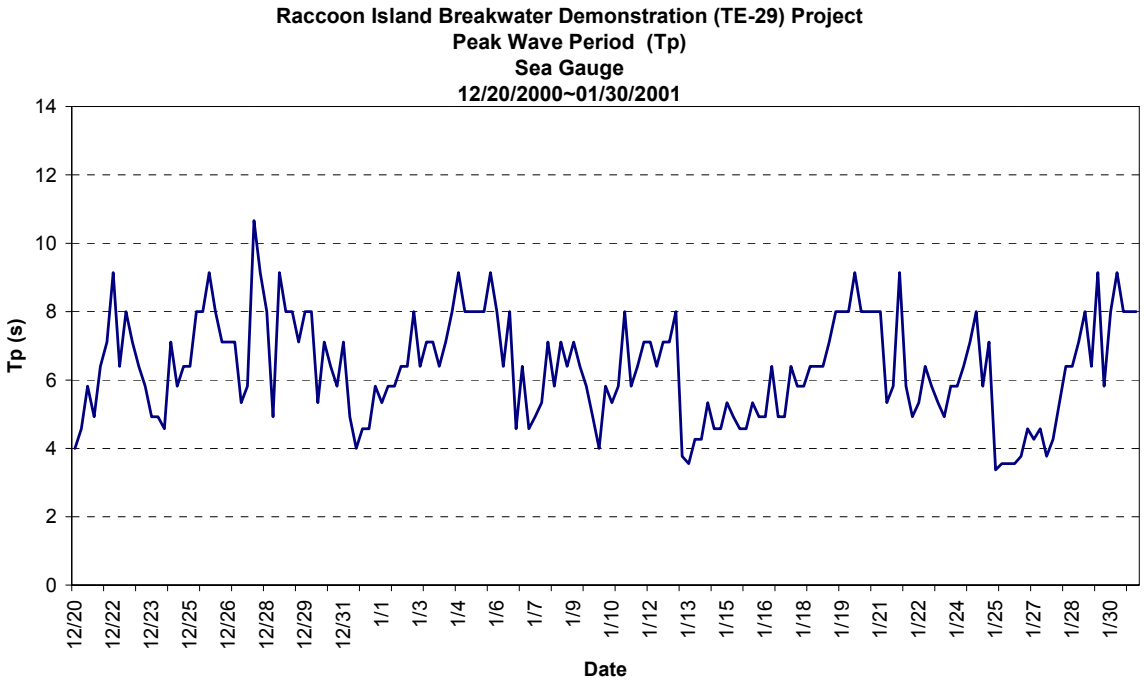

Figure 11. Peak wave period at deployment #4 (D4)

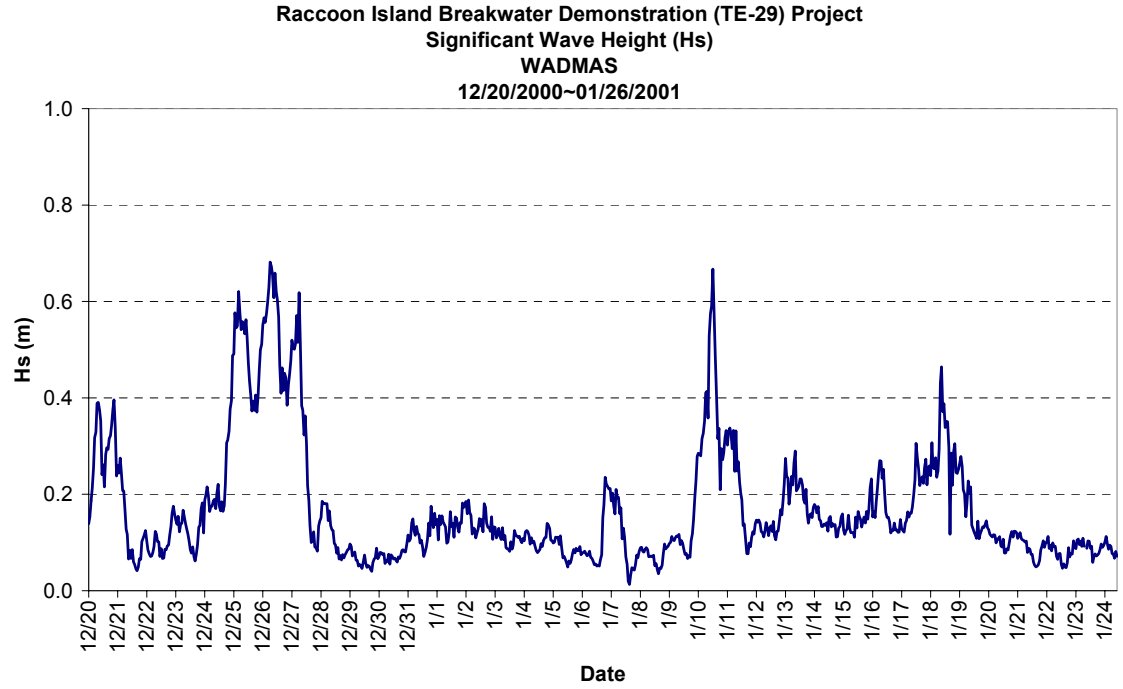

Figure 12. Significant wave height (Hs) at deployment #3 (D3).

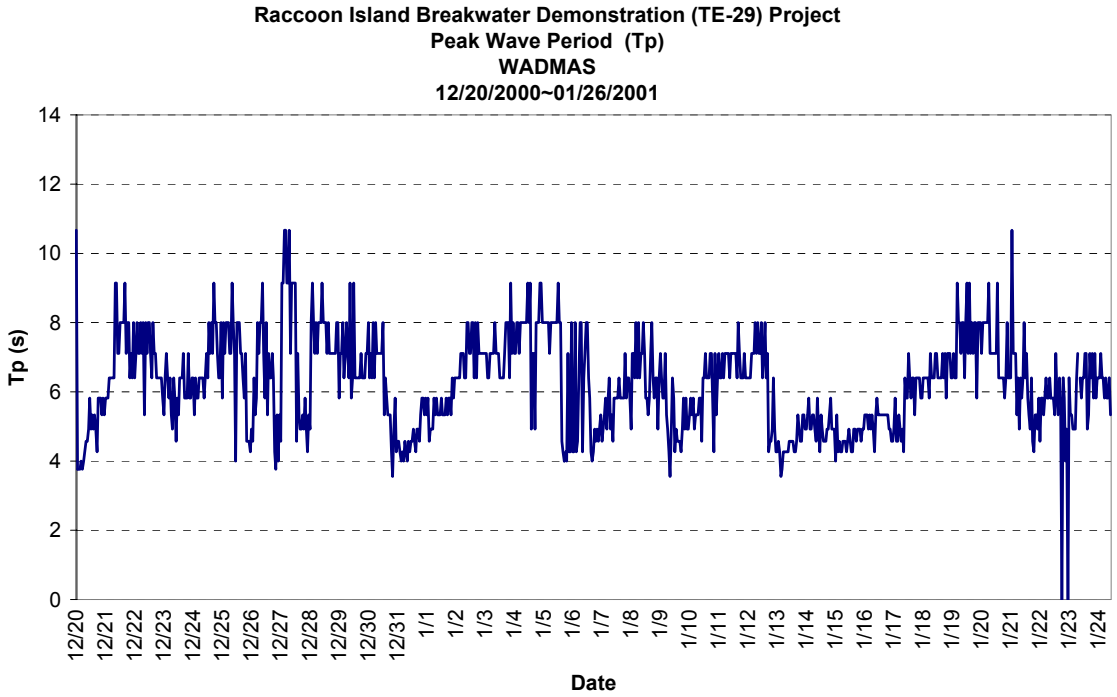

Figure 13. Peak wave period (Tp) at deployment #3 (D3).

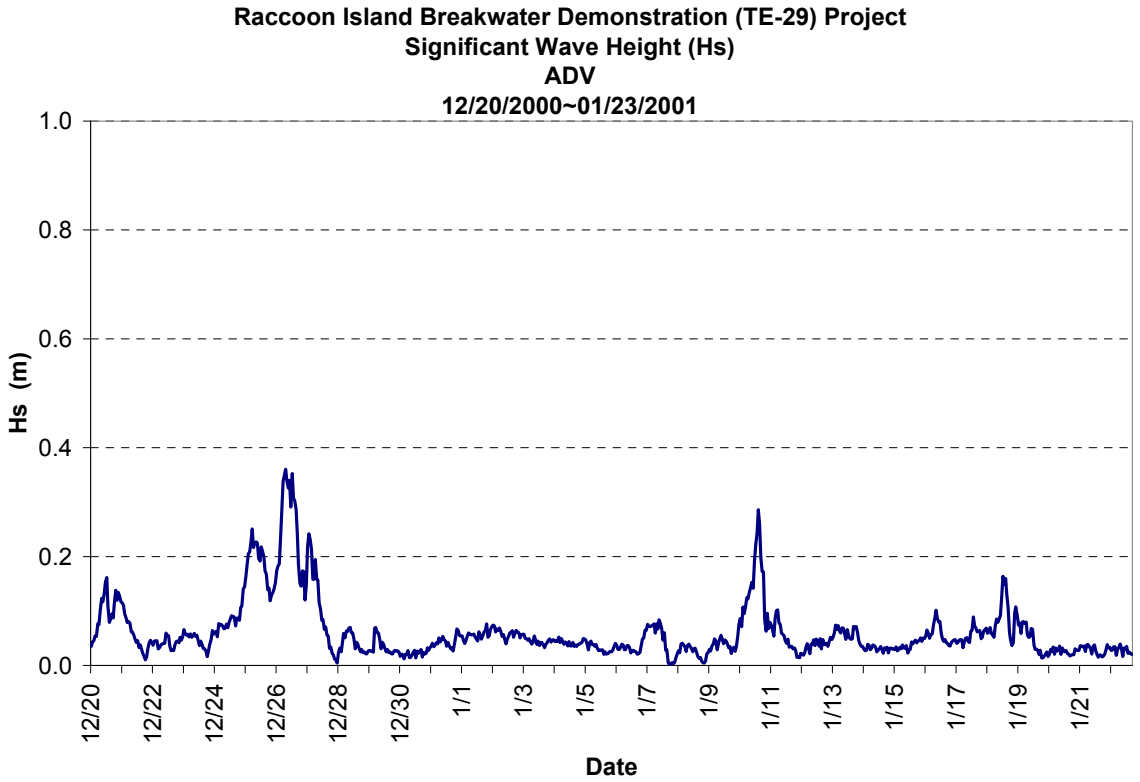

Figure 14. Significant wave height (Hs) at deployment #2 (D2).

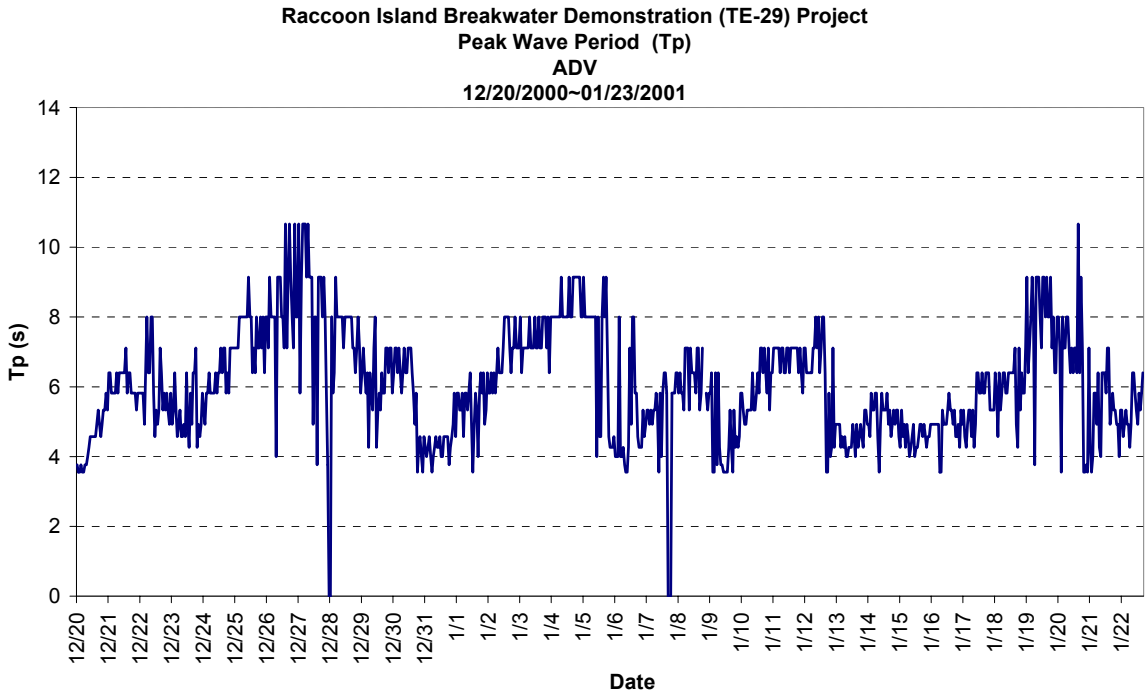

Figure 15. Peak wave period (Tp) at deployment #2 (D2).

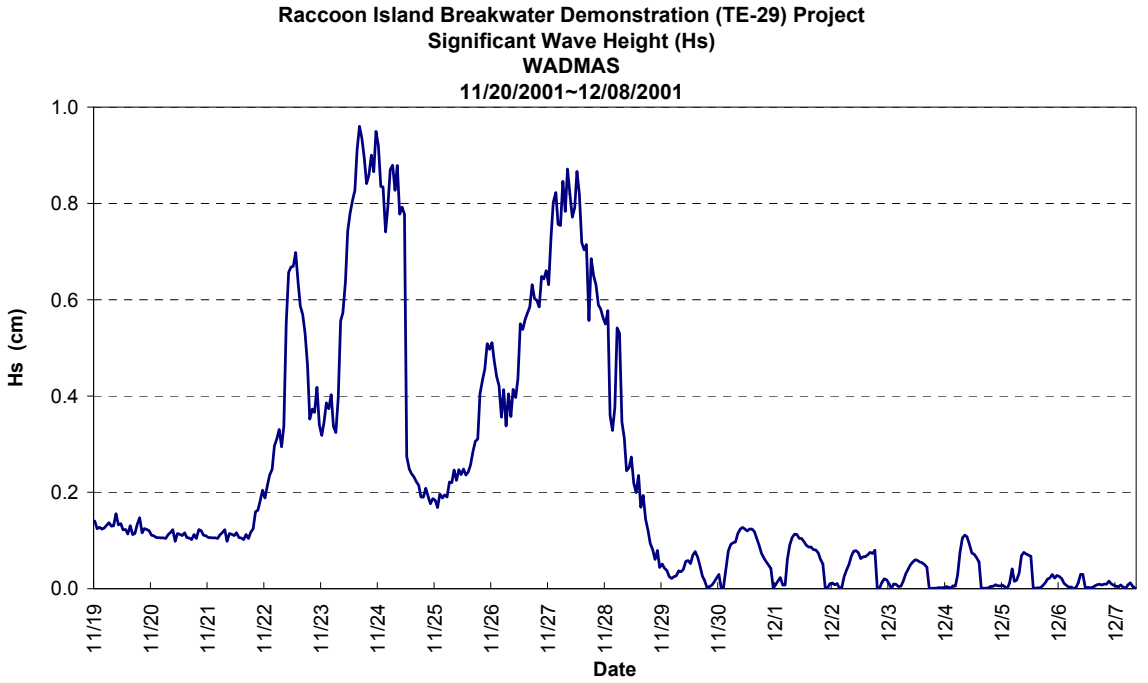

Figure 16. Significant wave height (Hs) at deployment #6 (D6).

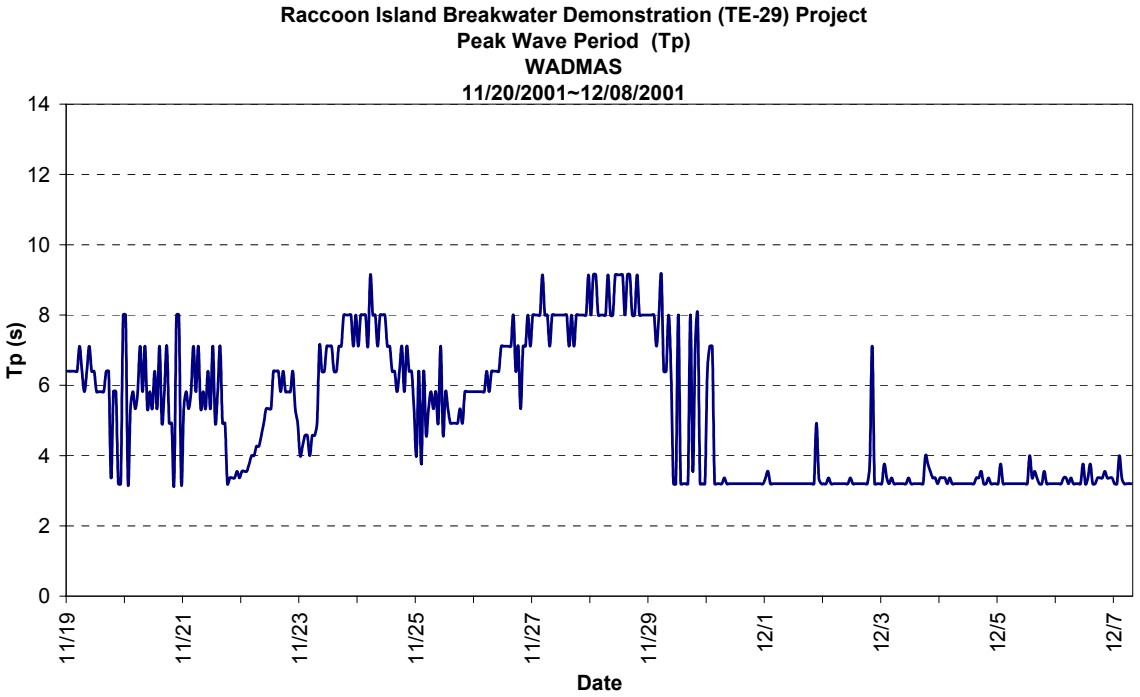

Figure 17. Peak wave period (Tp) at deployment #6 (D6).

Offshore wave measurements were carried out at deployment D6 on the shoal seaward of breakwater 2 at the 2.4 m (7.87 ft) isobath. Figures 16 and 17 provide significant wave height at D6 measured by WADMAS approximately 500 m (1,640.42 ft) from the breakwaters. Two storms are apparent from the time series where significant wave height ranged from 0.01 m to 0.96 m (0.03–3.15 ft) with an average of 0.22 m (0.72 ft). Wave period ranged from 3 s to 9 s with an average of 5 s. Longer period waves are associated with storm peaks when wave energy is at a maximum. The latter part of the time series of wave height shows a strong diurnal tidal signal during fair-weather wave conditions and wave periods drop to approximately 3.5 s.

Currents

ADV (D2)

Currents measured at D2, northeast of the easternmost breakwater (0), show a distinct asymmetry with the north (onshore) currents being stronger than the south

(offshore) currents (Figure 18) for the December-January time series. Similarly, higher currents to the west (longshore) predominate over those to the east, although highest peak speeds were recorded during eastward flowing currents (Figure 19). The mean vertical current distribution is shown in Figure 20 and maximum downward velocities of near 5.8 cm/s (0.19 ft/s) were recorded. Mean vertical current velocities ranged from 0.01 to 47.7 cm/s (0.0003–1.56 ft/s) with a mean value of 6.4 cm/s (0.21 ft/s) (Figure 21).

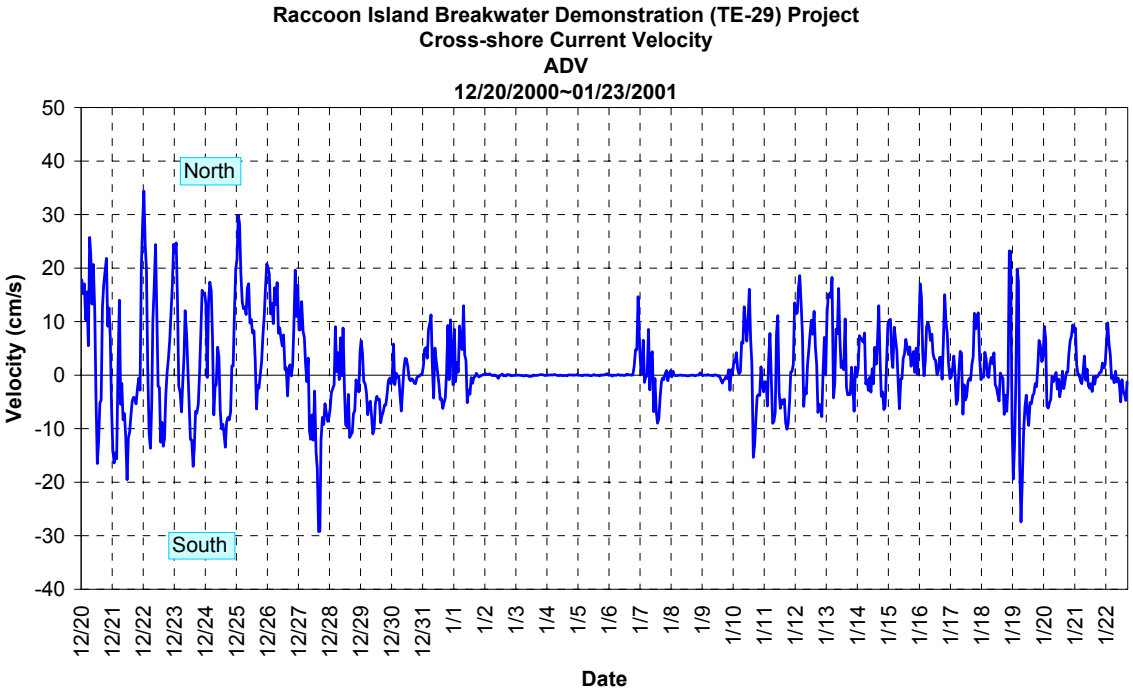

Figure 18. Time series of mean cross-shore current at D2.

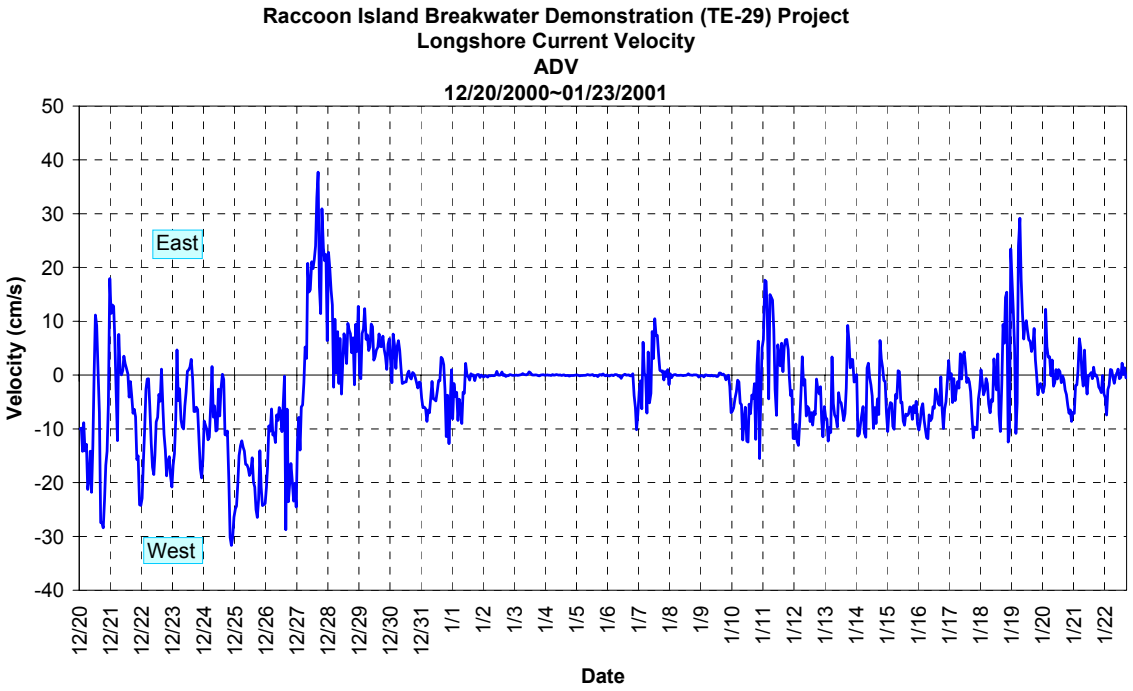

Figure 19. Time series of mean longshore current at D2.

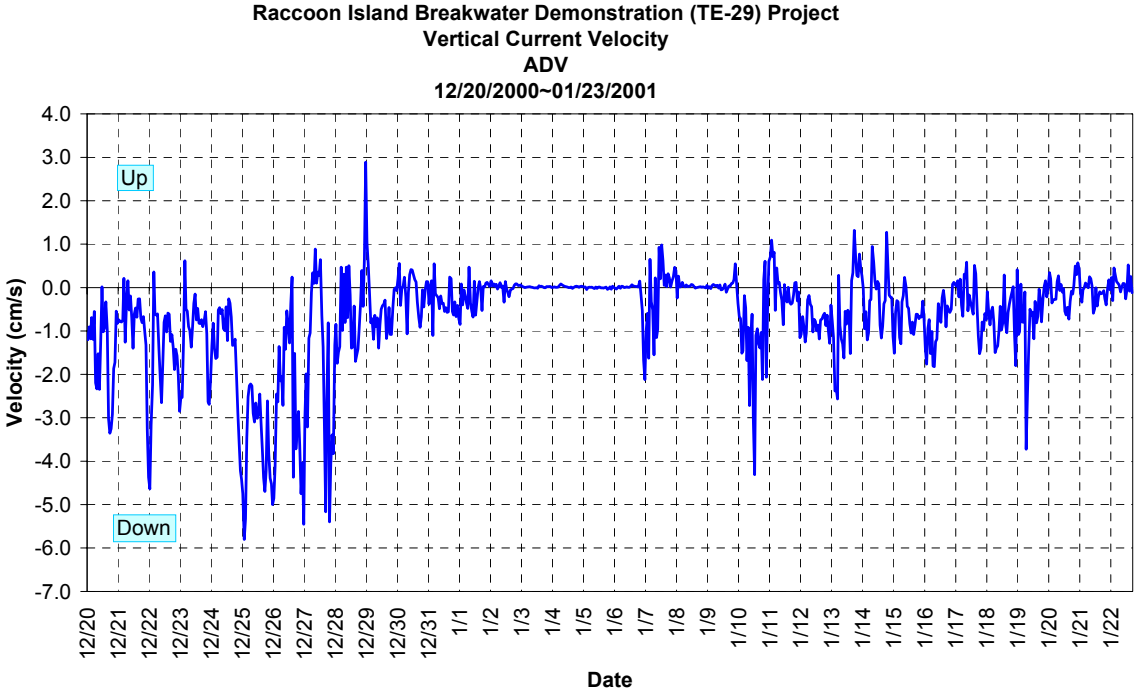

Figure 20. Time series of mean vertical current at D2.

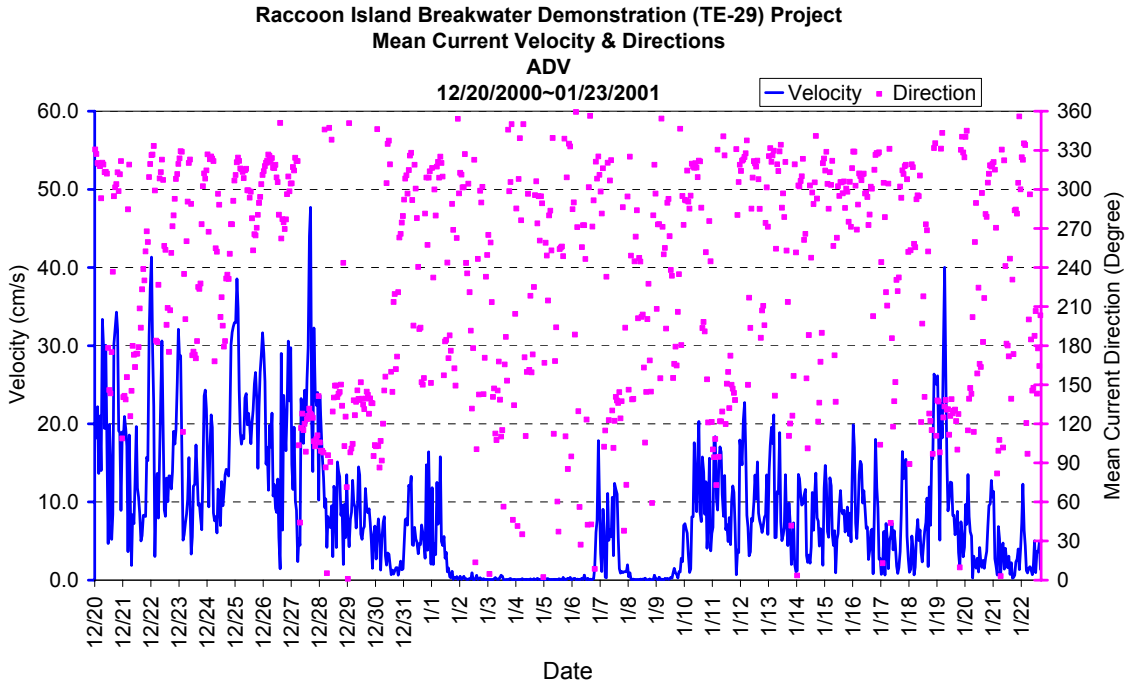

Figure 21. Time series of mean current and directions at D2.

ADV (D5)

Deployment #5 (D5) is located behind breakwater 0. The time scale covered extended from 9/27-10/15/01 and captured a significant cold front where wind gusts measured at CSI 5 exceeded 32 kts (16.46 m/s, 36.82 m/h) and waves approached 2 m (6.56 ft). The mean longshore current is shown for the entire time series in Figure 22. It is evident that the highest velocities are to the east at this site peaking at ~20 cm/s (0.66 ft/s). During the cold front event, however, maximum velocities of 55 cm/s (1.80 ft/s) to the west were recorded. The mean current velocity is 16.02 cm/s (0.53 ft/s) for this entire time series, but clearly, the importance of cold fronts on generating strong currents is apparent.

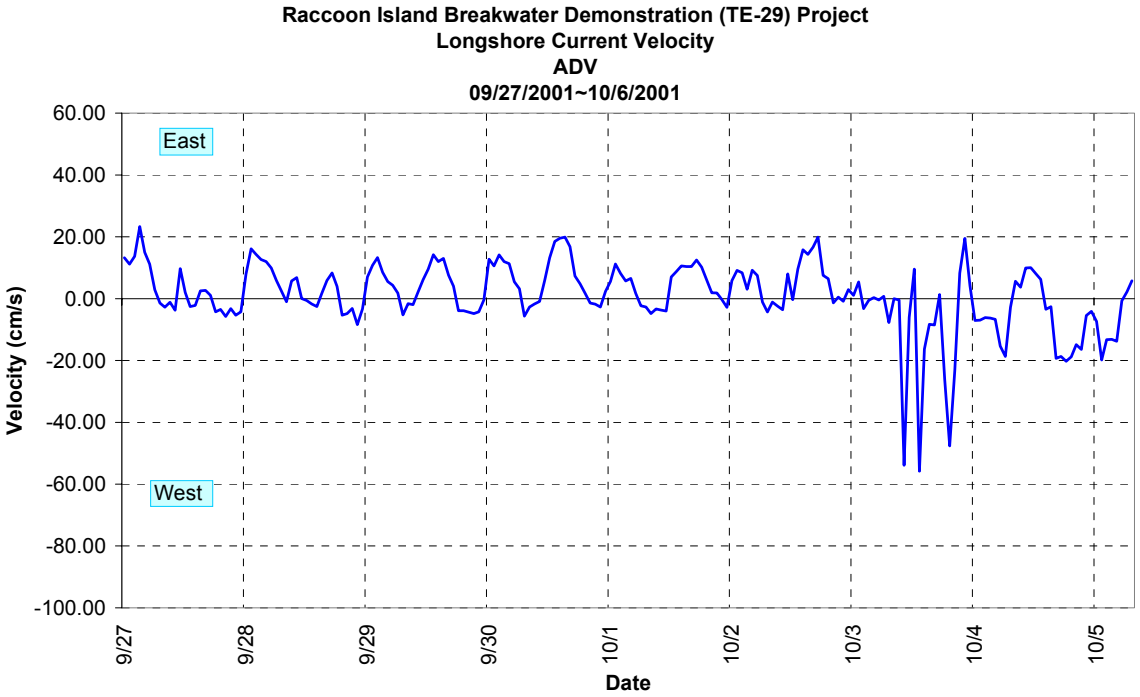

Figure 22. Time series of mean longshore current at D5.

The mean cross-shore current velocity is presented in Figure 23 for the same time series. Currents are generally symmetrical although stronger currents tend to be directed onshore. The significance of the frontal event is again apparent and maximum offshore current velocities of 92 cm/s (3.02 ft/s) were recorded moving offshore. The mean current distribution is presented in Figure 24 and maximum speeds of 109 cm/s (3.58 ft/s) are evident.

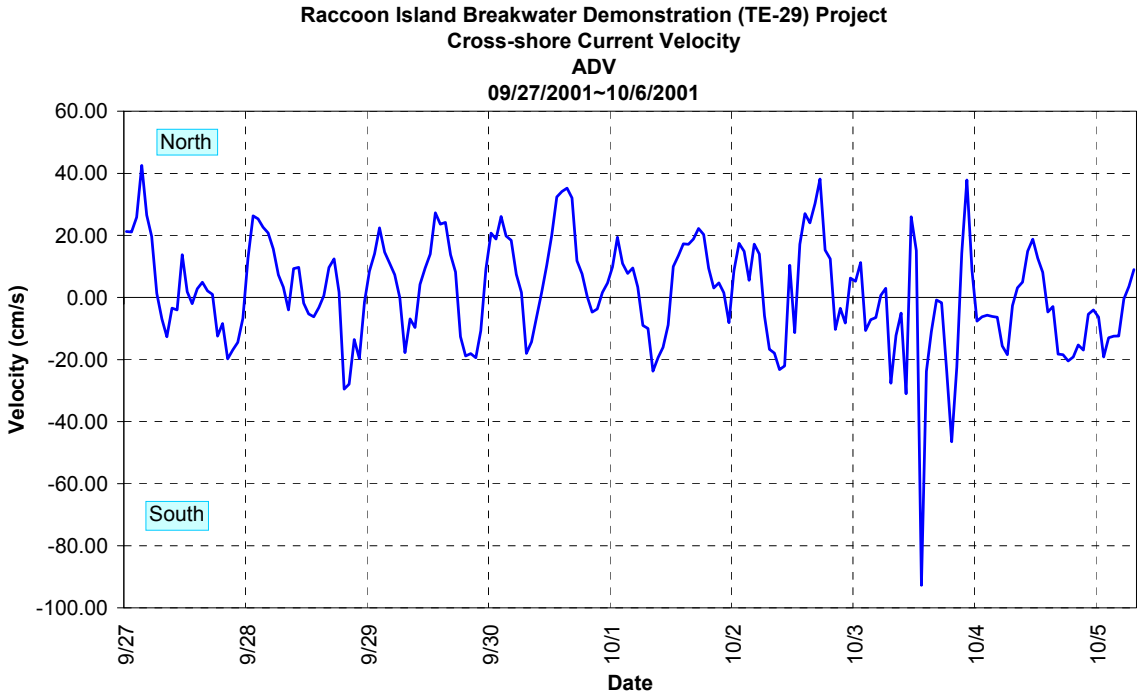

Figure 23. Time series of mean cross-shore current at D5.

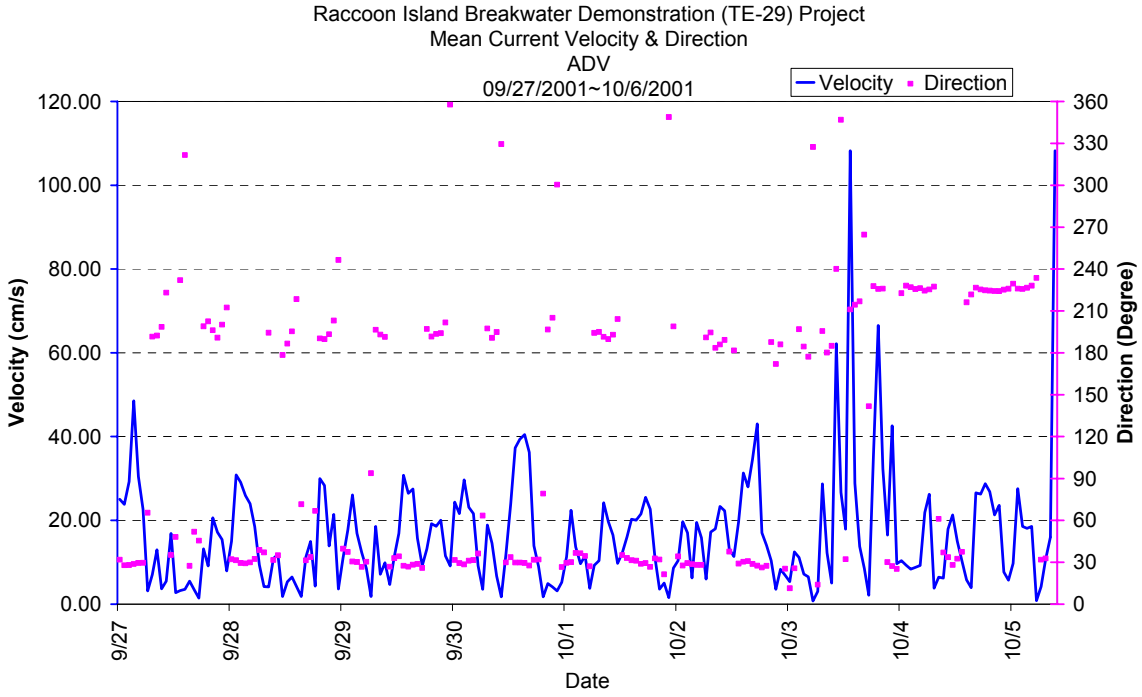

Figure 24. Time series of mean current at D5.

WADMAS (D3)

The WADMAS system was deployed in the gap between breakwaters 0 and 1 for the period 12/20/00-01/26/01. At least 4 cold front passages occurred during this deployment. As shown in Figures 25, 26 and 27, current velocity is highest at the top and mid sensors when compared to that near the bed. Maximum current speeds of slightly over 180 cm/s (5.91 ft/s) occurred during two storms near the top and mid portion of the water column. At the bed, current velocity exceeds 100 cm/s (3.28 ft/s) during 4 events and reached a maximum of ~150 cm/s (4.92 ft/s). These measurements indicate that extremely fast flowing currents are common through the gaps of these breakwaters, particularly along the east flank of the structures where the gaps are aligned with current flow from Caillou Bay and the Gulf of Mexico.

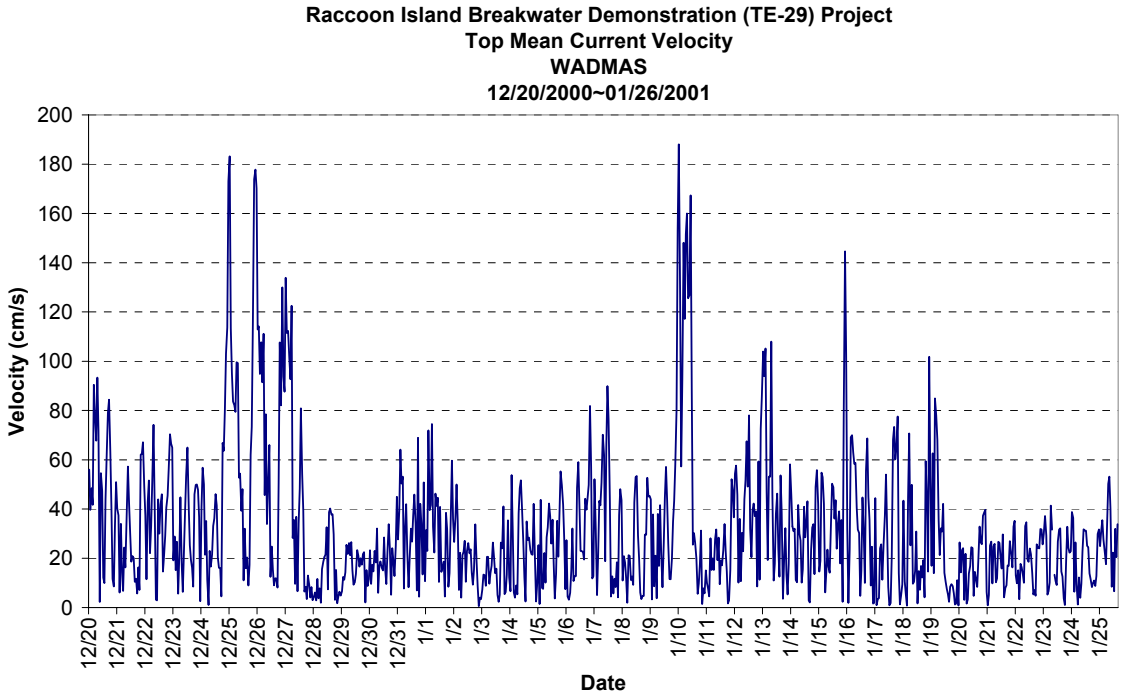

Figure 25. Time series of top current velocity at D3

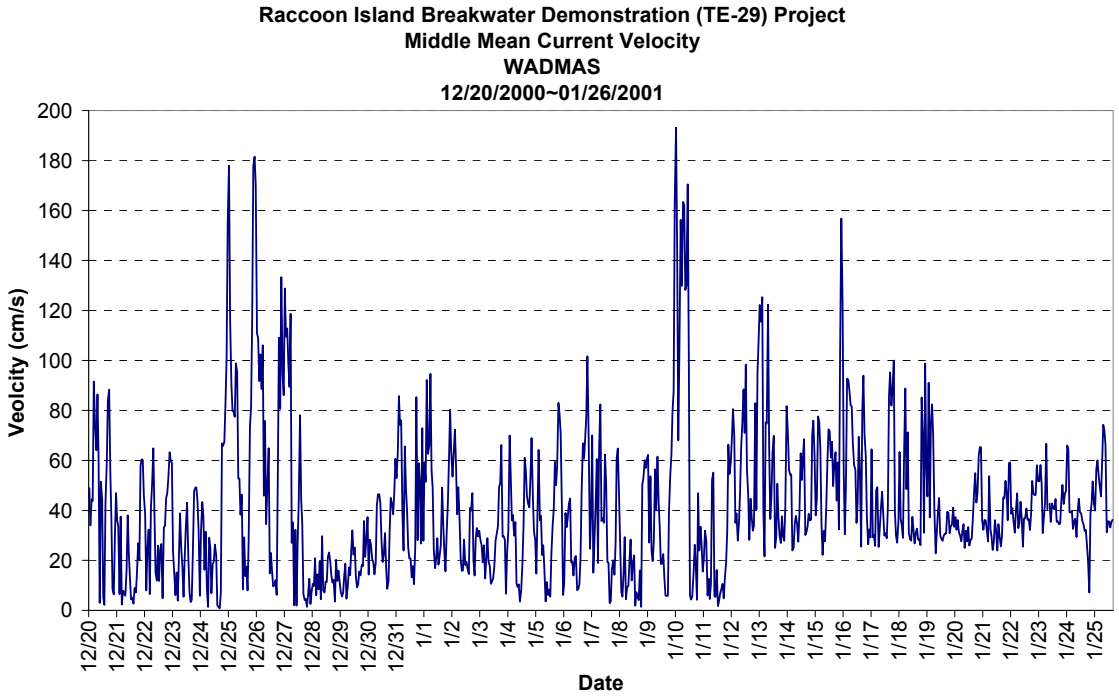

Figure 26. Time series of middle current velocity at D3

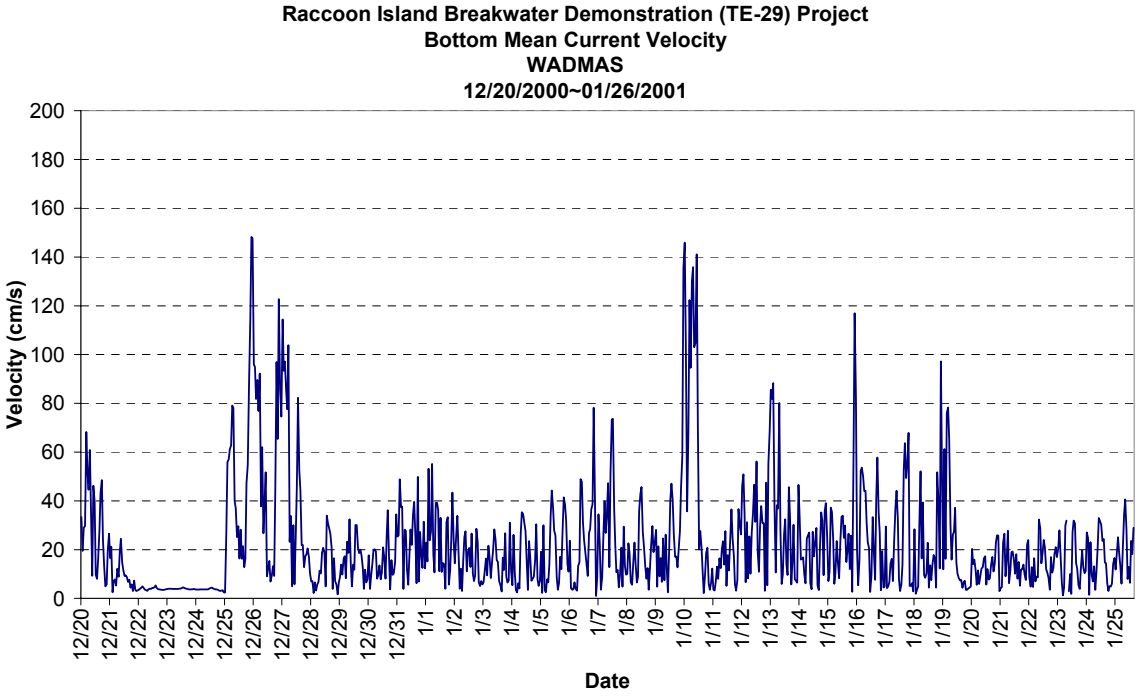

Figure 27. Time series of bottom current velocity at D3

WADMAS (D6)

The WADMAS system was deployed at D6 to investigate bottom boundary layer dynamics and sediment transport on the shoal and to establish possible linkages between this sand body acting as a source for sediment deposited in the lee and seaward of the breakwaters, as well as in the gaps between structures. The bottom, mid and top mean currents are shown in Figures 28, 29 and 30 respectively for the period 11/19/01-12/08/01. Two significantly energetic cold fronts are captured in the time series driving peak current velocities of near 80 cm/s (2.60 ft/s) at the bottom, ~100 cm/s (3.28 ft/s) at mid depth and 110 cm/s (3.61 ft/s) near the surface. These maximum currents correlate with the storm that peaked between 11/28 and 11/29, with sustained wind speeds of >32 kts (16.46 m/s, 36.82 m/h) measured blowing offshore at the nearby CSI 5 site. The remainder of the time series illustrates the diurnal tidal signal which entered a Tropic phase with maximum tidal range of ~0.75 m (2.46 ft).

Suspended sediment concentrations are shown for the bottom and top OBS sensors in Figure 31. Both storms are evident in this time series also at both sensor locations. As expected, suspended sediments are highest in the bottom boundary layer and exceed 5,000 g/l during both events. The water column does not appear to be completely saturated since the upper sensor recorded concentrations of 1,000 g/l and less during both events. The bottom current and wave shear velocity time series are shown in Figure 32. It is evident on comparison of the combined shear with suspended sediment concentrations near the bed that a phase lag exists between maximum combined shear and maximum suspended sediment concentration. This is due to the phasing of the combined shear and when the threshold velocity (3–3.5 cm/s; 0.1–0.11 ft/s) is actually attained.

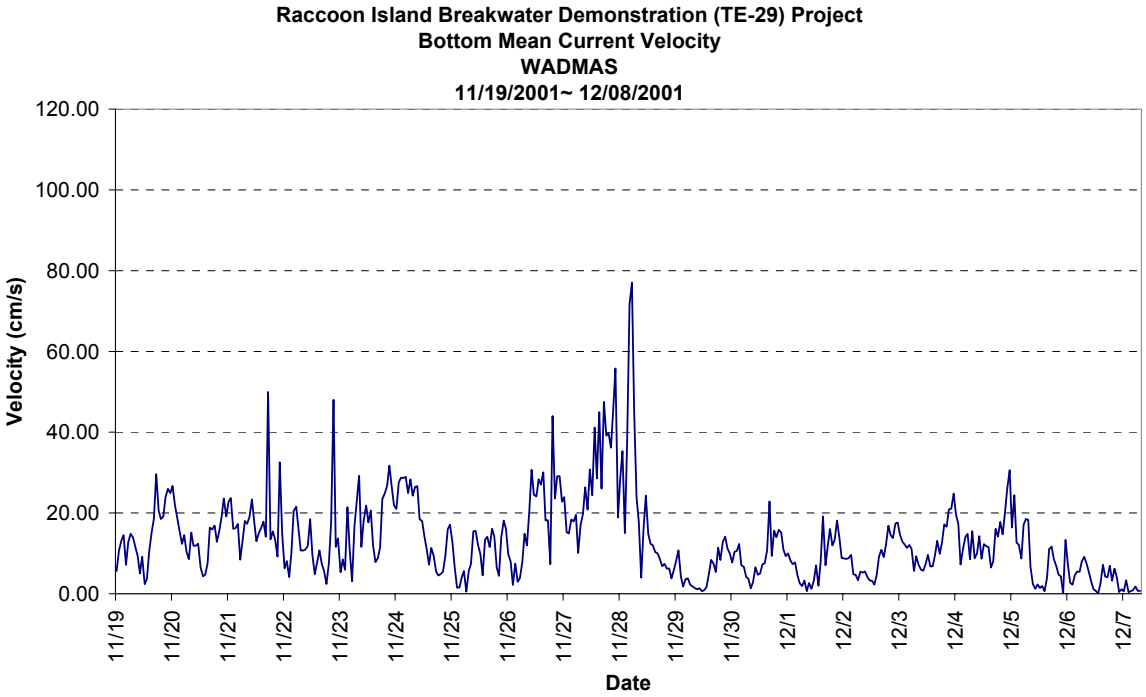

Figure 28. Time series of bottom current velocity at D6.

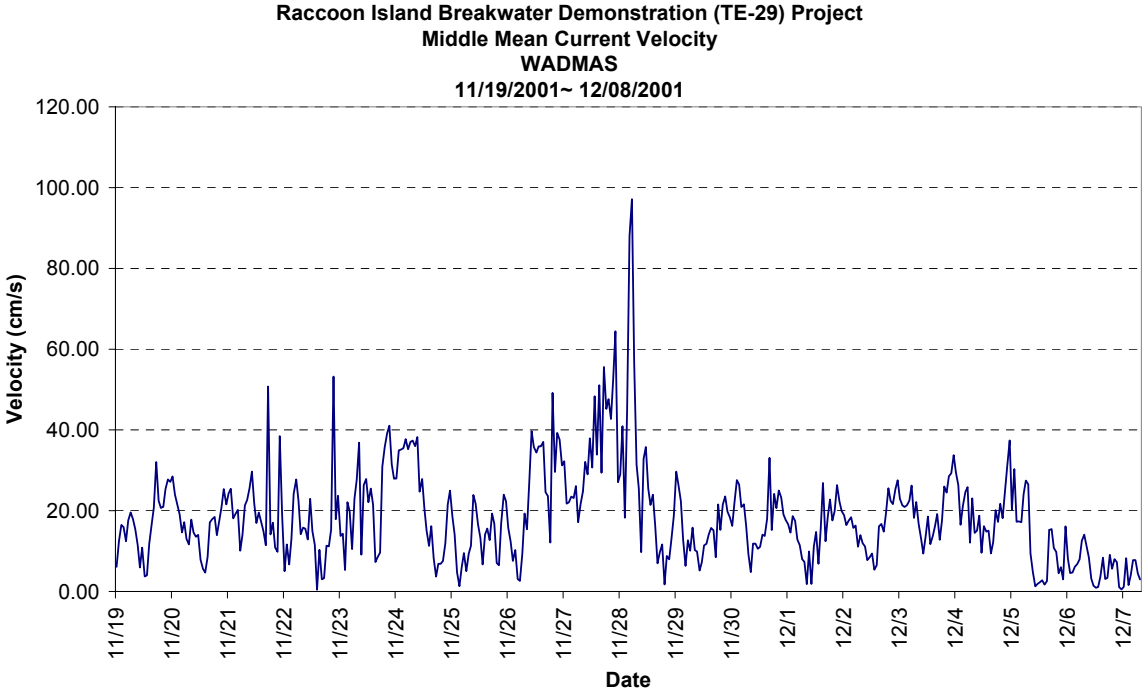

Figure 29. Time series of middle current velocity at D6.

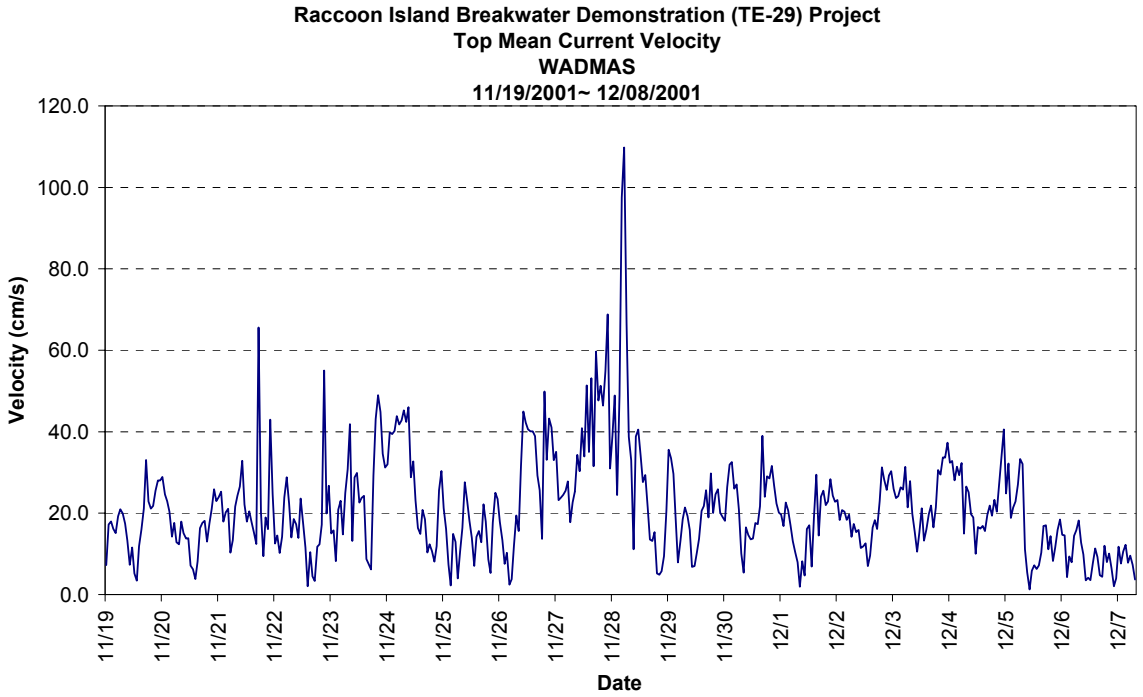

Figure 30. Time series of top current velocity at D6.

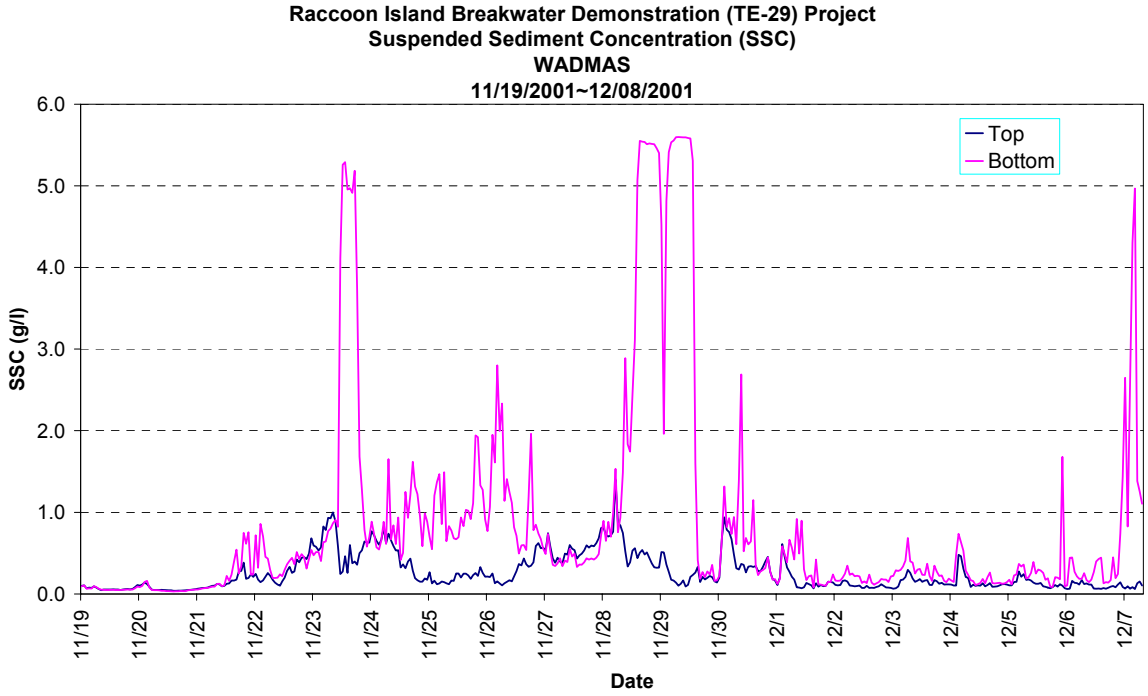

Figure 31. Time series of suspended sediment concentration at D6.

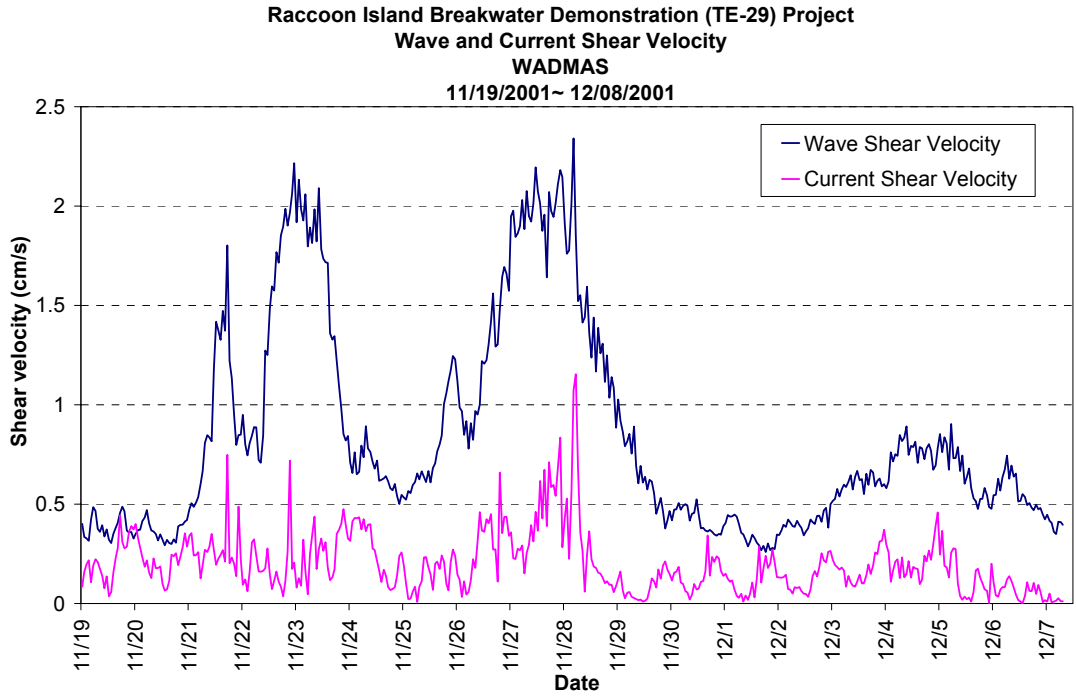

Figure 32. Time series of wave and current bed shear velocities at D6.

In Figures 33–36 sediment transport rates are presented for cross-shore (north and south) and longshore (east and west) components using bottom and top mounted OBS sensors. The cross-shore distribution obtained from the bottom OBS shows a net flux onshore throughout much of the time series with the exception of during the two stronger events when offshore transport peaks at 1.0 kg/m^2/s (0.2048 lb/ft^2/s). During the earlier storm (11/24/01), a maximum cross-shore transport rate of 0.8 kg/m^2/s (0.1639 lb/ft^2/s) was calculated. The longshore distribution is more symmetrical than the cross-shore, however a net flux to the west is generally apparent. Eastward transport of some 0.5 kg/m^2/s (0.1024 lb/ft^2/s) occurred during the first storm. A similar value is noted moving to the east during the second storm, followed by net flux to the west over a longer duration as the storm waned. In order to investigate phase coupling of both cross-shore and longshore transport with storm phase, significant wave height was superimposed on transport rates as shown in Figures 37 and 38 for the bottom OBS. Wave height increases to a maximum of 0.7 m (2.3 ft) and sediment transport is onshore. During this phase winds are from the south. Wind direction becomes northerly and waves are quickly attenuated resulting in a brief duration of sediment transport offshore. Waves begin to

increase in height as winds veer to the south and during which sediment transport is onshore. Onshore transport continues even when winds veer to the north as the post-frontal phase of the event occurs and wave energy decreases from 0.95 m (3.11 ft) to 0.2 m (0.66 ft). Onshore flux is evident until the waves are attenuated almost completely during the next wind veering event and winds blow from the north. As wave energy decreases and fair-weather waves prevail the significantly reduced flux of sediment is predominantly onshore. The longshore flux of sediment is predominantly westward during these events although two pronounced periods of eastward transport do occur during the increasing wave energy period as southerly winds veer to the north. The relationship between wind direction and wave energy is shown in Figure 39.

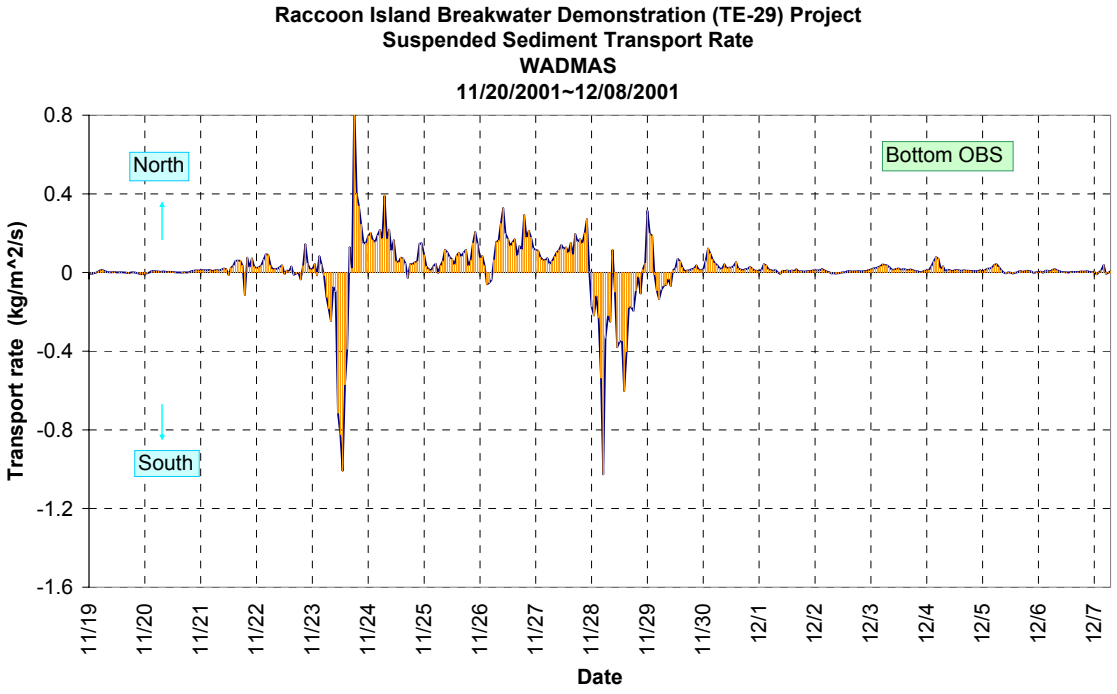

Figure 33. Time series of bottom cross shore suspended sediment transport rate at D6.

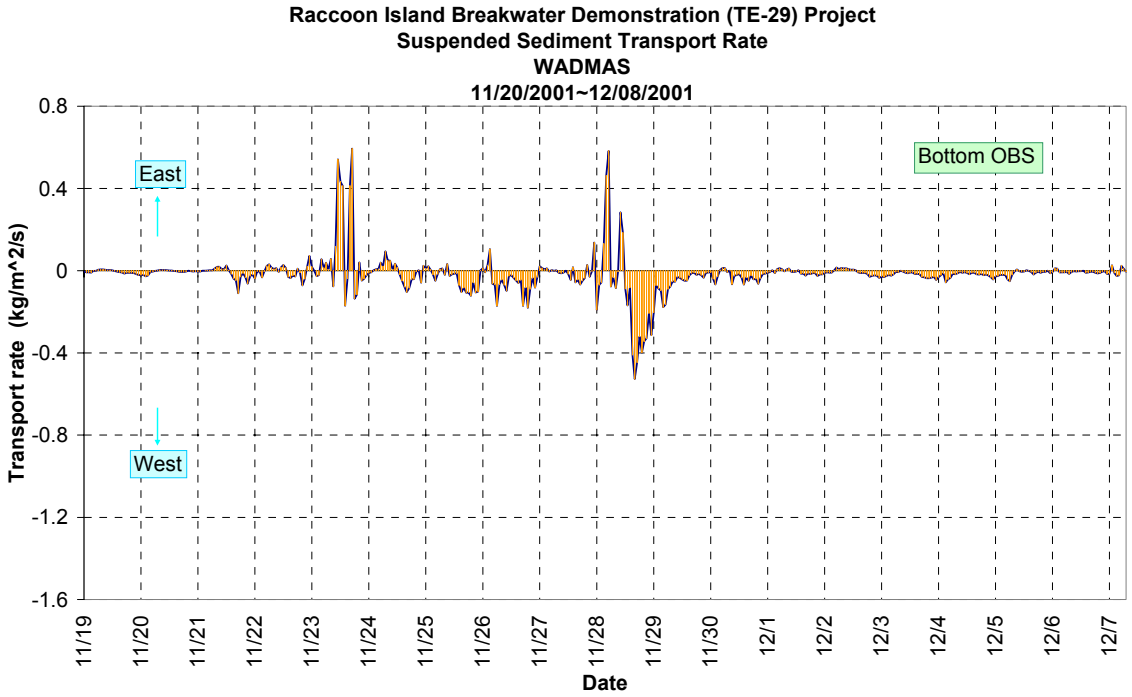

Figure 34. Time series of bottom long shore suspended sediment transport rate at D6.

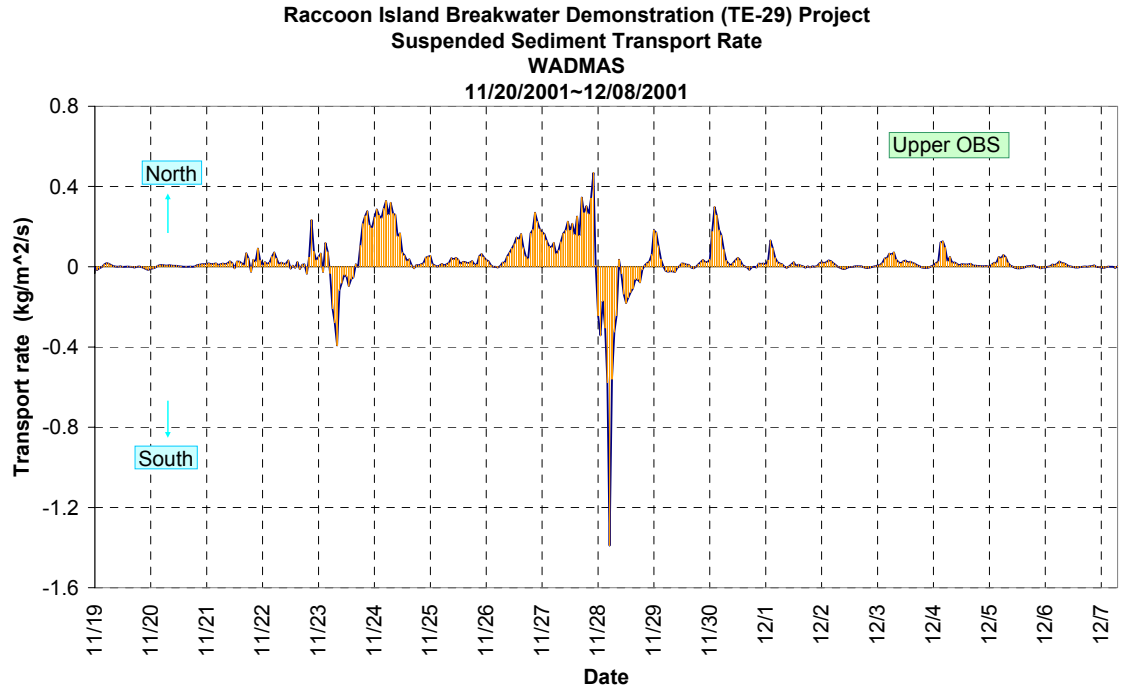

Figure 35. Time series of upper cross shore suspended sediment transport rate at D6.

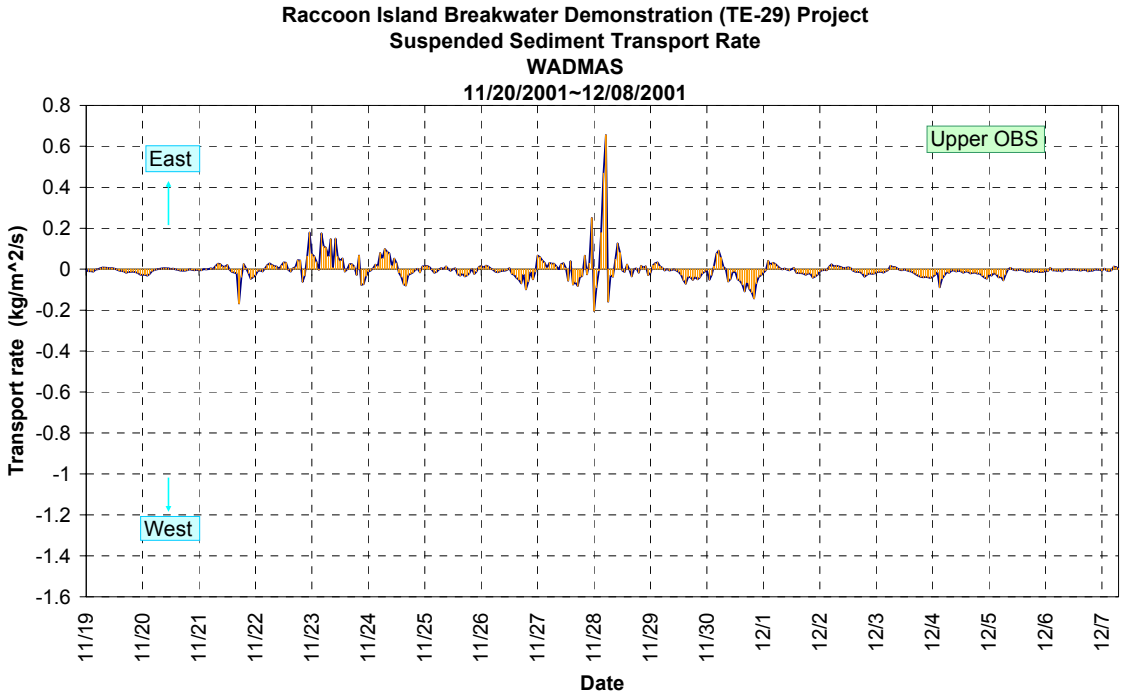

Figure 36. Time series of upper long shore suspended sediment transport rate at D6.

TRANSPORT DURING TWO TROPICAL CYCLONES

In late September and early October 2002, Raccoon Island was impacted by two tropical cyclones; Tropical Storm Isidore (September) and Hurricane Lili (October). The WADMAS was deployed at D7 prior to TS Isidore and successfully measured sediment transport during both events. As shown on Figure 40, peak suspended transport rates approximated 2.3 g/l for several days during Isidore. The storm's path was slightly east of Raccoon Island (Stone et al., 2003) and the system was slow moving, occupying much of the Gulf. Thus, the duration of high sediment resuspension was long, approximating 6 days. During Lili suspended sediment concentrations were lower and peaked at around 1.75 g/l. The duration of increased suspension was less than that of Isidore and approximated 2 days. Lili was an extremely fast moving system that made landfall over 150 km (93.2 mile) west of Raccoon Island. The distribution of sediment in both the

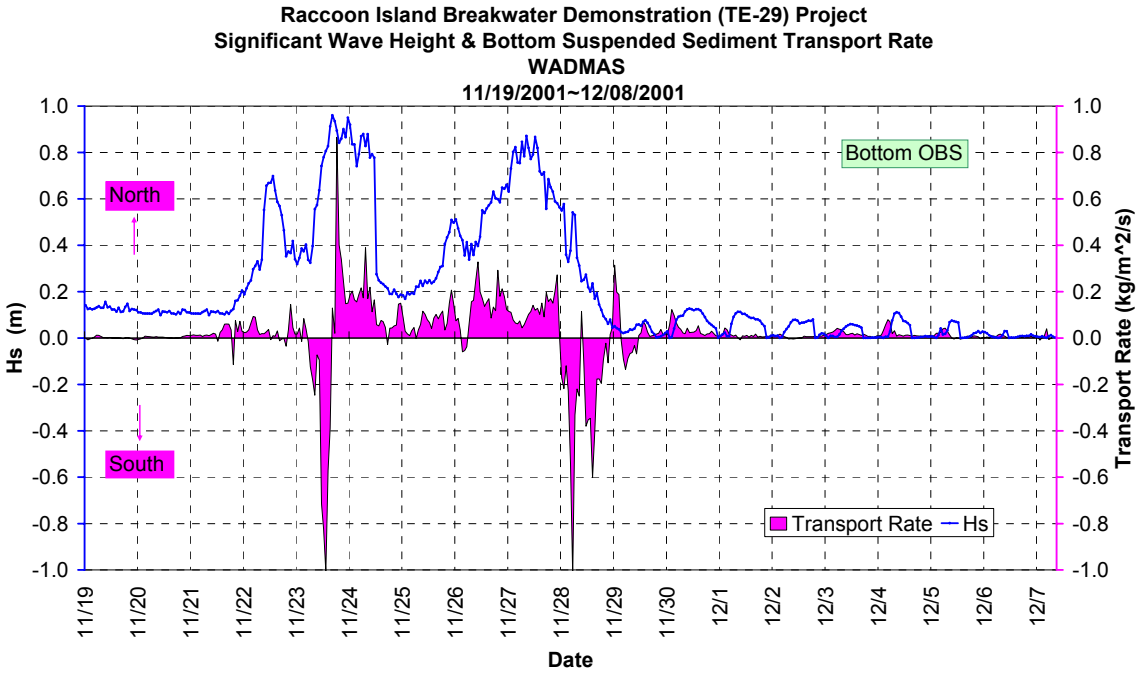

Figure 37. Time series of significant wave height and cross-shore suspended sediment transport rate at D6.

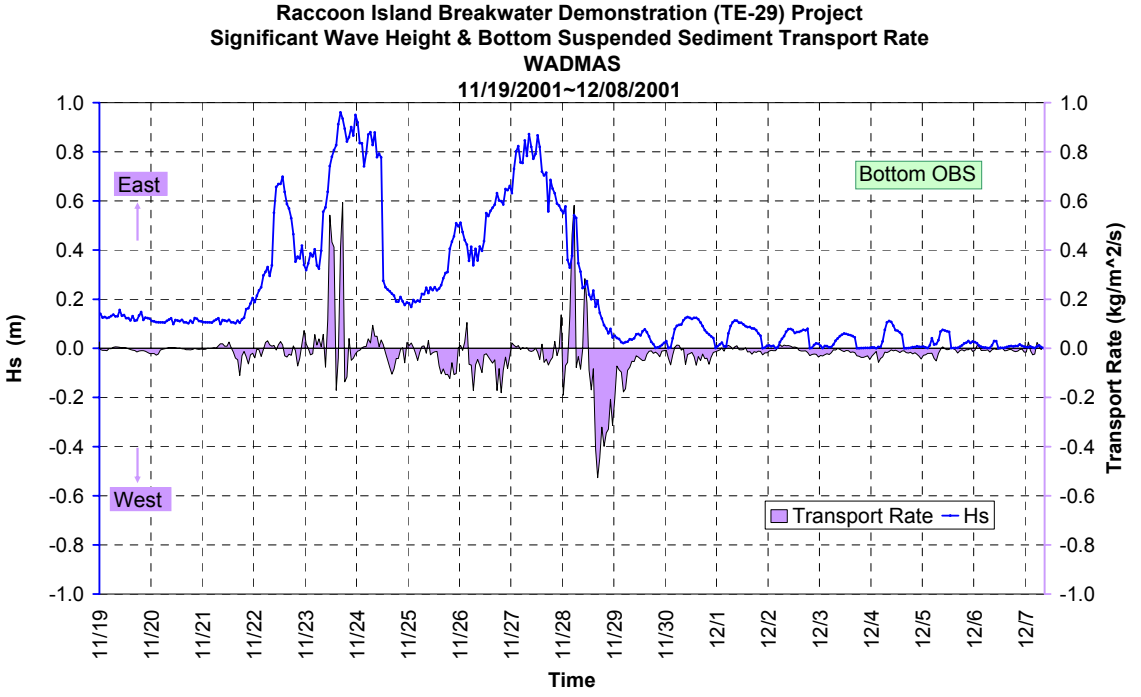

Figure 38. Time series of significant wave height and longshore suspended sediment transport rate at D6.

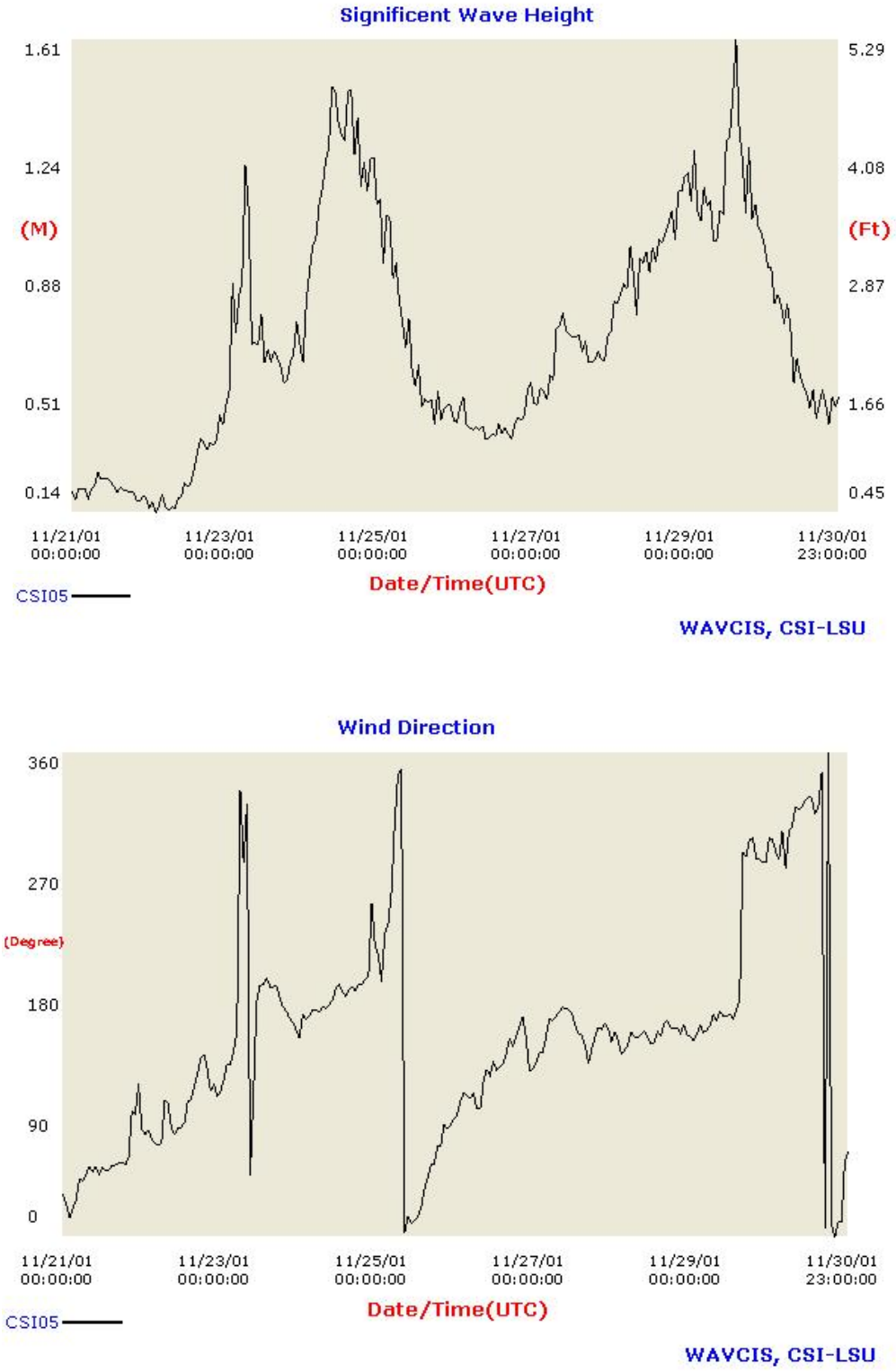

Figure 39. Wave height and wind relationship during three frontal passages at CSI 5.

cross shore and longshore directions is shown in Figures 41 and 42. The data show that net flux was to the north for virtually all of the 6 day period during Isidore reaching a maximum of near 100 kg/m^2/s (20.48 lb/ft^2/s) during the earlier part of the storm. Some 30 kg/m^2/s (6.14 lb/ft^2/s) was measured moving offshore as the system moved onshore and currents were directed southward. With the exception of a short duration at the end of the storm, net longshore flux was westward during Isidore and reached a maximum of 160 kg/m^2/s (32.77 lb/ft^2/s). Eastward transport approached 50 kg/m^2/s (10.24 lb/ft^2/s). Net flux was considerably less during Lili but again, a net westward flux is evident in the data with a maximum of 100 kg/m^2/s (20.48 lb/ft^2/s) being attained. A short lived pulse of sediment flux to the east occurred towards the end of the storm approximating 20 kg/m^2/s (4.10 lb/ft^2/s) (Figure 42).

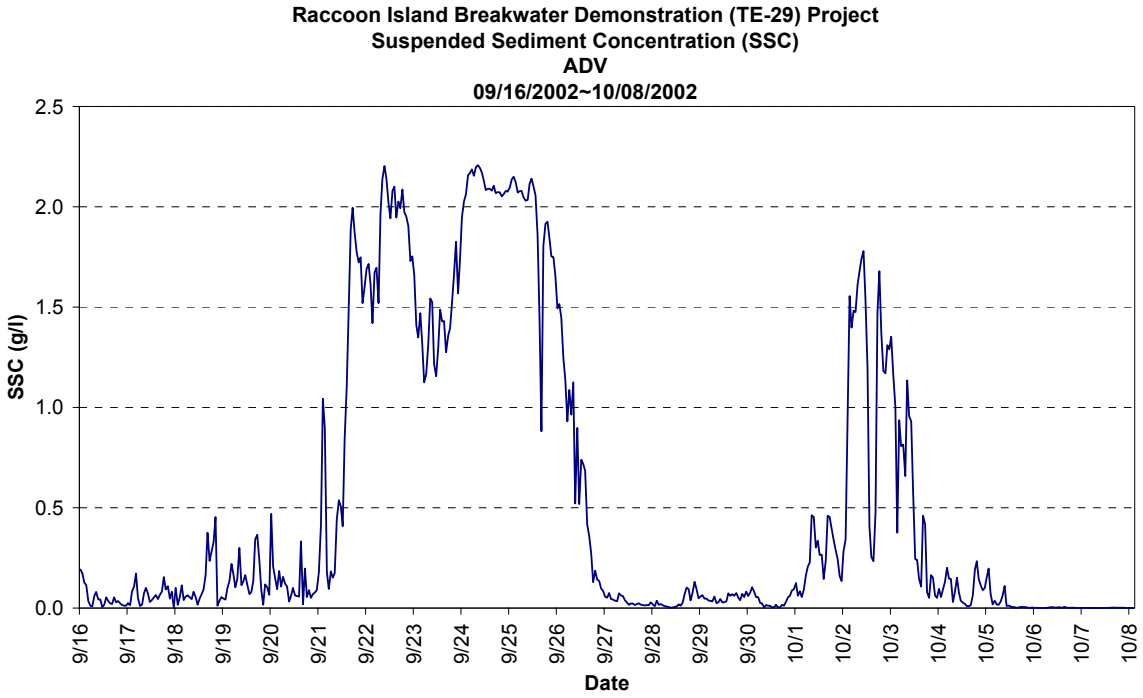

Figure 40. Time series of suspended sediment concentration at D7.

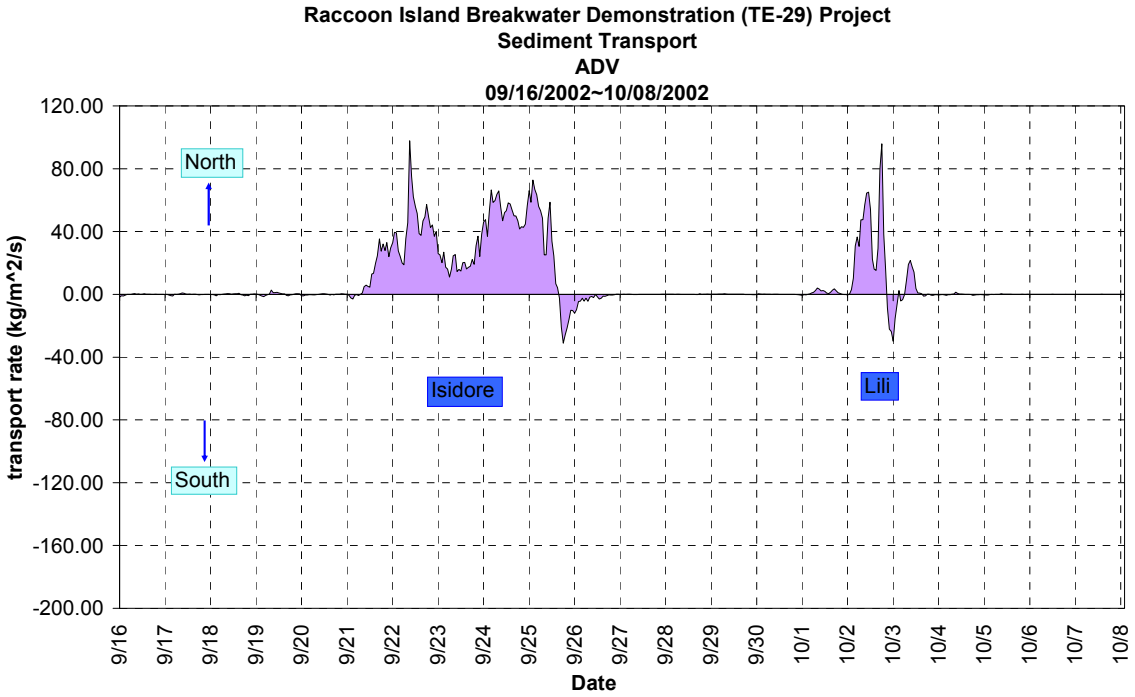

Figure 41. Time series of long shore suspended sediment transport rate at D7.

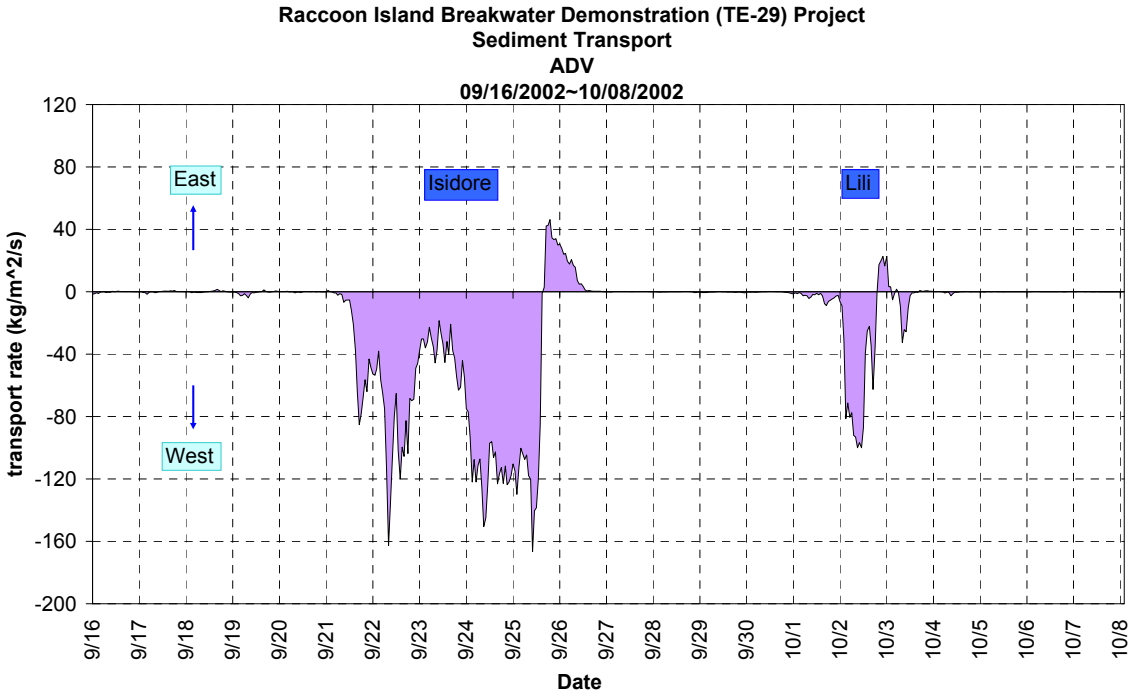

Figure 42. Time series of cross shore suspended sediment transport rate at D7.

SURFACE SEDIMENT CHARACTERISTICS

The locations of 80 sediment samples extracted from the study site are shown in Figure 43. The material sampled was generally orthoquartzitic with some silts and clays apparent. Granulometric data (Table 3) show the median particle diameter ranging from 0.01 (coarse silt) to 0.21 mm (fine sand) for the surface sediment. Figure 44 shows the mean size distribution (using the Folk and Ward, 1957 method). It is evident that sediment fines from east to west and the coarsest material is found in the vicinity of breakwaters 0-3. Sediment is very well sorted in the vicinity of the breakwaters and offshore on the shoal (Figure 45). To the west, sorting becomes moderate with patches of very poorly sorted sediment evident in a few locations. Kurtosis (Figure 46) is mesokurtic to leptokurtic although very leptokurtic sediments occur in a few spots.

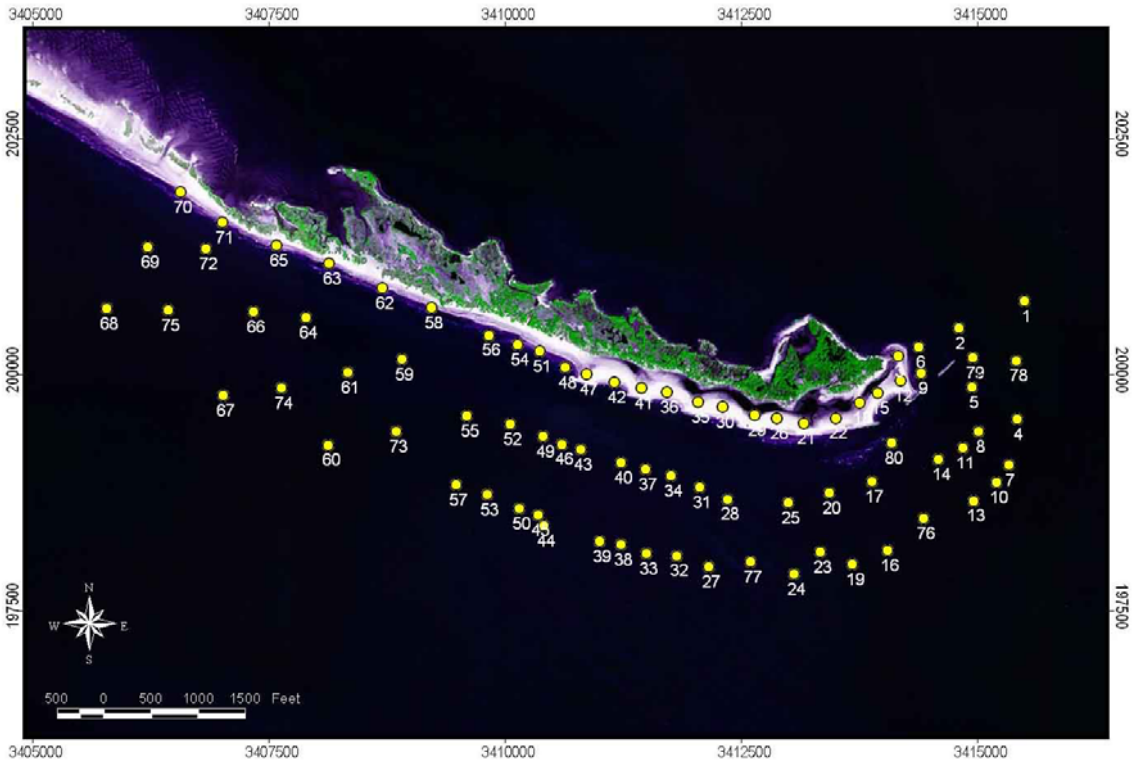

Figure 43. Location of bottom grab samples used for granulometric characterization.

Table 3. Summary on grain-size analysis of surface samples.

Sample No.	Mean Grain Size (mm)	Nomenclature (Folk & Ward, 1957)	Sample No.	Mean Grain Size (mm)	Nomenclature (Folk & Ward, 1957)
1	0.1148	Very fine sand	41	0.1528	Fine sand
2	0.1765	Fine sand	42	0.1568	Fine sand
3	0.1679	Fine sand	43	0.0301	Coarse silt
4	0.1638	Fine sand	44	0.1076	Very Fine sand
5	0.1374	Fine sand	45	0.0516	Very coarse silt
6	0.1920	Fine sand	46	0.1155	Very Fine sand
7	0.1696	Fine sand	47	0.1614	Fine sand
8	0.1273	Fine sand	48	0.1633	Fine sand
9	0.1716	Fine sand	49	0.1222	Very Fine sand
10	0.1303	Fine sand	50	0.2085	Fine sand
11	0.1692	Fine sand	51	0.1443	Fine sand
12	0.2080	Fine sand	52	0.1311	Fine sand
13	0.1507	Fine sand	53	0.0982	Fine sand
14	0.1725	Fine sand	54	0.1658	Fine sand
15	0.1952	Fine sand	55	0.1141	Very Fine sand
16	0.1532	Fine sand	56	0.1566	Fine sand
17	0.1864	Fine sand	57	0.0960	Very Fine sand
18	0.1904	Fine sand	58	0.0830	Very Fine sand
19	0.1547	Fine sand	59	0.1243	Very Fine sand
20	0.1601	Fine sand	60	0.1043	Very Fine sand
21	0.1637	Fine sand	61	0.1148	Very Fine sand
22	0.2104	Fine sand	62	0.1194	Very Fine sand
23	0.1475	Fine sand	63	0.1531	Fine sand
24	0.1449	Fine sand	64	0.1270	Fine sand
25	0.1511	Fine sand	65	0.1524	Fine sand
26	0.1727	Fine sand	66	0.1236	Very Fine sand
27	0.0618	Very coarse silt	67	0.1144	Very Fine sand
28	0.0257	Coarse silt	68	0.1108	Very Fine sand
29	0.1572	Fine sand	69	0.1212	Very Fine sand
30	0.1717	Fine sand	70	0.1676	Fine sand
31	0.1352	Fine sand	71	0.1632	Fine sand
32	0.0180	Coarse silt	72	0.1153	Very Fine sand
33	0.0380	Very coarse silt	73	0.1000	Very Fine sand
34	0.0402	Very coarse silt	74	0.0993	Very Fine sand
35	0.1548	Fine sand	75	0.1090	Very Fine sand
36	0.1666	Fine sand	76	0.1664	Fine sand
37	0.0423	Very coarse silt	77	0.0111	Medium silt
38	0.0457	Very coarse silt	78	0.1221	Very Fine sand
39	0.0485	Very coarse silt	79	0.1742	Fine sand
40	0.0237	Coarse silt	80	0.0842	Very Fine sand

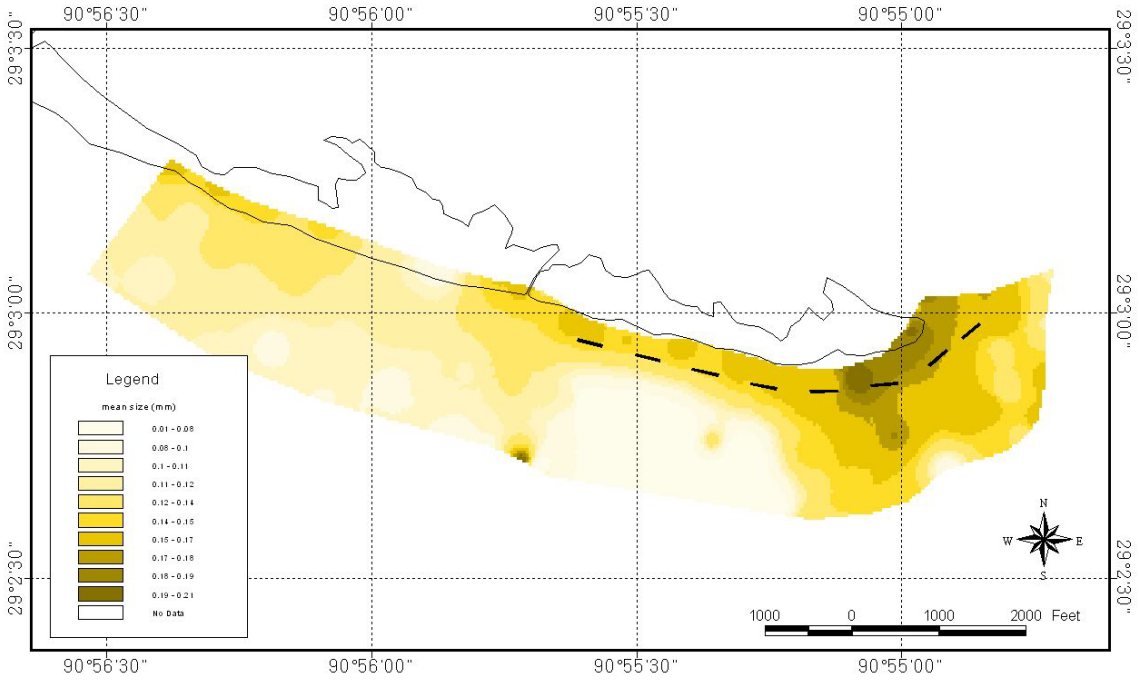

Figure 44. Mean grain-size distribution.

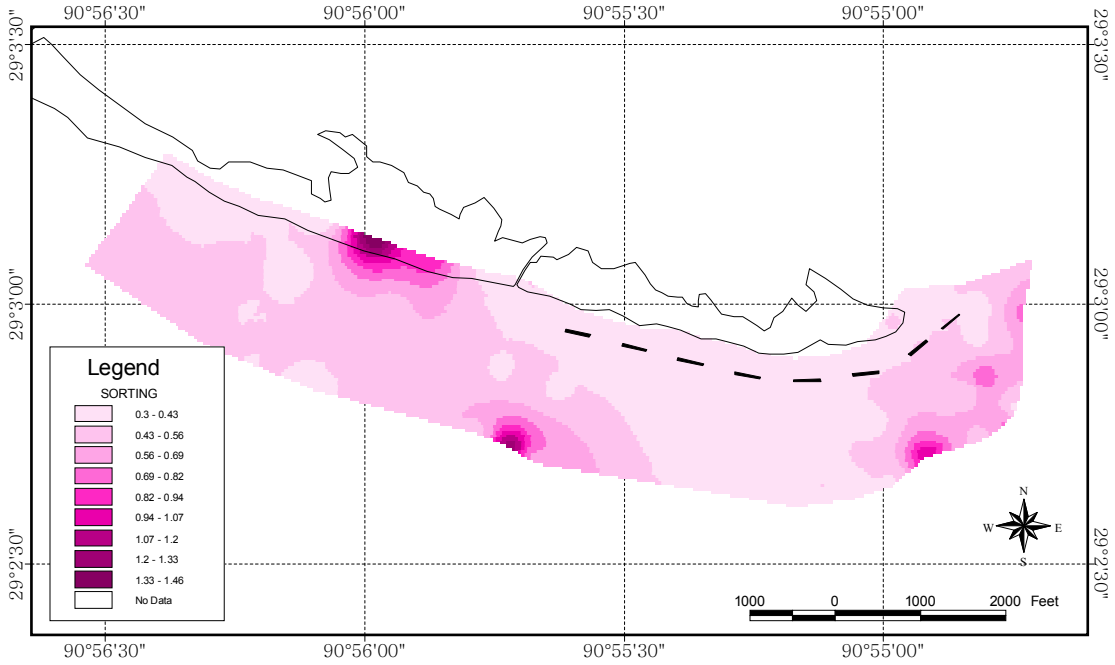

Figure 45. Sorting distribution.

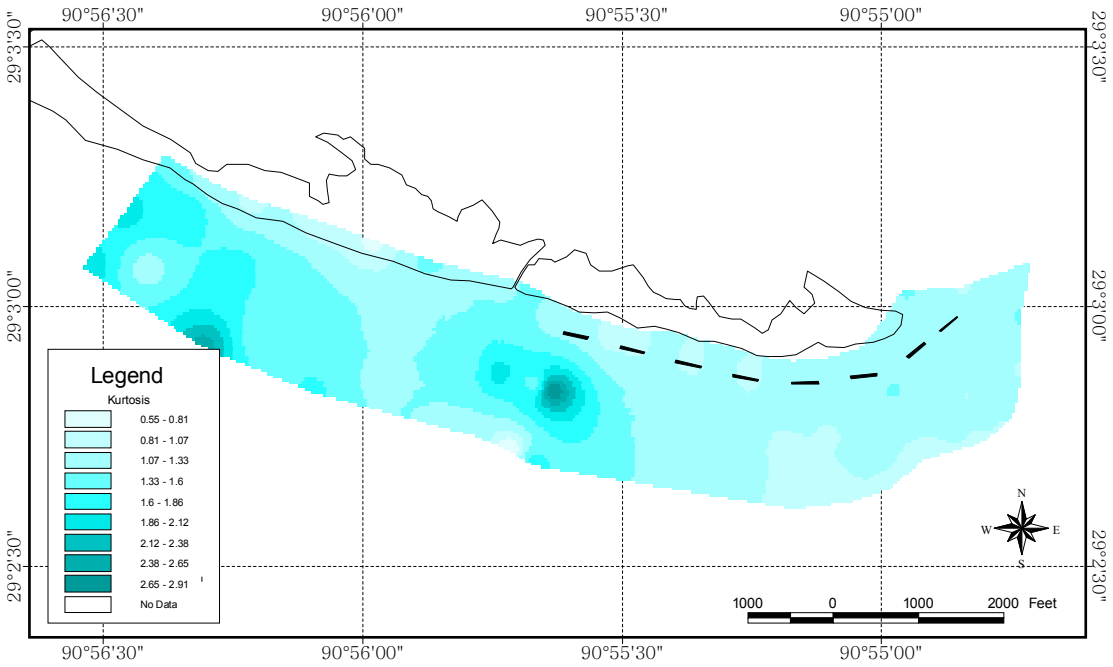

Figure 46. Kurtosis distribution.

SUB-SURFACE LITHOLOGY AND GRANULOMETRY

Five vibracores were extracted from the subsurface and three of these were on the shoal fronting the breakwaters (Figure 1 for location). The remaining two were extracted from the nearshore along the central and western flanks of Raccoon Island. The cores are referred to as RIC 1, RIC 2, RIC 4, RIC 5 and RIC 6. Using RIC 1 as an example, a photograph of the core and lithological log are presented in Figures 47 and 48. The remaining core photographs and logs are shown in the appendix. The thickness of respective layers in all cores is shown in Figure 49 along with relative sediment type distribution. More detailed granulometry is shown in Table 3.

RIC-1

This vibracore is 3.47 m (11.38 ft) in length and penetrated the sand wedge in the shoal area reaching the underlying mud. The core was divided into 8 layers according to grain-size (Table 4) and the contents of shell and organics, and numbered as 1 to 8 from top to bottom (Figure 51).

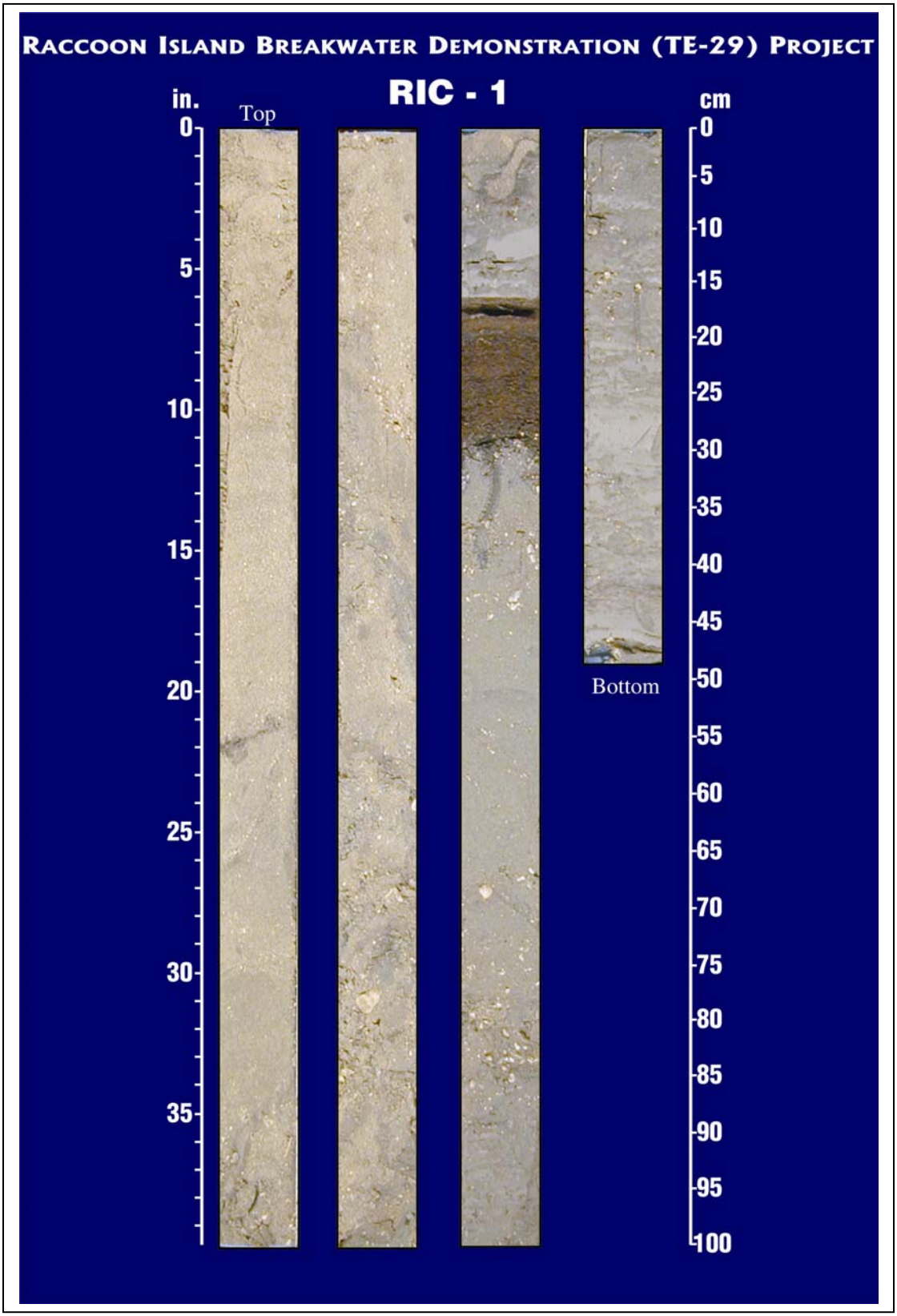

Figure 47. Photograph of core RIC 1 taken from the shoal seaward of the Raccoon Island breakwaters.

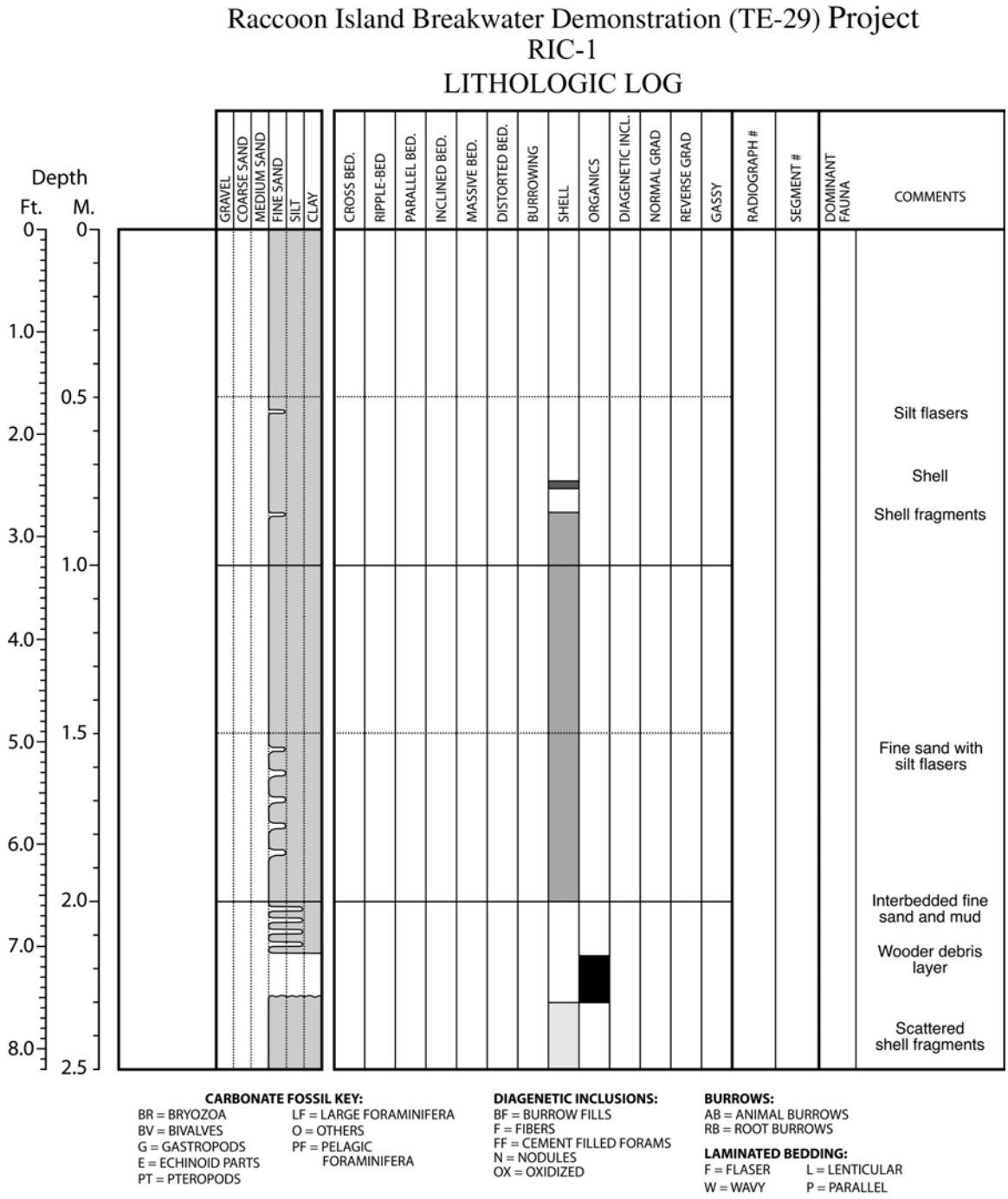

Figure 48. Lithological log of core RIC 1 taken from the shoal seaward of the Raccoon Island breakwaters.

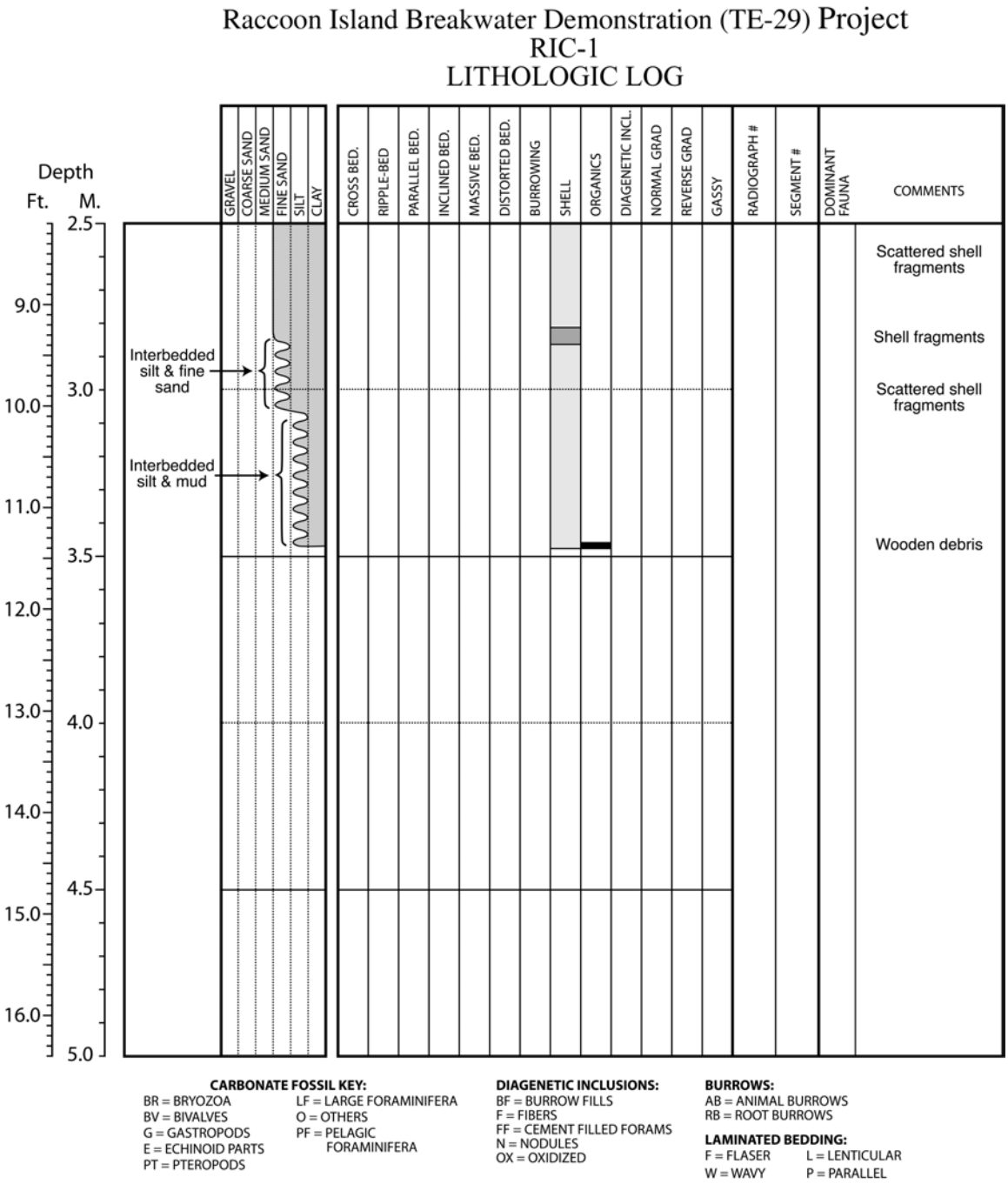

Figure 48 (continued). Lithological log of core RIC 1 taken from the shoal seaward of the Raccoon Island breakwaters.

Raccoon Island Breakwater Demonstration (TE-29) Project
Vibracore Sections

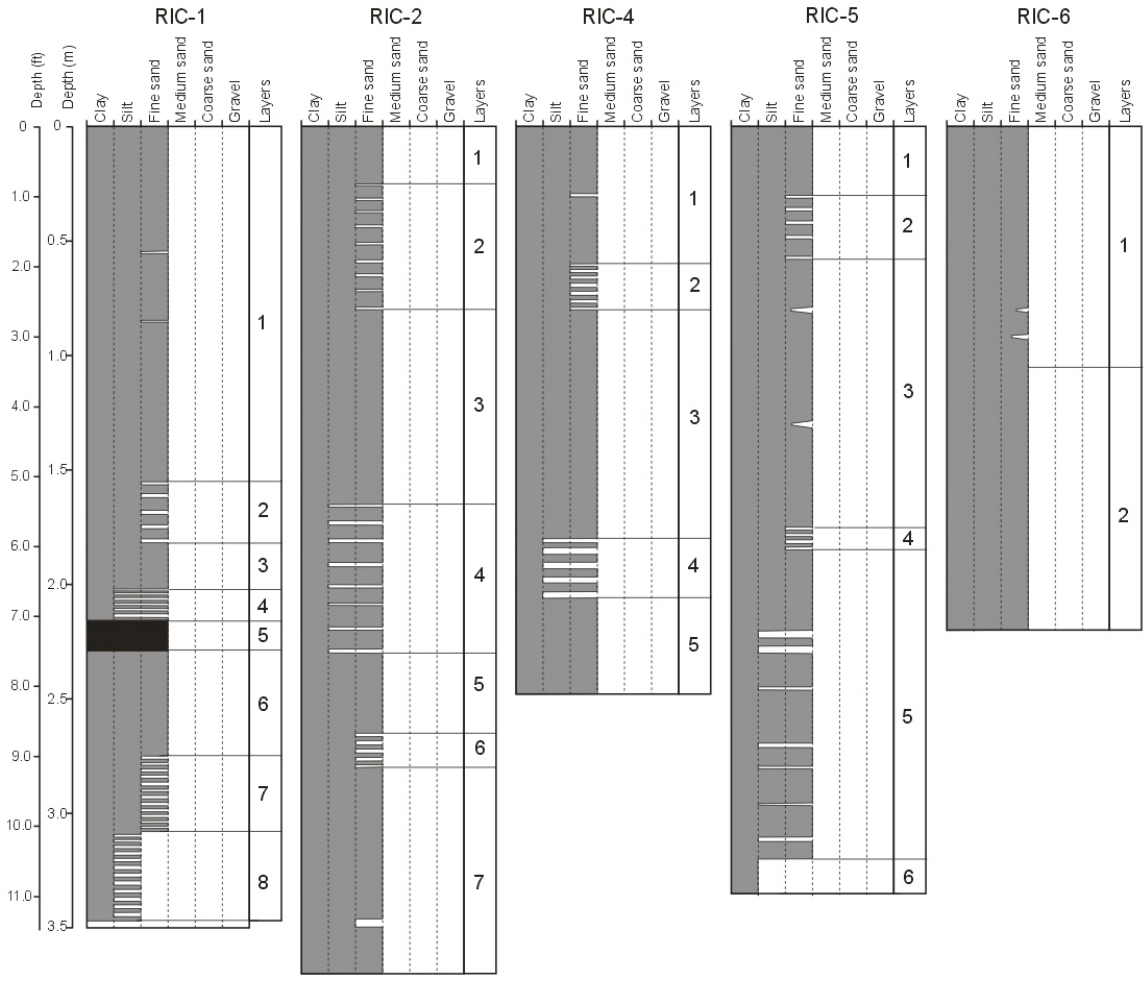

Figure 49. Vibracore sections. The relative distribution of sand, silt and clay is shown for each layer. Numbers show the respective layers defined according to grain-size, shell, and organic material present in the core.

Table 4. Grain-size summaries.

Core	Sample depth (ft/m)	Mean grain-size (mm)	Nomenclature (Folk & Ward, 1957)	Core	Sample depth (ft/m)	Mean grain-size (mm)	Nomenclature (Folk & Ward, 1957)
RIC-1	0.00/0.00	0.1630	Fine sand	RIC-2	0.00/0.00	0.1895	Fine sand
	1.64/0.50	0.1619	Fine sand		1.64/0.50	0.1583	Fine sand
	3.28/1.00	0.1660	Fine sand		3.28/1.00	0.1607	Fine sand
	4.92/1.50	0.1655	Fine sand		4.92/1.50	0.1382	Fine sand
	6.56/2.00	0.0948	Very fine sand		5.74/1.75	0.1273	Fine sand
	6.76/2.06	0.1364	Fine sand		6.10/1.86	0.0123	Medium silt
	6.92/2.11	0.0055	Fine silt		7.71/2.35	0.1520	Fine sand
	9.02/2.75	0.1528	Fine sand		9.02/2.75	0.0043	Fine silt
	9.51/2.90	0.0025	Very fine silt		10.17/3.10	0.1556	Fine sand
	11.15/3.40	0.0090	Medium silt		11.32/3.45	0.0292	Coarse silt
					11.65/3.55	0.1555	Fine sand
RIC-4	0.00/0.00	0.1331	Fine sand	RIC-5	0.00/0.00	0.1233	Very fine sand
	1.64/0.50	0.1284	Fine sand		1.21/0.37	0.0723	Very fine sand
	3.28/1.00	0.1422	Fine sand		1.64/0.50	0.1249	Very fine sand
	5.25/1.6	0.1322	Fine sand		3.28/1.00	0.0919	Very fine sand
	6.23/1.90	0.0073	Fine silt		4.92/1.50	0.1364	Fine sand
	6.43/1.96	0.1072	Very fine sand		6.56/2.00	0.1249	Very fine sand
	7.55/2.30	0.1780	Fine sand		7.38/2.25	0.0094	Medium silt
RIC-6	0.00/0.00	0.1181	Very fine sand		7.74/2.36	0.1526	Fine sand
	1.64/0.50	0.1158	Very fine sand		8.53/2.60	0.1646	Fine sand
	3.28/1.00	0.1379	Fine sand		9.51/2.90	0.1258	Fine sand
	4.92/1.50	0.1502	Fine sand		10.33/3.15	0.1514	Fine sand
	6.56/2.00	0.1512	Fine sand		10.66/3.25	0.0328	Very coarse silt

Layer 1, is composed of fine sands with a few silt flasers occurring at horizons of about 0.55 m (1.80 ft) and 0.85 m (2.79 ft) downcore. There was a shell found at about 0.7 m (2.30 ft) and shell fragments from 0.85 m (2.79 ft) to the bottom of this layer.

Layer 2 is composed fine sands with more silt flasers. There were shell fragments in this layer.

Layer 3 is composed of fine sand, with shell fragments.

Layer 4 is composed of interbeded fine sand and mud.

Layer 5 is completely composed of wooden debris.

Layer 6 is composed of fine sands, with scattered shell fragments throughout.

Layer 7 is composed of interbeded fine sands and silt, with scattered shell fragments.

Layer 8 is composed of interbeded silt and mud, with scattered shell fragments, and wooden debris at the bottom of the layer.

RIC-2

This vibracore is 3.7 m (12.14 ft) in length, and did not penetrate the sand wedge comprising the shoal. Seven layers were identified.

Layer 1, is composed of fine sands.

Layer 2, is composed of fine sands with silt flasers.

Layer 3, is composed of fine sands, with shell fragments, and a piece of wood at the top of this layer.

Layer 4, is composed of fine sands with mud intercalations, with scattered shell fragments. A thin shell fragments layer was found at the horizon of about 1.85 m (6.07 ft) deep, and a piece of wood at about 2.05 m (6.73 ft) deep.

Layer 5, is composed of fine sands, with scattered shell fragments throughout the entire layer, and an abundance of shell fragments at the bottom of it.

Layer 6, is composed interbeded fine sands and silts.

Layer 7, is composed of fine sands, wood particles were found at about 3.40 m (11.15 ft), on the top of the silt flaser.

RIC-4

This vibracore is 2.49 m (8.17 ft) in length, and was obtained on the western flank of the shoal fronting the breakwaters. The core did not penetrate the entire thickness of the shoal. The core was divided into 5 layers according to grain-size (Table 3) and the contents of shell and organics, and numbered as 1 to 5 from top to bottom (Figure 49).

Layer 1, is composed of fine sands.

Layer 2, is composed of interbeded fine sands and silts, shell fragments and wooden fragments were found at the top of this layer.

Layer 3, is composed of fine sands. Large shell fragments were found at the horizon of 1.3 m (4.27 ft), and scattered shell fragments were also found in this layer.

Layer 4, is composed of interbeded fine sands and muds, shell fragments were also found in the upper part of this layer.

Layer 5, is composed of fine sands, with shell fragments in the upper portion with scattered shell fragments in the lower section.

RIC-5

This vibracore is 3.32 m (10.89 ft) in length and is located along the western flank of Raccoon Island. The core penetrated the sand veneer to the underlying mud. The core was divided into 6 layers.

Layer 1, is composed of fine sands.

Layer 2, is composed of fine sands, with silt flasers.

Layer 3, is composed of fine sands, with two silt flasers. Shell fragments were found at a horizon 1.2 m (3.94 ft) down-core, and wood debris was found at two horizons some 1.3 (4.27 ft) m and 1.4 m (4.59 ft) down-core.

Layer 4, is composed of interbeded fine sands and silts.

Layer 5, is composed of fine sands, with mud flasers. Shell fragments were found from 2.4 m to 2.72 m (7.87 to 8.92 ft) down-core and 3.0 to 3.2 m (9.84 to 10.50 ft) respectively. A shell fragment layer was found at a horizon located 3.22 – 3.25 m (10.56 – 10.66 ft) down-core, and wooden debris was found at a second horizon located 1.87 – 1.89 m (6.14 – 6.20 ft) down-core.

Layer 6, is composed of mud.

RIC-6

This vibracore is 2.2 m (7.22 ft) in length, and was extracted from the nearshore approximately halfway along the island. The core did not penetrate the sand veneer. The core was divided into 2 layers.

Layer 1, is composed of fine sands, with two silt flasers, shell was found at about 0.7 m (2.30 ft) down-core.

Layer 2, is composed of fine sands, with shell/shell fragments. Wood particles were found at about 1.62 m (5.31 ft) down-core and again at 1.72 – 2.2 m (5.64 – 7.22 ft).

Sand Thickness on the Shoal

Using a sand thickness of 2.85 m (9.35 ft) obtained from vibracore RIC-1, an approximate volume of sand comprising the shoal fronting the breakwaters of 1.22 million cubic meters (1.6 million cubic yards) was calculated. This is a conservative estimate in that the 1.83 m (6 ft) isobath was used to delineate the shoal perimeter (Figure

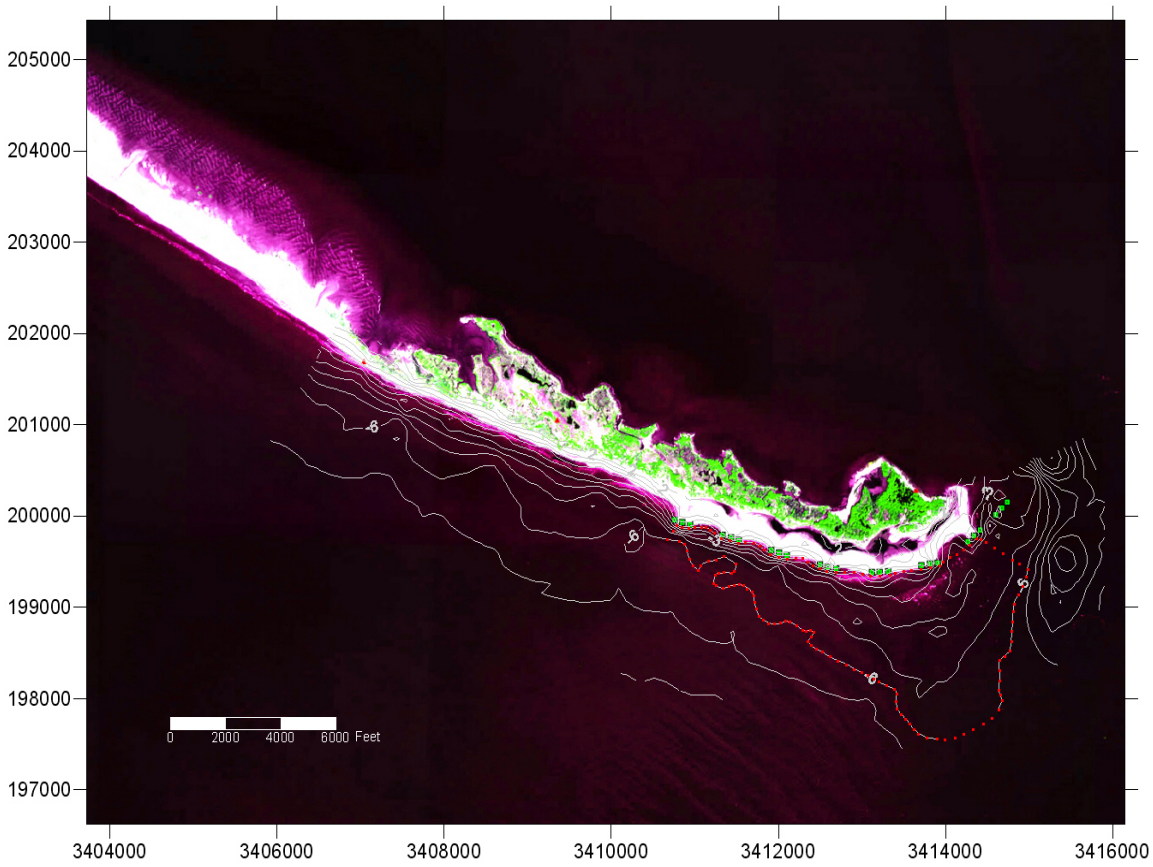

Figure 50. Image of Raccoon Island showing shoal fronting the breakwaters delineated by the 1.83 m (6 ft) isobath. Bathymetry is based on a May 2002 survey (relative to NAVD88).

50). There is additional sand that extends beyond the survey area at least to the 2.13 m (7 ft) isobath.

BATHYMETRY AND TOPOGRAPHY

Initial Survey (12 months)

Since construction in 1997, the breakwaters at Raccoon Island induced dramatic change in sedimentation patterns. Post-construction monitoring of the beach and nearshore was carried out by Stone et al. 1998a, 1998b, 1998c, and 1999. A sequence of aerial photographs and a LIDAR image is presented in Figures 51-54 to provide a summary of morphological response to breakwater construction. Five surveys were conducted between 10/97 and 09/98. Surveys were resumed 11/00, 05/01, 11/01 and

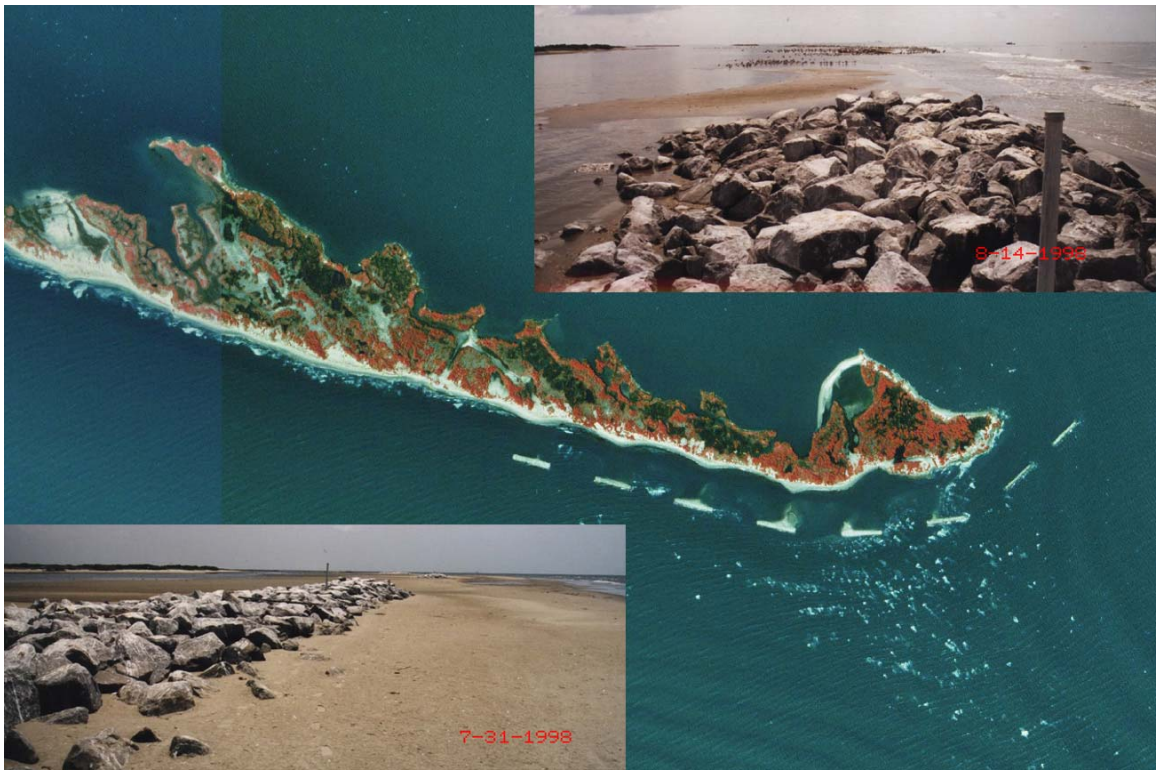

Figure 51. Upper, images of Raccoon Island breakwaters in 1998. Lower, image of breakwaters in 1999.

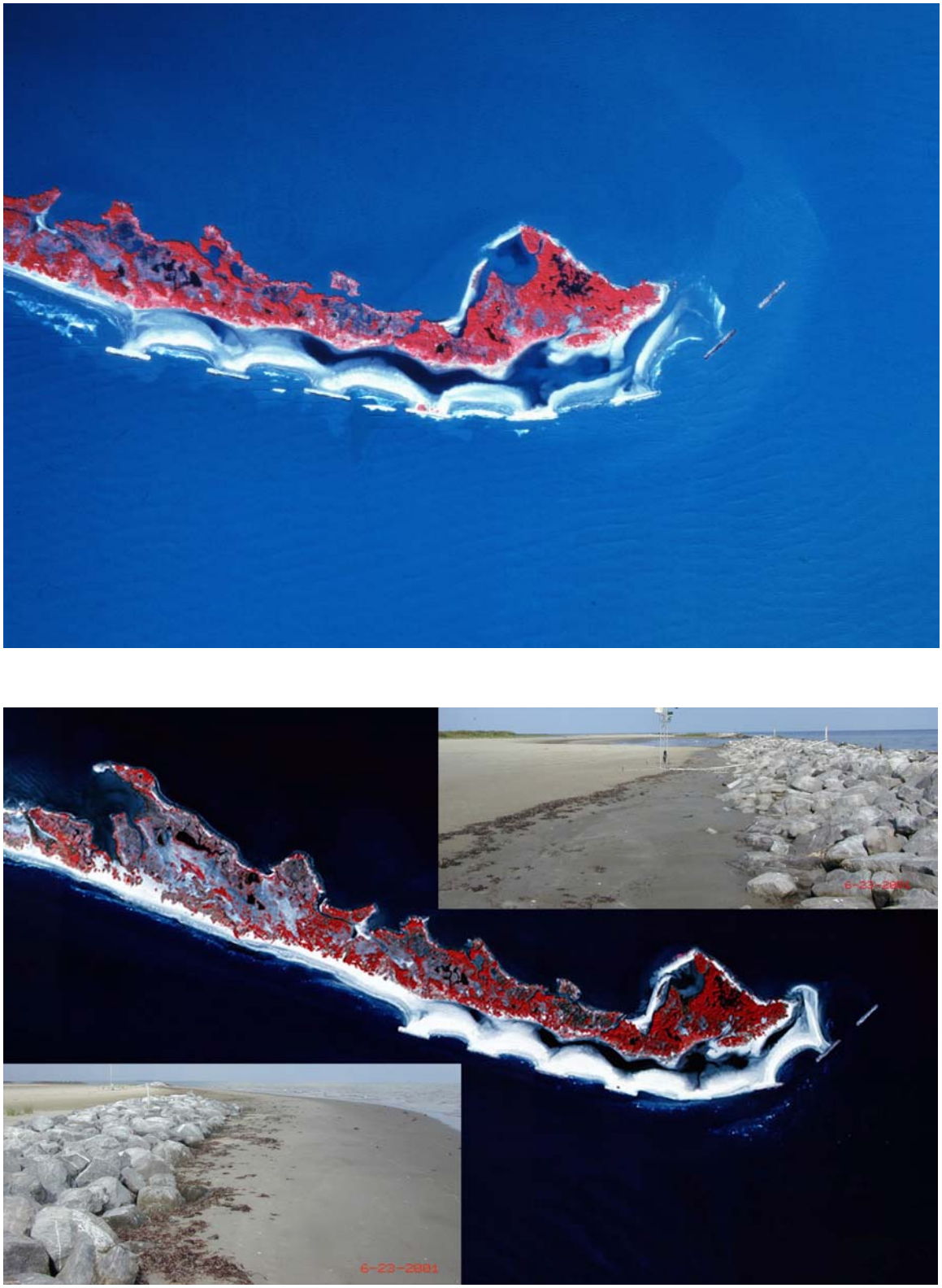

Figure 52. Upper, image of Raccoon Island breakwaters in 2000. Lower, images of breakwaters in 2001.

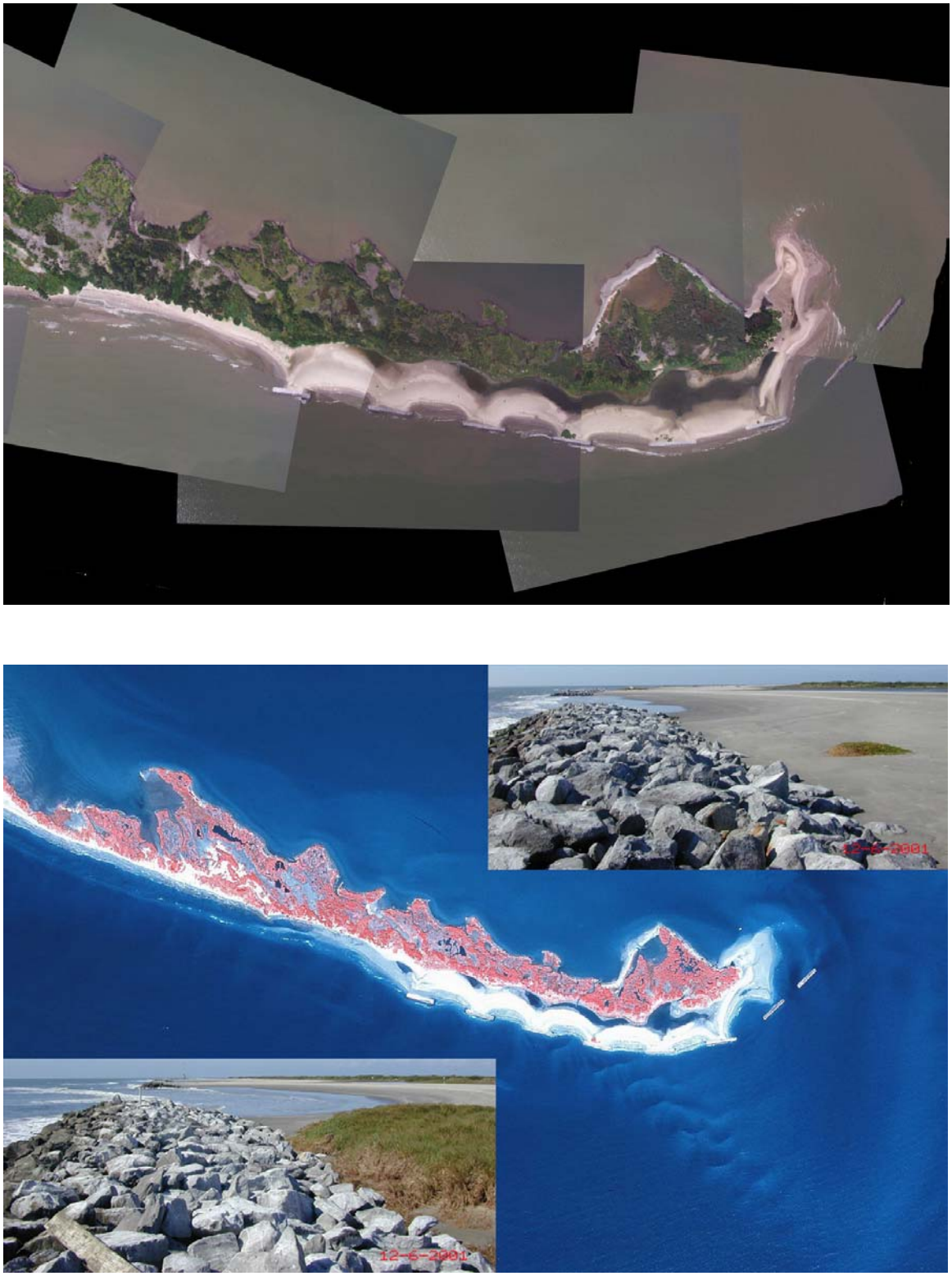

Figure 53. Upper, image of Raccoon Island breakwaters in 2001. Lower, images of breakwaters in late 2001.

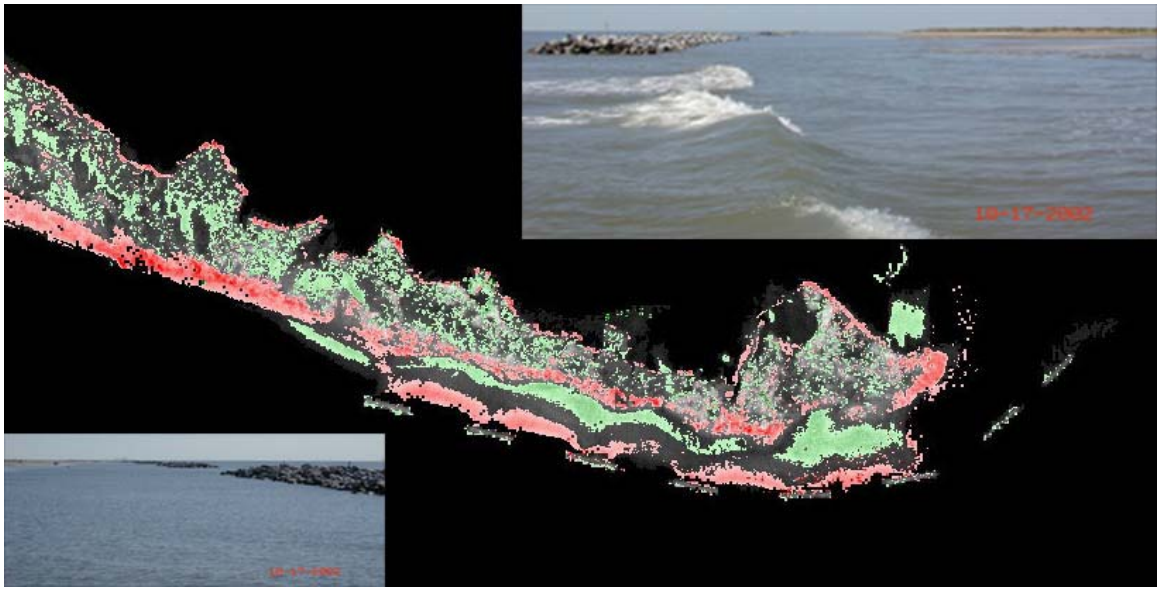

Figure 54. Images of Raccoon Island breakwaters in 2002 after Tropical Storm Isidore and Hurricane Lili. Red color on Lidar image represents erosion and green color represents deposition (Courtesy of Dr. A. Sallenger, USGS).

5/02. The following sequence of changes was observed via data obtained from the initial monitoring effort:

1. Approximately 3 months after breakwater construction, a salient was observed along the Raccoon Island shoreline, resulting in moderate shoreline gain landward of the center of the breakwaters and recession landward of the gaps between the segments (Figure 51);
2. Approximately 6 months post-construction, substantial sand accumulation was measured directly landward of the center of the breakwaters, resulting in an emerged sand body. The development of the salient appeared to have reached quasi-equilibrium (Figure 51);
3. Approximately 9 months post-construction, sand accumulation in the vicinity of the breakwaters continued and extended to the gaps, resulting in a continuous sand body connecting breakwaters 3-6. Substantial amounts of sand emerged Gulfward of the structures. A substantial salient developed landward of the center of the westernmost breakwater, resulting in a local shoreline gain of over 20 meters (65.62 feet) (Figure 51);

4. Approximately 12 months post-construction, sand accumulation between the breakwaters and shoreline continued, while the sand that accumulated Gulfward of the structures was eroded. The salient developed landward of the center of the westernmost segment was almost completely eroded and the shoreline returned to its previous location, indicating that the westernmost salient was temporary and probably related to seasonal wave characteristics.

Compared to conditions during the October 1997 and March 1998 field experiments, significant morphological changes occurred according to the July 1998 and September 1998 measurements. The morphological changes are discussed quantitatively later in this report. A large sand body emerged both landward and seaward of the breakwaters as observed during the July 1998 measurements, spanning breakwaters 4, 5 and 6 and partly 3. The emerged sand body filled the gaps between the above mentioned breakwaters. The water body landward of the breakwaters became much shallower when compared to the beginning of the project. The morphological conditions changed significantly during the four months between March 1998 and July 1998 surveys. These morphological changes significantly altered the function of the structures due to accumulation between the gaps and seaward of the breakwaters.

Data obtained from the September 1998 field experiment suggest that a significant volume of sediment that had accumulated seaward of the breakwaters had been eroded between the July and September surveys. Field observation and beach surveys indicate that some of the sediment had been transported landward and accumulated between the breakwaters and the shoreline. It is also conceivable that some of this material was reworked offshore and deposited as bars. The breakwaters remained connected by the emerged sand body and blocked Gulf waves from reaching the shoreline, similar to the conditions encountered during the July 1998 measurements. Profiles are presented in Figures 55, 56 and 57 at three locations showing the extent of sedimentation occurring behind and between breakwaters 6 and 7. In October 1997, shortly after construction, water depths were approximately -3 ft. (-0.91 m) (NAVD88); In May 2002, the same location had undergone deposition and the elevation had changed

to +3 ft (0.91 m), aggradation of 6 ft (1.82 m). Similar trends were noted in the gap between breakwaters 6 and 7 and in the lee of breakwater 7.

Bi-Annual Surveys 2000-2002

Transect lines surveyed in November 2000, May 2001, November 2001 and May 2002 are shown in Figure 1. A detailed description of change for each survey comparison is given for each transect in Appendix 4. Summaries of those data are presented in Table 5. In figures 58–65, surveys are presented as bathymetric/topographic maps and bathymetric/topographic change for respective survey comparisons. All data are referenced to NAVD88.

In all surveys, the shoal located off the eastern portion of Raccoon Island is clearly apparent. Survey comparisons indicate that the shoal undergoes seasonal variability showing erosional trends in the winter (November-May) and deposition in the summer (May-November) (Figures 60, 62 and 64). This occurrence is summarized in Figure 66 for all transects. Net change over the two year period is very distinct (Figure 65); the eastern three breakwaters have shown to be erosional behind the structures and offshore on the shoreface. The likelihood of deposition behind these structures was largely inhibited because of the occurrence of a tidal channel which actively scoured during winter months. East of breakwater 0 the west flank of the pass between Raccoon and Whiskey islands is actively shoaling.

West of breakwater 3, the trend is depositional behind the structures and for an area expanding from breakwater 3-6 offshore. At the toe of the structures, however, the upper shoreface is erosional. West of the breakwaters the shoreface and beach is predominantly erosional, with a hot spot immediately west of breakwater 7. This is in part due to an interruption by the breakwaters of east to west longshore transport. However, examination of Figure 65 suggest that the shoreface west of the breakwaters was erosional, over the study period, although intermittent deposition did occur at some locations during summer periods (Figures 62 and 64).

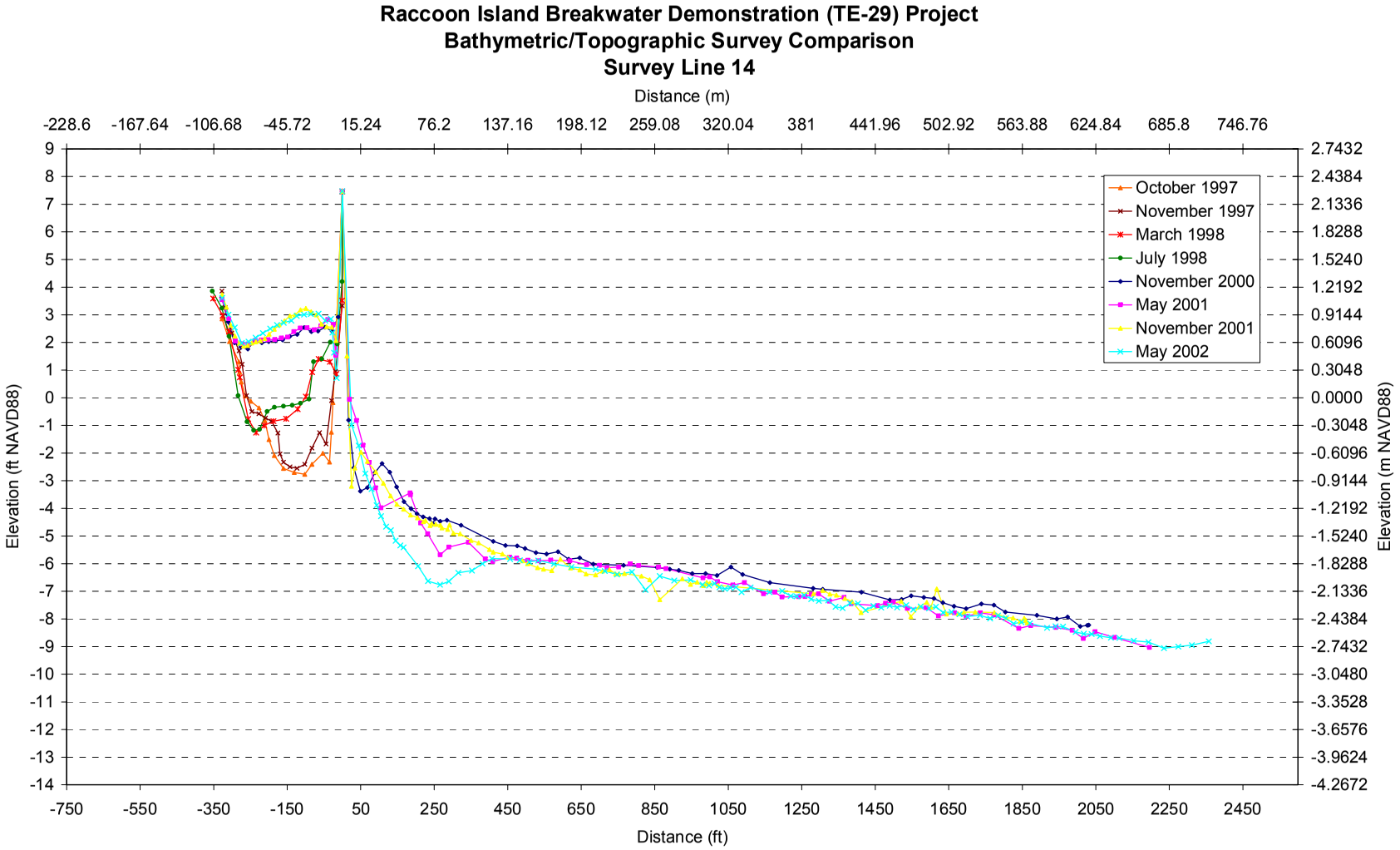

Figure 55. Bathymetric/topographic survey comparisons at transect line 14---breakwater 6.

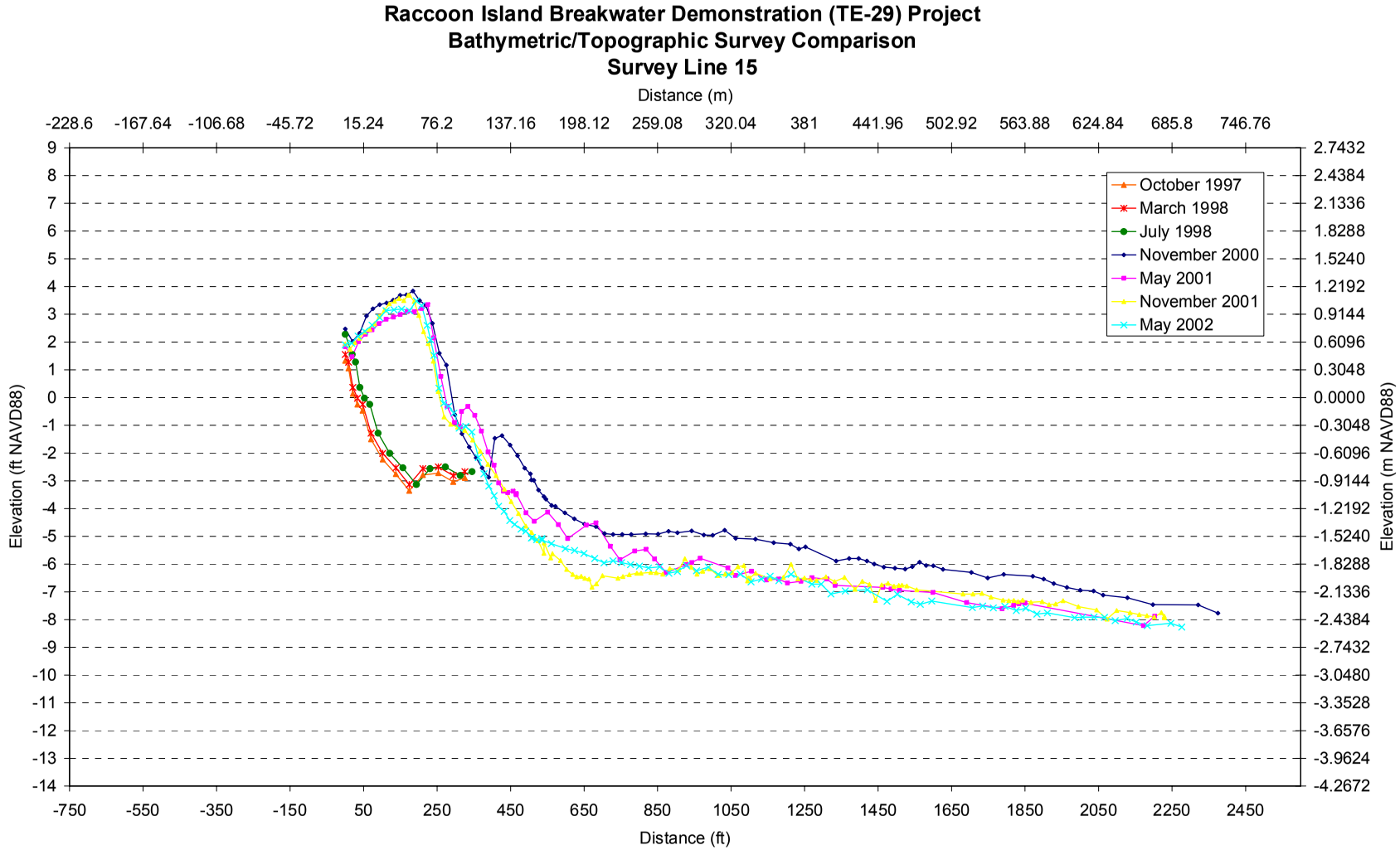

Figure 56. Bathymetric/topographic survey comparisons at transect line 15---between breakwaters 6 and 7.

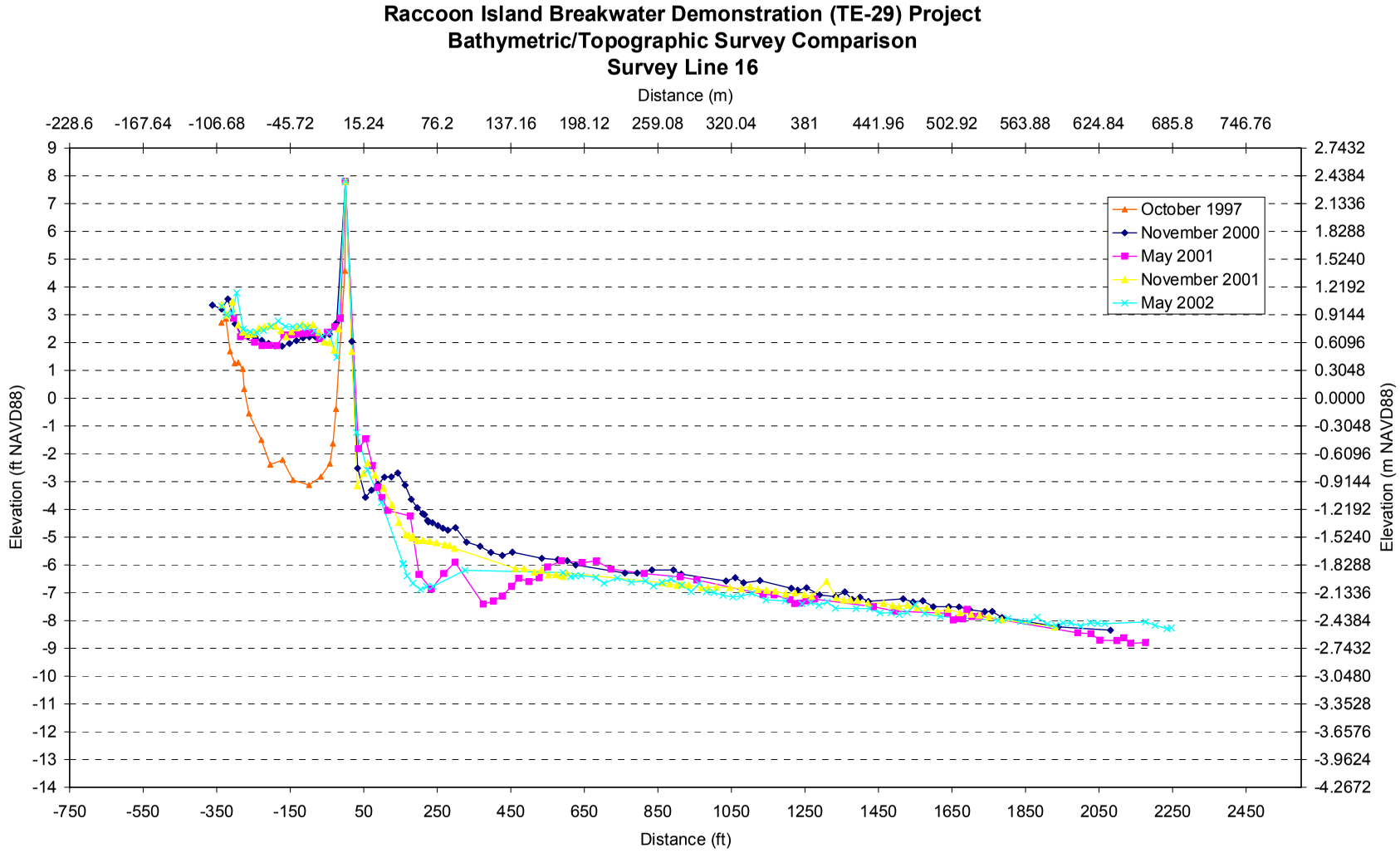

Figure 57. Bathymetric/topographic survey comparisons at transect line 16---at breakwater 7.

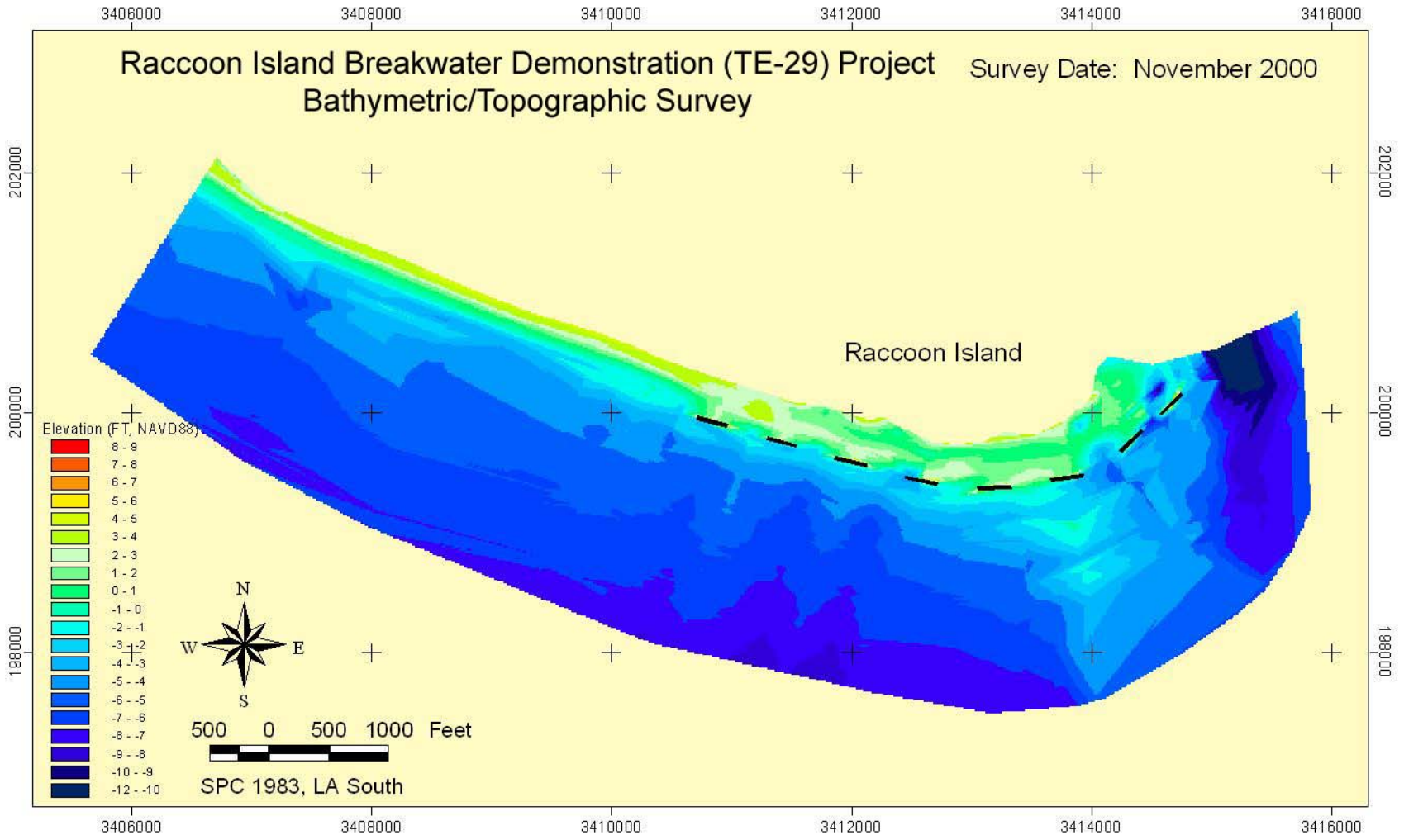

Figure 58. Bathymetry and topography of Raccoon Island surveyed in November 2000 (datum NAVD88).

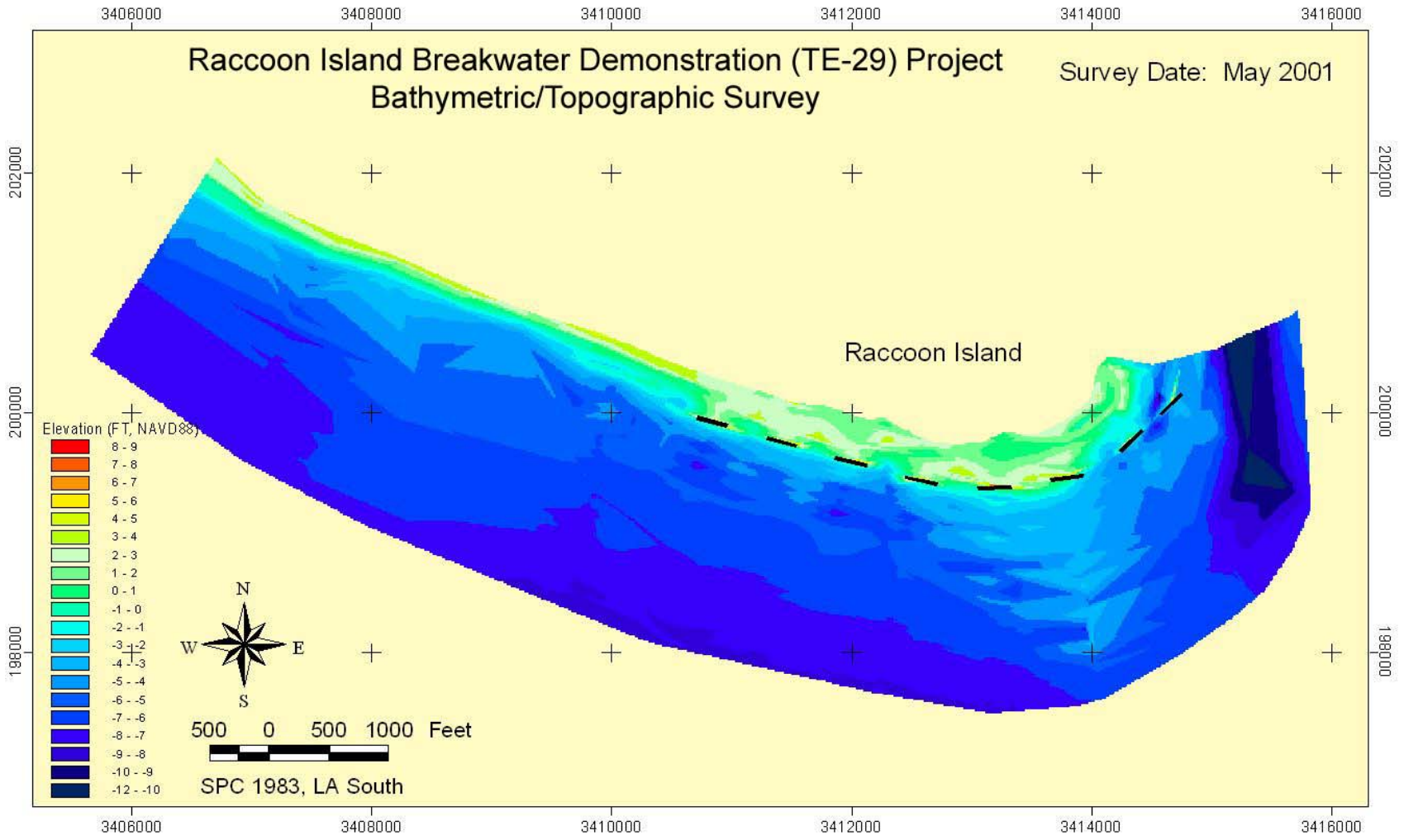

Figure 59. Bathymetry and topography of Raccoon Island surveyed in May 2001 (datum NAVD88).

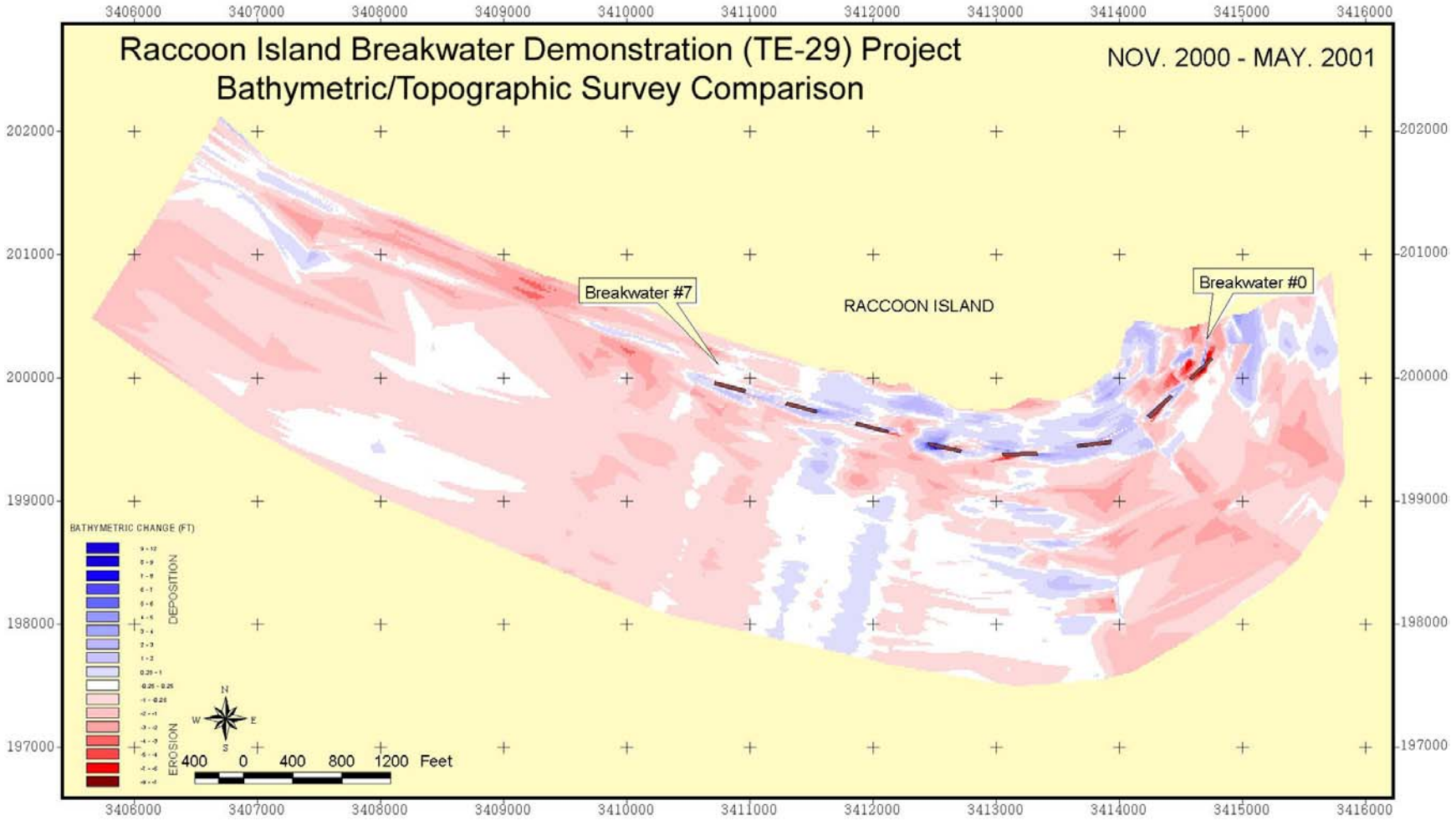

Figure 60. Bathymetric/Topographic Changes from November 2000 to May 2001, obtained by using ArcGIS. The map is in the State Plane Coordinates 1983, Louisiana South 1702. On this map, deposition is shown in blue while erosion is shown in red.

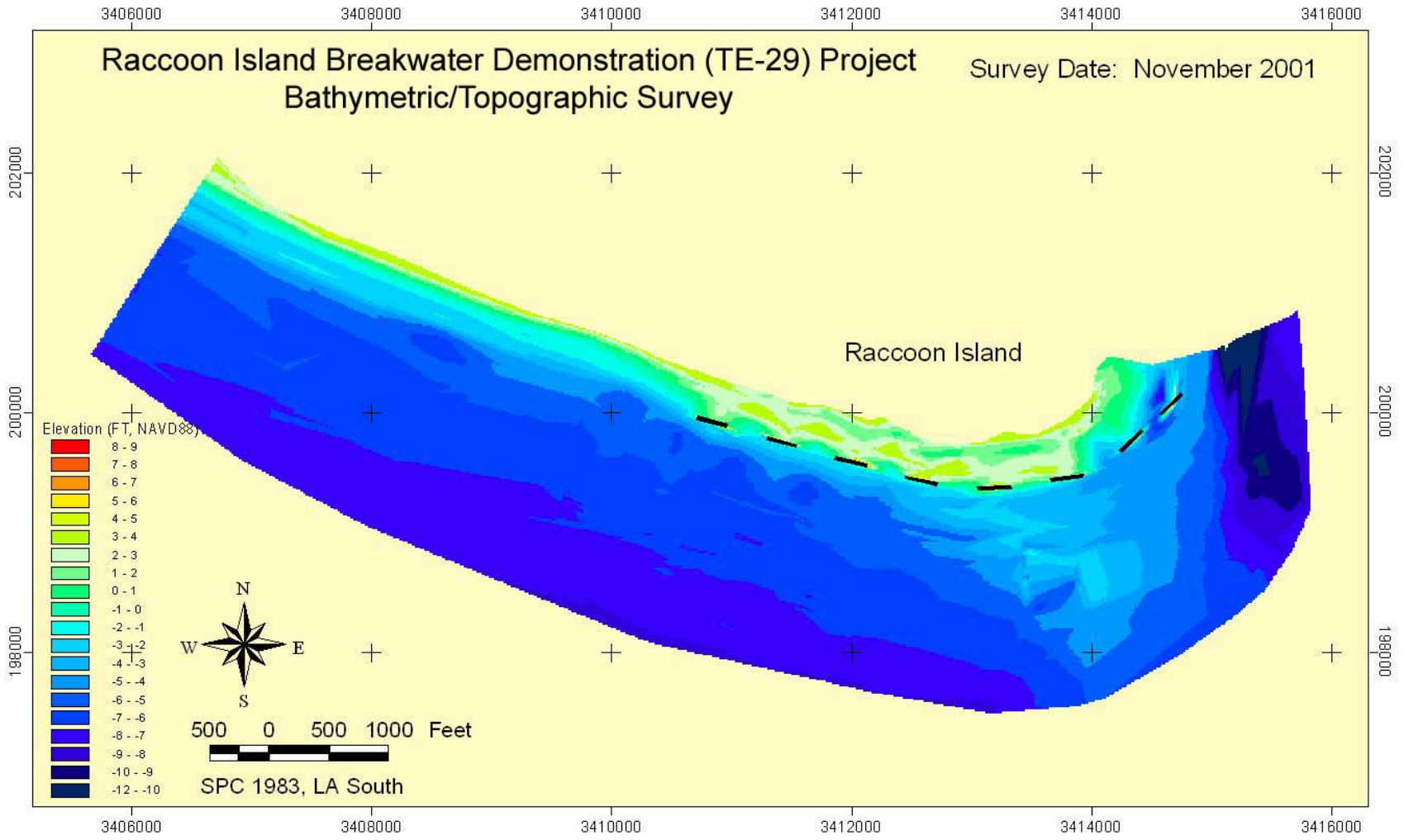

Figure 61. Bathymetry and topography of Raccoon Island surveyed in November 2001 (datum NAVD88).

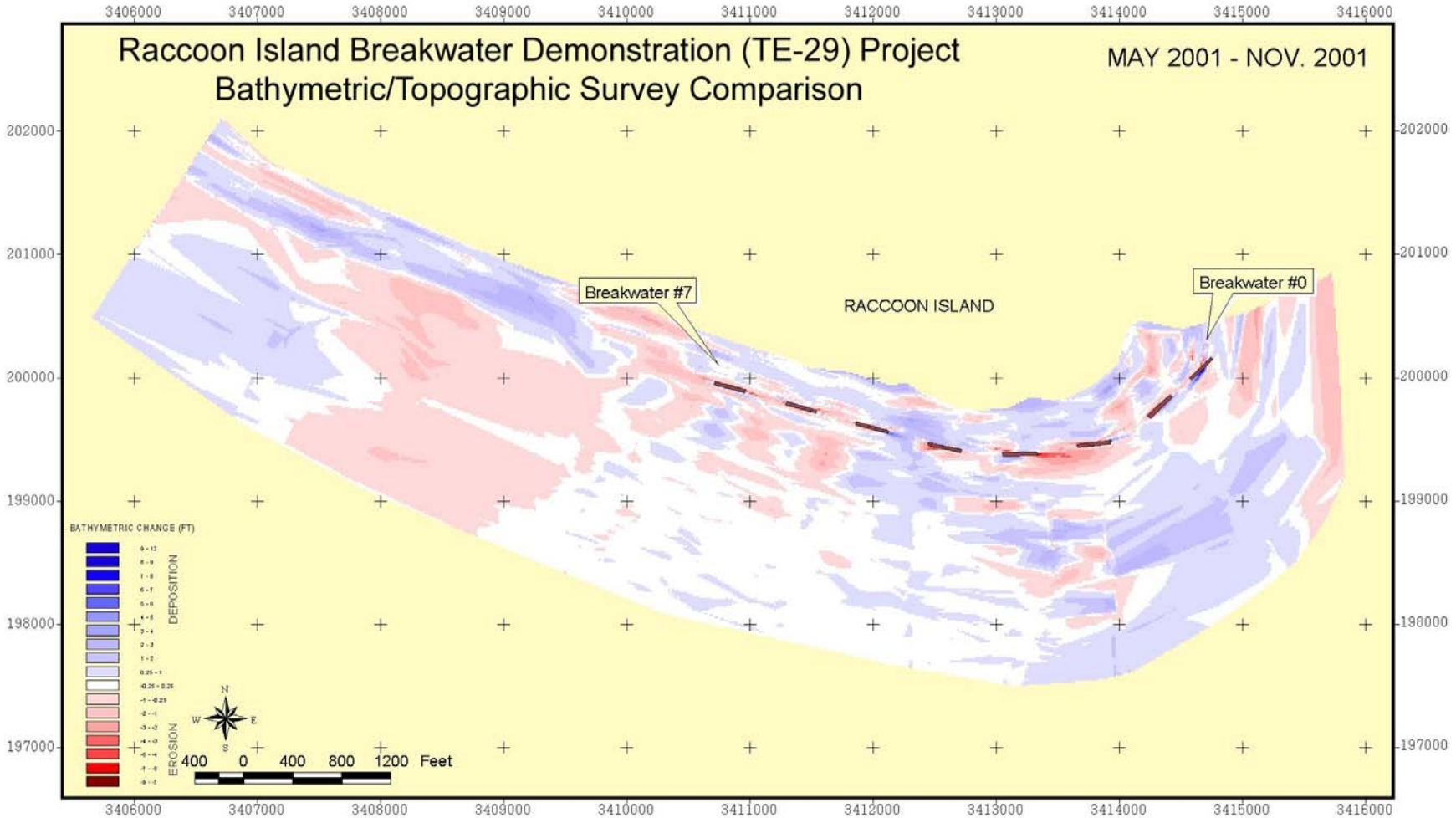

Figure 62. Bathymetric/Topographic Changes from May 2001 to November 2001, obtained by using ArcGIS. The map is in the State Plane Coordinates 1983, Louisiana South 1702. On this map, deposition is shown in blue while erosion is shown in red.

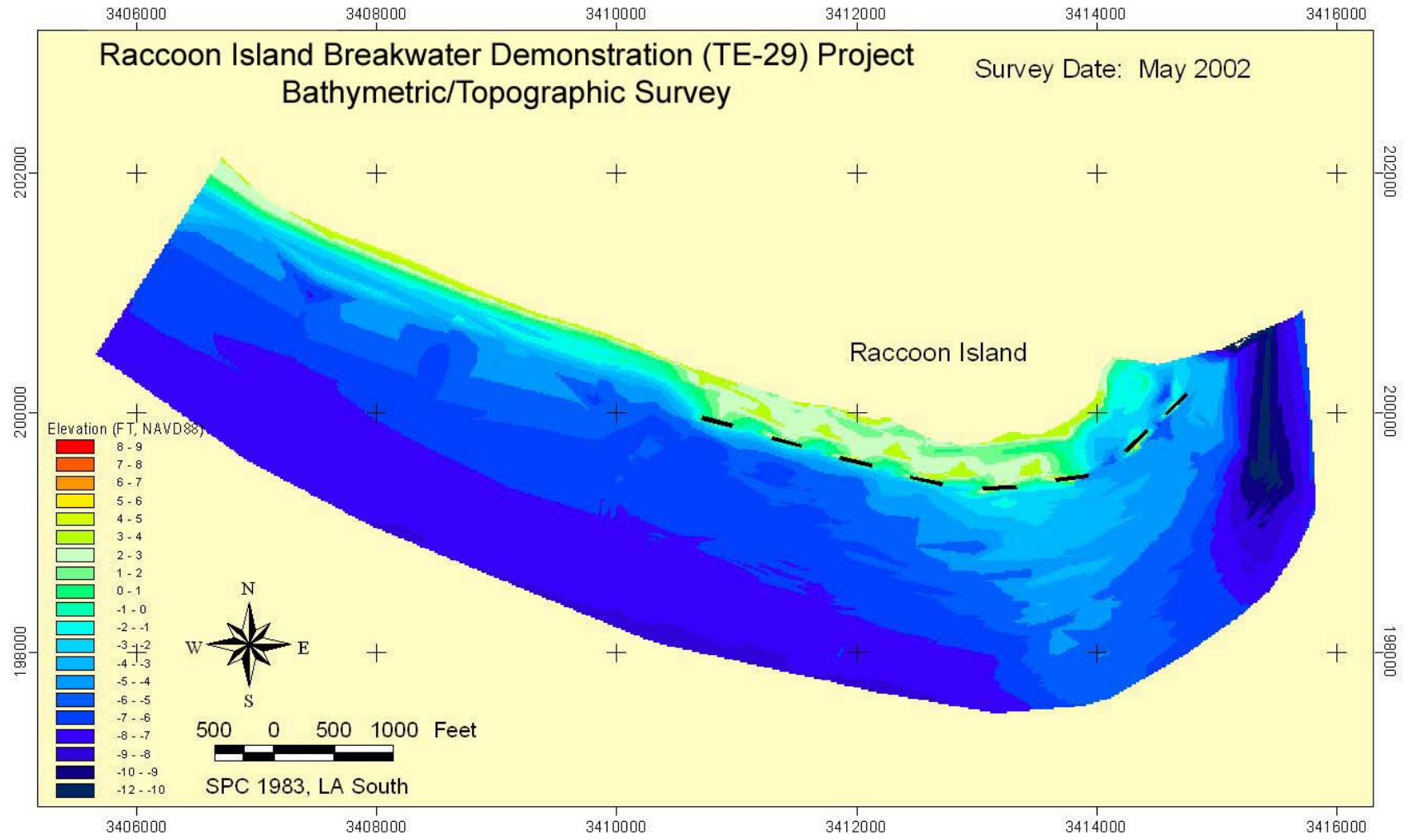

Figure 63. Bathymetry and topography of Raccoon Island surveyed in May 2002 (datum NAVD88).

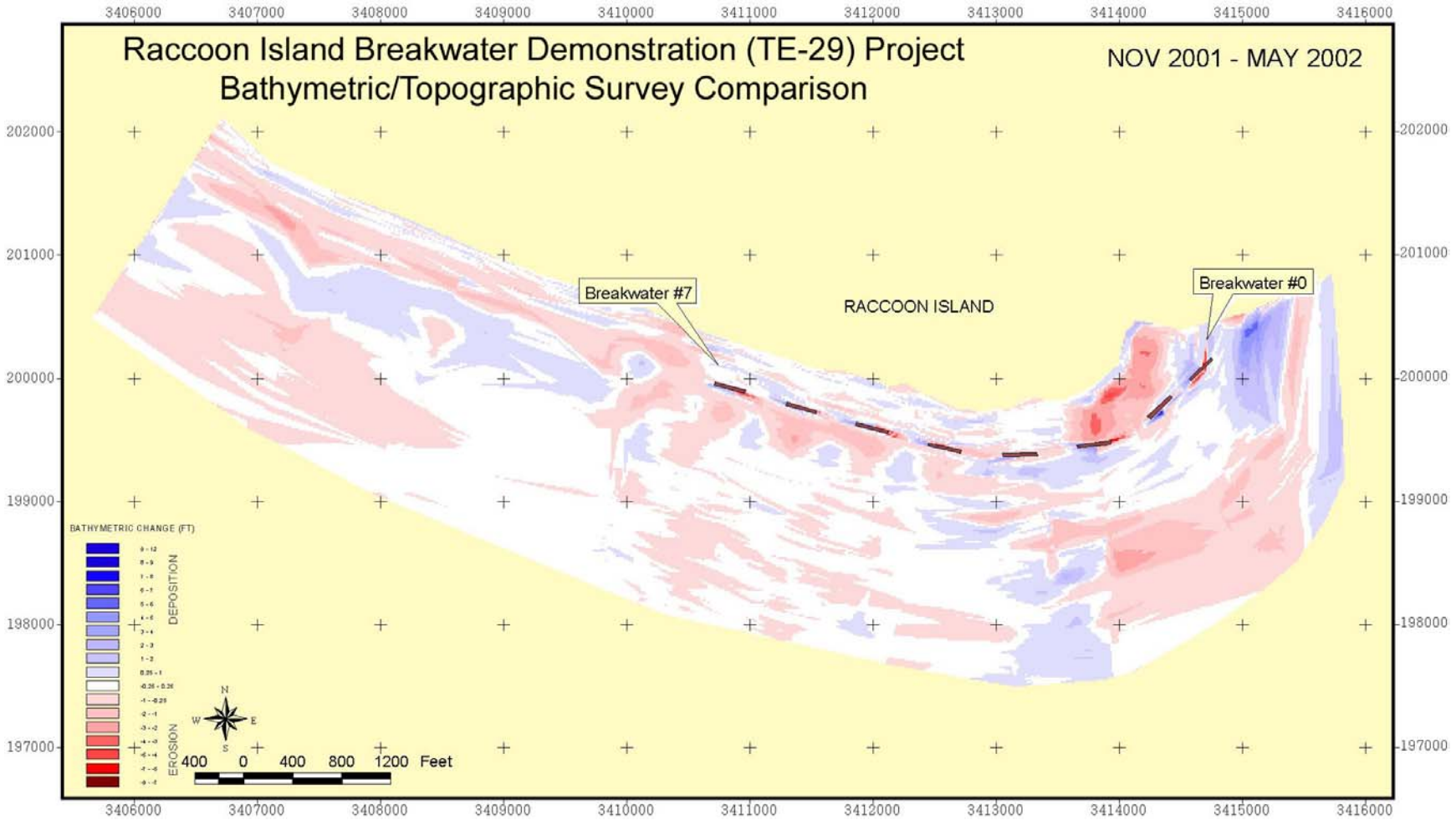

Figure 64. Bathymetric/Topographic Changes from November 2001 to May 2002, obtained by using ArcGIS. The map is in the State Plane Coordinates 1983, Louisiana South 1702. On this map, deposition is shown in blue while erosion is shown in red.

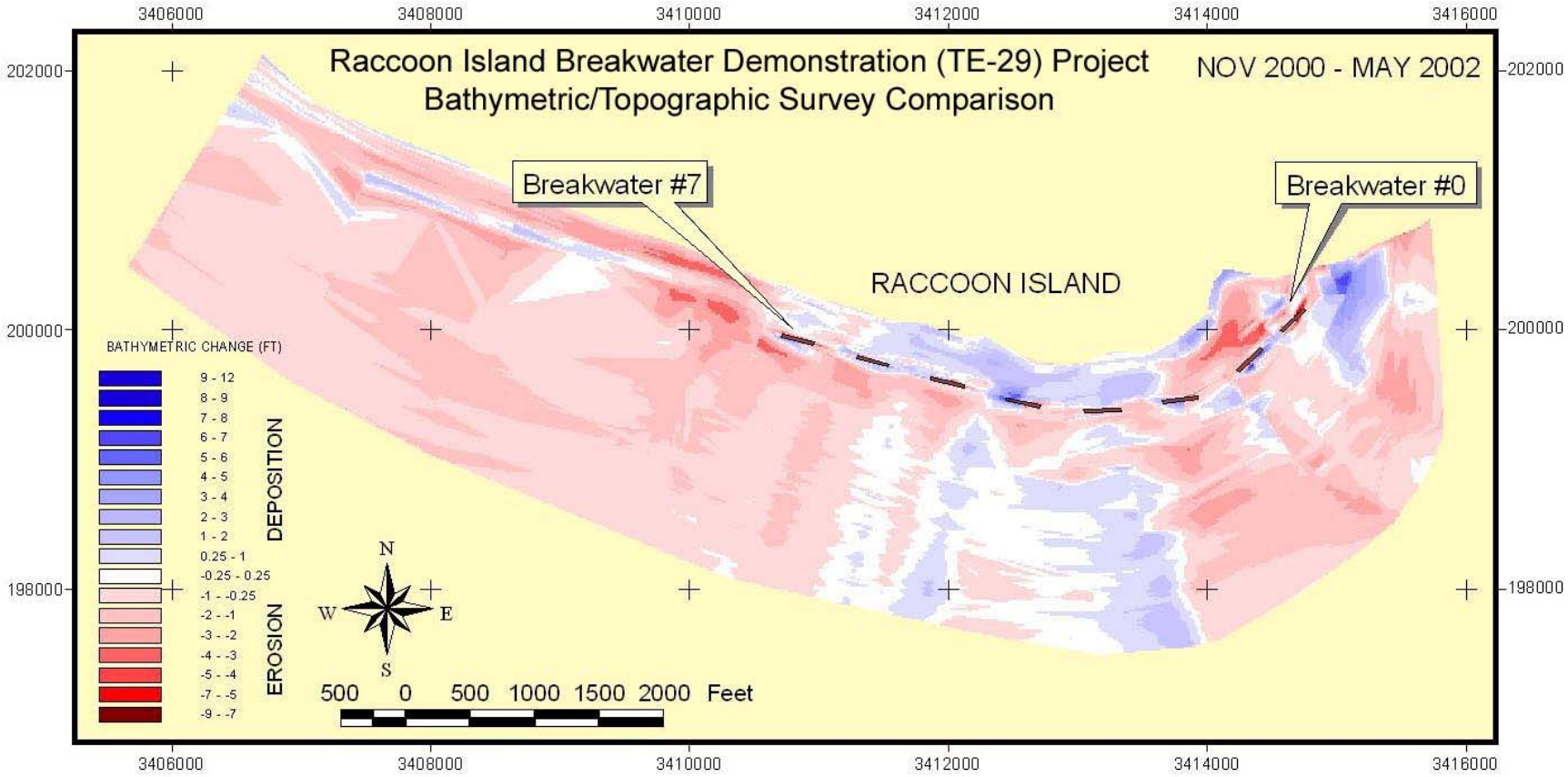

Figure 65. Bathymetric/Topographic Changes from November 2000 to May 2002, obtained by using ArcGIS. The map is in the State Plane Coordinates 1983, Louisiana South 1702. On this map, deposition is shown in blue while erosion is shown in red.

Table 5. Sediment volume changes during the survey periods. Shaded rows show the volume changes that occurred behind the breakwaters. Volumes calculated to the 4.572 m (15 ft) isobath.

Survey Line	Survey	XOn (ft/m)	XOff (ft/m)	Volume (yd^3ft^{-1}/m^3m^{-1})	Volume Changes to the previous survey (yd^3ft^{-1}/m^3m^{-1})
L1	2000-11	0/0	2000/609.6	804.58/2015.27	
	2001-05	0/0	2000/609.6	744.56/1864.83	-60.02/-150.43
	2001-11	0/0	2000/609.6	735.27/1841.80	-9.29/-23.04
	2002-05	0/0	2000/609.6	742.65/1860.18	7.38/18.38
L2	2000-11	-500/-152.4	0/0	227.35/571.04	
	2001-05	-500/-152.4	0/0	235.00/588.86	7.65/17.82
	2001-11	-500/-152.4	0/0	244.62/612.96	9.62/24.10
	2002-05	-500/-152.4	0/0	237.48/595.08	-7.14/-17.88
	2000-11	0/0	1500/457.2	484.44/1213.17	
	2001-05	0/0	1500/457.2	454.24/1137.36	-30.20/-75.81
	2001-11	0/0	1500/457.2	457.20/1144.82	2.96/7.46
	2002-05	0/0	1500/457.2	442.09/1106.89	-15.11/-37.93
L3	2000-11	-200/-60.96	2000/609.6	845.46/2117.62	
	2001-05	-200/-60.96	2000/609.6	818.22/2049.84	-27.25/-67.77
	2001-11	-200/-60.96	2000/609.6	816.44/2044.80	-1.77/-5.04
	2002-05	-200/-60.96	2000/609.6	778.41/1949.79	-38.03/-95.01
L4	2000-11	-500/-152.4	0/0	303.96/761.82	
	2001-05	-500/-152.4	0/0	284.29/712.46	-19.67/-49.36
	2001-11	-500/-152.4	0/0	279.92/701.49	-4.37/-10.97
	2002-05	-500/-152.4	0/0	263.31/659.79	-16.60/-41.70
	2000-11	0/0	1600/487.68	563.13/1410.37	
	2001-05	0/0	1600/487.68	564.42/1413.73	1.29/3.36
	2001-11	0/0	1600/487.68	553.61/1386.47	-10.81/-27.26
	2002-05	0/0	1600/487.68	537.30/1345.63	-16.31/-40.84
L5	2000-11	-150/-45.72	2000/609.6	839.15/2102.22	
	2001-05	-150/-45.72	2000/609.6	831.55/2082.94	-7.60/-19.28
	2001-11	-150/-45.72	2000/609.6	851.50/2133.16	19.95/50.22
	2002-05	-150/-45.72	2000/609.6	815.47/2042.75	-36.03/-90.42
L6	2000-11	-400/-121.92	0/0	245.83/616.12	
	2001-05	-400/-121.92	0/0	252.26/632.21	6.43/16.09
	2001-11	-400/-121.92	0/0	251.14/629.43	-1.11/-2.78
	2002-05	-400/-121.92	0/0	230.55/577.82	-20.59/-51.61
	2000-11	0/0	1900/579.12	845.42/2118.49	
	2001-05	0/0	1900/579.12	758.71/1900.75	-86.72/-217.74
	2001-11	0/0	1900/579.12	771.30/1932.41	12.59/31.66
	2002-05	0/0	1900/579.12	751.95/1883.92	-19.35/-48.49
L7	2000-11	0/0	2200/670.56	927.34/2323.51	
	2001-05	0/0	2200/670.56	931.23/2333.28	3.89/9.76

Table 5 (cont.). Sediment volume changes during the survey periods. Shaded rows show the volume changes that occurred behind the breakwaters. Volumes calculated to the 4.572 m (15 ft) isobath.

L7	2001-11	0/0	2200/670.56	939.27/2353.50	8.04/20.22
	2002-05	0/0	2200/670.56	947.79/2374.83	8.52/21.32
L8	2000-11	-400/-121.92	0/0	245.11/614.37	
	2001-05	-400/-121.92	0/0	241.05/604.17	-4.06/-10.20
	2001-11	-400/-121.92	0/0	253.66/635.81	12.61/31.64
	2002-05	-400/-121.92	0/0	253.68/635.84	0.03/0.03
	2000-11	0/0	1700/518.16	665.83/1668.21	
	2001-05	0/0	1700/518.16	630.06/1578.52	-35.77/-89.69
	2001-11	0/0	1700/518.16	674.49/1689.80	44.43/111.28
	2002-05	0/0	1700/518.16	693.23/1736.99	18.73/47.19
L9	2000-11	0/0	2200/670.56	867.14/2172.68	
	2001-05	0/0	2200/670.56	821.15/2057.40	-45.99/-115.29
	2001-11	0/0	2200/670.56	871.47/2183.61	50.33/126.21
	2002-05	0/0	2200/670.56	872.85/2187.07	1.38/3.46
L10	2000-11	-300/-91.44	0/0	183.27/459.41	
	2001-05	-300/-91.44	0/0	188.85/473.38	5.57/13.97
	2001-11	-300/-91.44	0/0	192.94/483.64	4.09/10.26
	2002-05	-300/-91.44	0/0	193.40/484.75	0.46/1.11
	2000-11	0/0	1900/579.12	660.58/1654.81	
	2001-05	0/0	1900/579.12	627.06/1570.82	-33.52/-83.99
	2001-11	0/0	1900/579.12	639.76/1602.89	12.70/32.08
	2002-05	0/0	1900/579.12	627.94/1573.11	-11.82/-29.78
L11	2000-11	0/0	2200/670.56	858.57/2151.24	
	2001-05	0/0	2200/670.56	821.85/2059.20	-36.72/-92.04
	2001-11	0/0	2200/670.56	841.95/2109.51	20.10/50.31
	2002-05	0/0	2200/670.56	842.22/2110.47	0.27/0.96
L12	2000-11	-350/-106.68	0/0	221.83/556.04	
	2001-05	-350/-106.68	0/0	220.61/552.98	-1.21/-3.06
	2001-11	-350/-106.68	0/0	226.81/568.57	6.20/15.59
	2002-05	-350/-106.68	0/0	228.29/572.23	1.48/3.66
	2000-11	0/0	2000/609.6	679.30/1701.97	
	2001-05	0/0	2000/609.6	643.29/1611.59	-36.02/-90.39
	2001-11	0/0	2000/609.6	649.30/1626.71	6.01/15.12
	2002-05	0/0	2000/609.6	640.77/1605.23	-8.53/-21.48
L13	2000-11	0/0	2200/670.56	843.71/2114.11	
	2001-05	0/0	2200/670.56	826.68/2071.60	-17.03/-42.51
	2001-11	0/0	2200/670.56	821.47/2058.24	-5.21/-13.36
	2002-05	0/0	2200/670.56	808.46/2025.78	-13.01/-32.46
L14	2000-11	-320/-97.54	0/0	205.56/515.33	
	2001-05	-320/-97.54	0/0	206.69/518.16	1.13/2.83
	2001-11	-320/-97.54	0/0	209.62/525.51	2.93/7.35
	2002-05	-320/-97.54	0/0	209.48/525.15	-0.14/-0.36

Table 5 (cont.). Sediment volume changes during the survey periods. Shaded rows show the volume changes that occurred behind the breakwaters. Volumes calculated to the 4.572 m (15 ft) isobath.

L14	2000-11	0/0	2000/609.6	661.42/1657.16	
	2001-05	0/0	2000/609.6	641.13/1606.25	-20.29/-50.92
	2001-11	0/0	2000/609.6	638.84/1600.43	-2.29/-5.82
	2002-05	0/0	2000/609.6	620.87/1555.53	-17.97/-44.90
L15	2000-11	0/0	2200/670.56	881.22/2208.48	
	2001-05	0/0	2200/670.56	814.15/2040.13	-67.06/-168.34
	2001-11	0/0	2200/670.56	800.70/2006.46	-13.46/-33.67
	2002-05	0/0	2200/670.56	792.05/1984.68	-8.65/-21.78
L16	2000-11	-300/-91.44	0/0	193.29/484.56	
	2001-05	-300/-91.44	0/0	192.86/483.46	-0.42/-1.10
	2001-11	-300/-91.44	0/0	195.31/489.61	2.45/6.15
	2002-05	-300/-91.44	0/0	196.35/492.18	1.04/2.57
	2000-11	0/0	2000/609.6	652.77/1635.55	
	2001-05	0/0	2000/609.6	622.30/1559.20	-30.46/-76.35
	2001-11	0/0	2000/609.6	631.19/1581.52	8.89/22.32
	2002-05	0/0	2000/609.6	612.07/1533.48	-19.12/-48.04
L17	2000-11	0/0	2000/609.6	841.32/2110.34	
	2001-05	0/0	2000/609.6	840.30/2107.77	-1.01/-2.57
	2001-11	0/0	2000/609.6	777.48/1950.23	-62.82/-157.55
	2002-05	0/0	2000/609.6	759.48/1905.06	-18.01/-45.16
L18	2000-11	0/0	2000/609.6	794.16/1990.37	
	2001-05	0/0	2000/609.6	715.25/1792.35	-78.91/-198.02
	2001-11	0/0	2000/609.6	705.29/1767.38	-9.96/-24.97
	2002-05	0/0	2000/609.6	679.49/1702.65	-25.80/-64.73
L19	2000-11	0/0	2000/609.6	787.83/1974.48	
	2001-05	0/0	2000/609.6	721.81/1808.92	-66.02/-165.56
	2001-11	0/0	2000/609.6	709.81/1778.81	-12.00/-30.11
	2002-05	0/0	2000/609.6	697.62/1748.25	-12.18/-30.56
L20	2000-11	0/0	2000/609.6	792.65/1986.69	
	2001-05	0/0	2000/609.6	725.03/1817.05	-67.63/-169.64
	2001-11	0/0	2000/609.6	708.31/1775.02	-16.71/-42.03
	2002-05	0/0	2000/609.6	696.08/1744.33	-12.24/-30.69
L21	2000-11	0/0	220/67.06	114.96/288.21	
	2001-05	0/0	220/67.06	112.19/281.25	-2.77/-6.96
	2001-11	0/0	220/67.06	120.54/302.24	8.35/21.00
	2002-05	0/0	220/67.06	117.58/294.76	-2.96/-7.48
L22	2000-11	0/0	2000/609.6	774.08/1940.42	
	2001-05	0/0	2000/609.6	743.40/1863.57	-30.68/-76.85
	2001-11	0/0	2000/609.6	700.09/1754.78	-43.31/-108.79
	2002-05	0/0	2000/609.6	682.76/1711.10	-17.34/-43.68
L23	2000-11	0/0	200/60.96	127.40/319.45	
	2001-05	0/0	200/60.96	115.67/290.00	-11.73/-29.45

Table 5 (cont.). Sediment volume changes during the survey periods. Shaded rows show the volume changes that occurred behind the breakwaters. Volumes calculated to the 4.572 m (15 ft) isobath.

	2001-11	0/0	200/60.96	119.05/298.47	3.39/8.47
	2002-05	0/0	200/60.96	117.86/295.51	-1.19/-2.96
L24	2000-11	0/0	2000/609.6	738.43/1851.07	
	2001-05	0/0	2000/609.6	694.91/1741.87	-43.52/-109.20
	2001-11	0/0	2000/609.6	717.82/1799.31	22.91/57.43
	2002-05	0/0	2000/609.6	687.45/1723.21	-30.36/-76.10
L25	2000-11	0/0	230/70.10	132.83/333.05	
	2001-05	0/0	230/70.10	133.78/335.42	0.94/2.37
	2001-11	0/0	230/70.10	128.39/321.95	-5.38/-13.48
	2002-05	0/0	230/70.10	128.34/321.83	-0.05/-0.12
L26	2000-11	0/0	2000/609.6	806.44/2022.05	
	2001-05	0/0	2000/609.6	740.98/1857.69	-65.47/-164.36
	2001-11	0/0	2000/609.6	754.09/1890.64	13.12/32.94
	2002-05	0/0	2000/609.6	746.65/1872.04	-7.44/-18.59

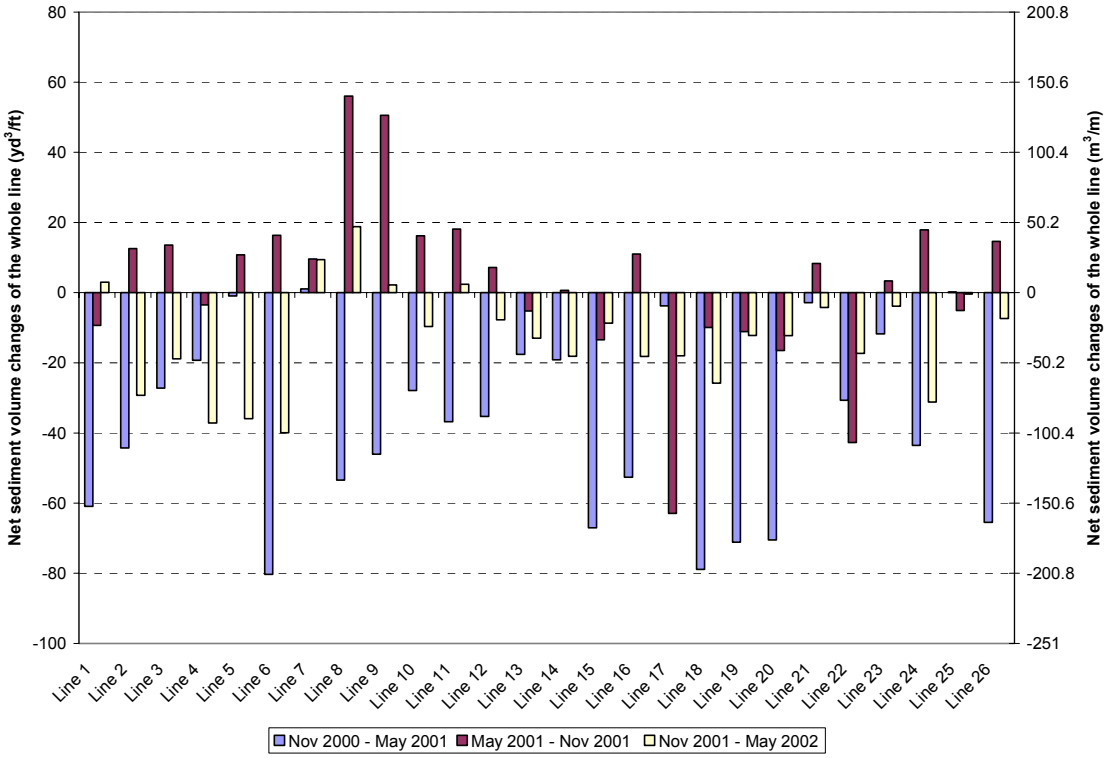

Figure 66. Summaries of sediment volume changes of each survey line during the three survey seasons. Negative values represent erosion, and positive values represent deposition.

The seasonal movement of sand to and from the shoreface was accomplished at some locations by sand wave migration, onshore in the summer and offshore in the winter. Lines 6 and 7 at breakwater 2 are examples. The ridges attain elevations up to ~0.914 m (3 ft) and disappear to the west along the shoreface.

Change Landward and Seaward of Breakwaters

Sediment volume change was also calculated for those areas landward and seaward of the breakwaters to obtain a better understanding of erosion deposition trends. As shown in Figure 67, for the period November 2000 to May 2001, deposition occurred behind breakwaters 0, 2, 4, and 6, whereas erosion occurred behind breakwaters 1, 3, 5, and 7. Maximum erosion occurred behind breakwater 1 with 49.36 m^3/m (19.67 yd^3/ft) being lost. Maximum deposition occurred behind breakwater 0, with 17.82 m^3/m (7.65 yd^3/ft) being gained. For the period May 2001 to November 2001, deposition occurred behind breakwaters 0, 3, 4, 5, 6, and 7 while erosion occurred behind breakwaters 1 and 2. Maximum erosion occurred behind breakwater 1, with 10.97 m^3/m (4.37 yd^3/ft) being lost. Maximum deposition occurred behind breakwater 3, with some 31.64 m^3/m

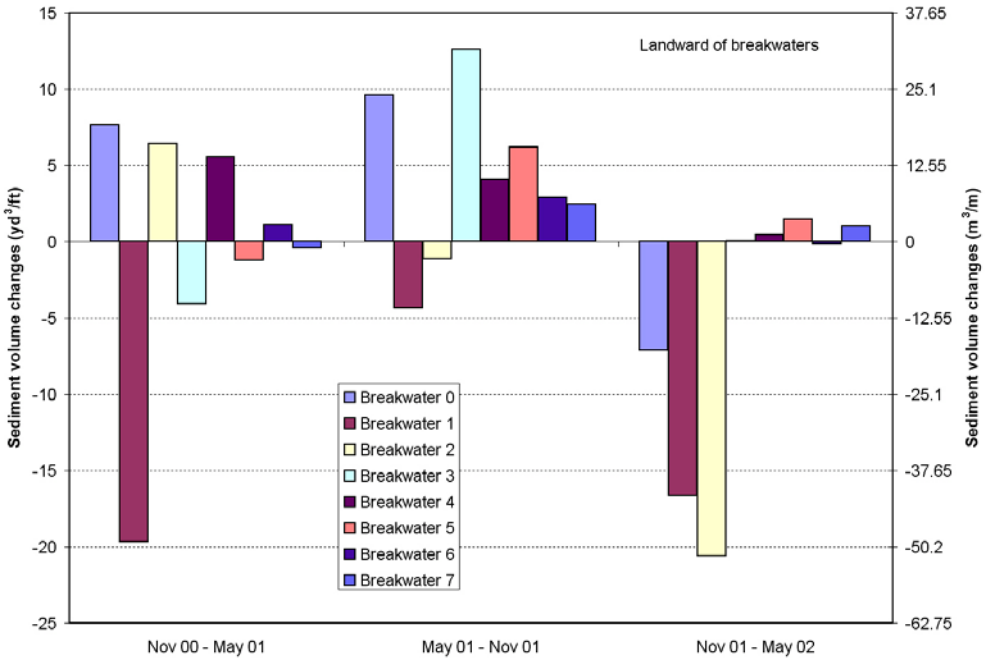

Figure 67. Sediment volume changes of behind breakwater part of the eight survey lines through the breakwaters. Negative values represent erosion, while positive values represent deposition.

(12.61yd^3/ft) being gained. For the period November 2001 to May 2002, a significant amount of erosion occurred behind breakwaters 0, 1, and 2, and substantially less behind breakwater 6. Deposition occurred behind breakwaters 3, 4, 5, and 7. Maximum erosion occurred behind breakwater 2, with some 51.61 m^3/m (20.59 yd^3/ft) being lost. Maximum deposition occurred behind breakwater 5, where 3.66 m^3/m (1.48 yd^3/ft) of sediment were deposited.

Seaward of the breakwaters to the 4.572 m (15 ft) isobath, there is also a seasonal trend evident in the data (Figure 68). From November 2000 to May 2001, the shoreface was eroded almost all across that portion fronting the breakwaters with only slight deposition of 3.36 m^3/m (1.29 yd^3/ft) occurring in front of breakwater 1. Maximum erosion of 217.74 m^3/m (86.72 yd^3/ft) occurred in front of breakwater 2. Between May 2001 and November 2001, deposition occurred in front of breakwaters 0, 2, 3, 4, 5, and 7,

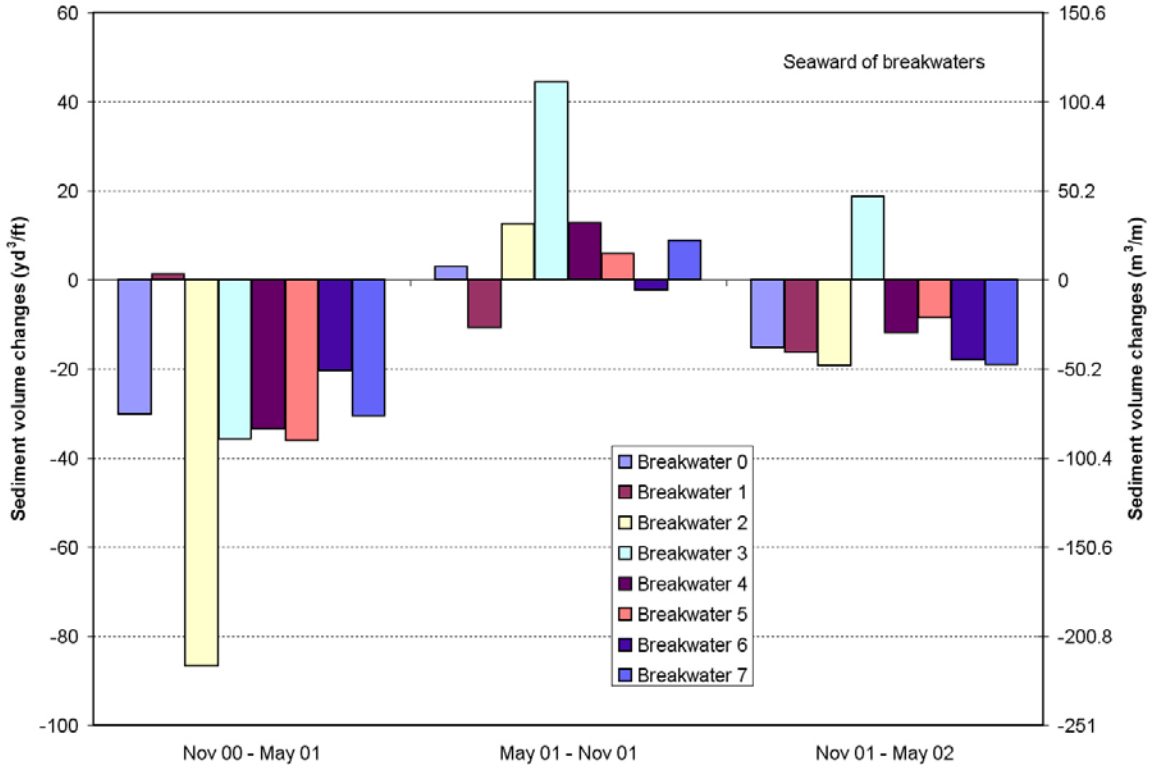

Figure 68. Sediment volume changes of the part in front of the breakwater of the eight survey lines through the breakwaters. Negative values represent erosion, while positive values represent deposition.

and erosion in front of breakwaters 1 and 6. Maximum deposition of 111.28 m^3/m (44.43 yd^3/ft) occurred in front of breakwater 3. Finally, for the period of November 2001 to May 2002, erosion occurred throughout almost all of the site with the exception of breakwater 3. Here some 47.19 m^3/m (18.73 yd^3/ft) of deposition occurred. Maximum erosion approximating 48.49 m^3/m (19.35 yd^3/ft) occurred in front of breakwater 2.

In Figure 69 the entire volume of sediment accumulation landward and seaward (to the 4.572 m; 15 ft isobath) is presented for the two year survey period. The volume change is presented in Table 6. Between November 2000 and May 2001, sediment accumulated behind the breakwaters resulting in an increase in volume from 0.704 million cu meters (mcum) [0.921 million cubic yards (mcuy)] to 0.712 mcum (0.931 mcuy), an increase of 8,000 cum (10,000 cuy). Between May 2001 and November of that year, the total volume decreased by 2,000 cum (3,000 cuy) to 0.710 mcum (0.928 mcuy). Between November 2001 and May 2002, sediment volume continued to decrease behind the breakwaters by 15,000 cum (19,000 cuy), an all time low of 0.695 mcum (0.909 mcuy) over the survey period.

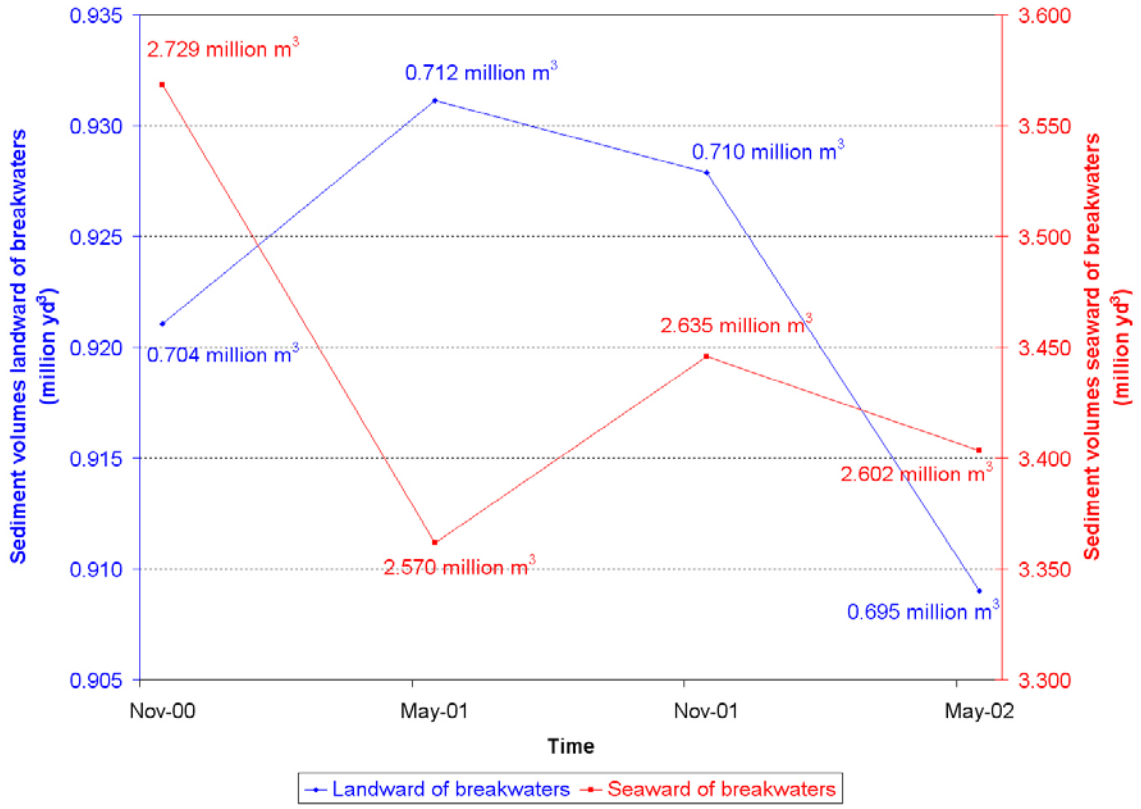

Figure 69. Sediment volume changes of entire areas landward and seaward of the breakwaters.

Seaward of the breakwaters the total volume of sand to the 4.572 m (15 ft) isobath shows a similar downward trend. As shown in Figure 69 and Table 6, in November 2000 the volume approximated 2.729 mcum (3.569 mcuy). Comparison of this volume with that calculated from the May 2001 survey shows a decrease in volume to 2.570 mcum (3.362 mcuy), a loss of 159,000 cum (207,000 cuy). This erosional trend was reversed between May 2001 and November 2001 when the total volume increased to 2.635 mcum (3.446 mcuy), a net gain of 65,000 cum (84,000 cuy). Finally, between November 2001 and May 2002, 33,000 cum (43,000 cuy) was eroded from the site when the total volume decreased to 2.602 mcum (3.403 mcuy).

Table 6. Sediment volume and change landward and seaward of breakwaters. Seaward volumes calculated to the 4.572 m (15ft) isobath. (Note - = erosion)

	Survey Date	Volume (yd^3 × million)	Volume change compared to previous survey (yd^3)	Volume (m^3 × million)	Volume change compared to previous survey (m^3)
Landward of breakwaters	Nov-00	0.921		0.704	
	May-01	0.931	10,000	0.712	8,000
	Nov-01	0.928	-3,000	0.710	-2,000
	May-02	0.909	-19,000	0.695	-15,000
Seaward of breakwaters	Nov-00	3.569		2.729	
	May-01	3.362	-207,000	2.570	-159,000
	Nov-01	3.446	84,000	2.635	65,000
	May-02	3.403	-43,000	2.602	-33,000

The sediment budget presented above suggests that over the entire survey period, a net loss of sand approximating 9,174 cum (12,000 cuy) was experienced behind the breakwaters. Approximately 126,916 cum (166,000 cuy) was lost from the offshore site.

SYNTHESIS AND IMPLICATIONS FOR PROJECT DESIGN

Introduction

The breakwaters at Raccoon Island caused deposition of sediment in an extremely unique manner, one that to our knowledge has not been documented in the scientific literature. Only one vaguely similar example is known along the Massachusetts coast, however, the genesis of those features is not well understood. The typical response to breakwaters along a coast is the formation of salients along the beach, which given an abundance of sediment in the nearshore, begin over time to prograde offshore towards the structure. Many salients develop into tombolos where they become attached to the landward side of the breakwater. This response has been documented extensively in the scientific and engineering literature and is presented in Figure 70 (upper). At Raccoon Island, however, the formation of salients was quickly followed by the formation of what Stone et al. (1999) refer to as Reverse Salients, i.e., sand bodies formed behind the structures that have prograded onshore. The model of development for the Raccoon breakwaters is shown in Figure 70 (middle). This response was not anticipated; in fact according to the engineering literature (Pope and Dean, 1986), the development of neither salients or conventional tombolos was anticipated given the distance of the structures offshore, the depth in which they had been constructed, structure length and gap width (Figure 70, lower). Therefore, it became imperative that a better understanding of why Raccoon Island responded to the breakwaters in the way it did to be obtained. It is worthwhile to recap the objectives and rationale of this project to ensure focus of the perceived implications associated with these findings and breakwater performance at Raccoon Island.

The unanticipated response of Raccoon Island to the structures and magnitude of sediment accumulation warranted further investigation. This was deemed particularly important given the perceived notion that application of breakwaters along Louisiana's Gulf-facing coast was the panacea for mitigating all coastal erosion problems. Utilizing this restoration technique in other locations, necessitates a greater understanding of the

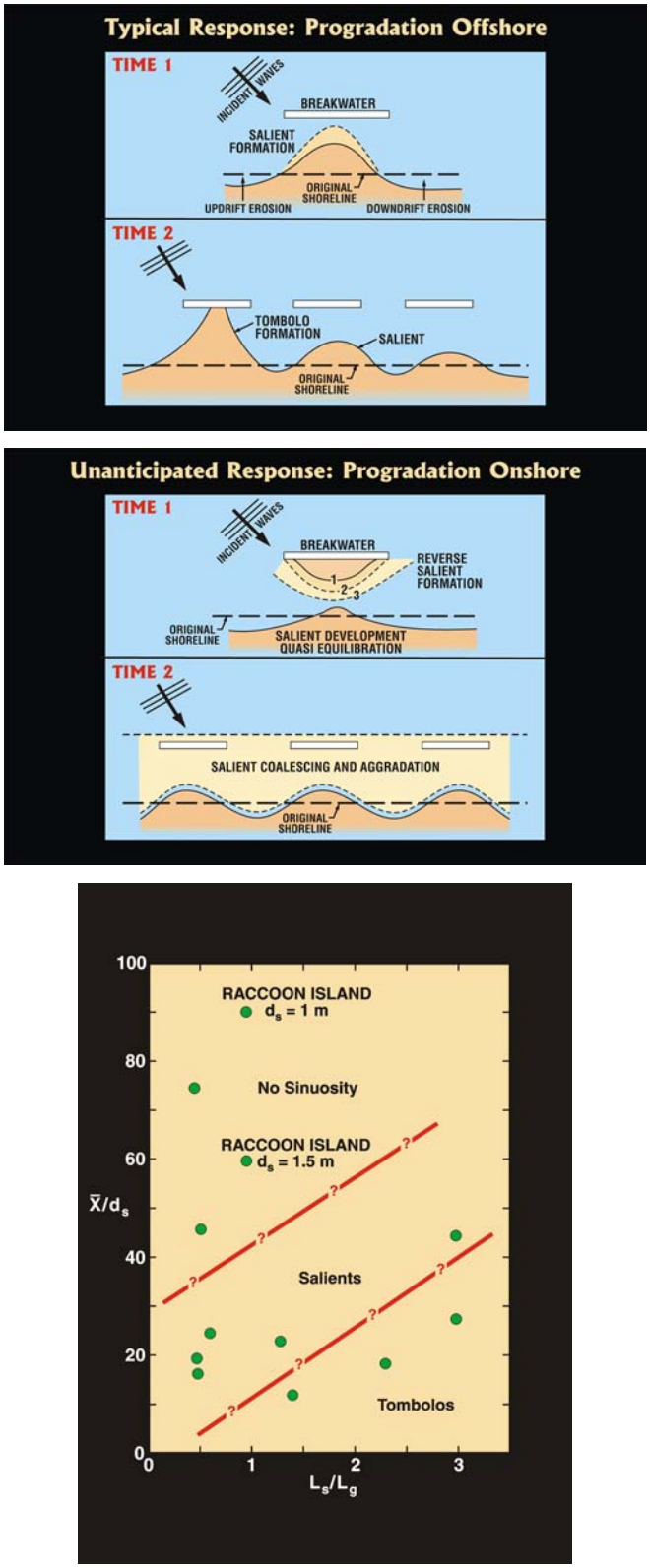

Figure 70. Upper, typical response of nearshore to breakwater construction. Middle, model of the response of Raccoon Island to breakwaters. Bottom, documented response of beaches to structures based on design criteria where X = distance offshore, d_s = depth at structure, L_s = structure length and L_g = gap width according to Pope and Dean, (1986).

questions that required answering beyond those of the original CWPPRA monitoring effort. Thus, several questions were carefully formulated and presented by both LDNR staff and LSU scientists. These were as follows:

1. Why did sand accumulation begin preferentially along the western flank of the breakwater array (7, 6, 5, 4 and 3 respectively)?
2. Where is the primary sand source for the sediment that accumulated in the vicinity of the breakwaters within the initial 12-month monitoring period and beyond should the trend continue?
3. What is the volume of sediment that comprises the source and what is the projected longevity and availability to nearshore processes of this source?
4. What are the precise roles of longshore and cross-shore sediment transport at the site?
5. How is the beach west of the structures responding to breakwater construction?
6. Can the design criteria used to construct the breakwaters be refined to maximize sediment accumulation at this and other prospective sites?
7. Are the trends that have been established for the first 12 months of monitoring likely short or longer-term?

Each of the above questions is addressed below.

Question 1: Why did sand accumulation begin preferentially along the western flank of the breakwaters array (7, 6, 5, 4 and 3 respectively)?

Sand appears to have been preferentially deposited along breakwaters 3-7 due to the presence of the shoal and the orientation of the structures. A channel exists between breakwaters 0 and 1 and considerably more scour is evident along the eastern flank of the structures than to the west. Much of the resuspension of sediment along the eastern three breakwaters can be accomplished during cold fronts with one such example occurring during late September and the first part of October. Winds exceeded 32 kts (16.46 m/s, 36.82 m/h) and waves approached 2 m (6.56 ft) on the shoreface. Maximum velocities of 55 cm/s (1.80 ft/s) to the west were recorded on the flanks of the channel at breakwaters 0

and 1. The mean current velocity was 16.02 cm/s (0.53 ft/s) for the entire time series, but clearly, the importance of cold fronts on generating strong currents was apparent.

In addition to the above findings, the WADMAS system was deployed in the gap between breakwaters 0 and 1 for the period 12/20/00–01/26/01. At least 4 cold front passages occurred during this deployment. Maximum current speeds of slightly over 180 cm/s (5.91 ft/s) occurred during two storms near the top and mid portion of the water column at this location. At the bed, current velocity exceeded 100 cm/s (3.28 ft/s) during 4 events and reached a maximum of ~150 cm/s (4.92 ft/s). These are important data and indicate that extremely fast flowing currents are common through the gaps of these breakwaters, particularly along the east flank of the structures where the gaps are aligned with current flow from Caillou Bay and the Gulf of Mexico (north–south). This explains why sediment did not accumulate behind breakwaters 0 and 1 in the same manner it accumulated behind the remainder of the breakwaters to the west. Some sand began accumulating behind breakwater 2 by 2000, but not to the extent of the remaining breakwaters to the west.

These data indicate that the orientation of the structure relative to tidal channels and larger tidal bay systems is important. The eastern end of Raccoon Island has suffered considerable erosion since the construction of the breakwaters, although the two do not appear to be related. Extremely high velocity tidal currents and both low frequency waves from the Gulf during pre-frontal stages in addition to high frequency waves driven by strong northerly winds during post-frontal events appear to be the primary cause of this erosion over the shorter term (years). A simple and possible solution to reduce this localized erosion maybe a structure built perpendicular to breakwater 0 and attached to the beach on the eastern end of the island. The data presented here would provide an excellent basis for developing an engineering solution to this problem.

Question 2: Where is the primary sand source for the sediment that accumulated in the vicinity of the breakwaters within the initial 12-month monitoring period and beyond should the trend continue?

The primary sand source for the eastern end of Raccoon Island appears to be the shoal adjacent to the breakwaters. A brief review of the historical evolution of this section of coast is helpful in understanding the genesis of this shoal. As shown in Figure 71, historic shoreline change between the late 1880's and 1990 shows that Raccoon Island was rapidly narrowing in place, a phenomenon commonly mistaken in Louisiana for barrier island rollover and landward migration. Thus, the subaerial parts of the island were transformed over this approximate 100 year time span to submarine shoals. Bathymetric comparisons show that the shoal off the breakwaters has been erosional historically (Figure 72) as has the eastern end of Raccoon Island. Reliance on the concept of bar bypassing from an updrift source, e.g., Whiskey Island is not, therefore, necessary to supply sand to the breakwaters. Given the proximity of the shoal to Coupe Colin, which separates Raccoon and Whiskey islands, and the strength of tidal currents through local tidal channels, it is conceivable that some reworking is due to inlet processes. As discussed in more detail earlier in this report, and summarized below, the transformation of the subaerial barrier to a shoal is a satisfactory mechanism by which the sand source can be local. Longshore sand transport from an updrift source may contribute some, however, over the survey period beginning 2000 and ending 2002, an adequate volume of sand was eroded from the shoal making it a viable sand source.

The hydrodynamic, sediment transport processes and patterns indicate that the shoal located on the eastern flank of Raccoon Island adjacent to the breakwaters is the immediate source of sand that has accumulated around the breakwaters. The WADMAS system was deployed on the shoal proper to investigate bottom boundary layer dynamics and sediment transport and to establish possible linkages between this sand body acting as a source for sediment deposited in the lee and seaward of the breakwaters, as well as in the gaps between structures.

The data presented and discussed earlier in this report point again to the importance of winter storms associated with cold fronts and increased wave-current conditions. Barring tropical cyclones, these constitute the meteorological forcing needed to resuspend sediment on the inner shelf. Two significantly energetic cold fronts were captured during a deployment on the shoal and instruments measured current velocities of near 80 cm/s (2.62 ft/s) at the bottom, ~100 cm/s (3.28 ft/s) at mid depth and 110 cm/s (3.61 ft/s) near the surface. Suspended sediments were highest in concentration on the sea bed (the bottom boundary layer) and exceed 5,000 g/l (41.73 lb/gal) during both events.

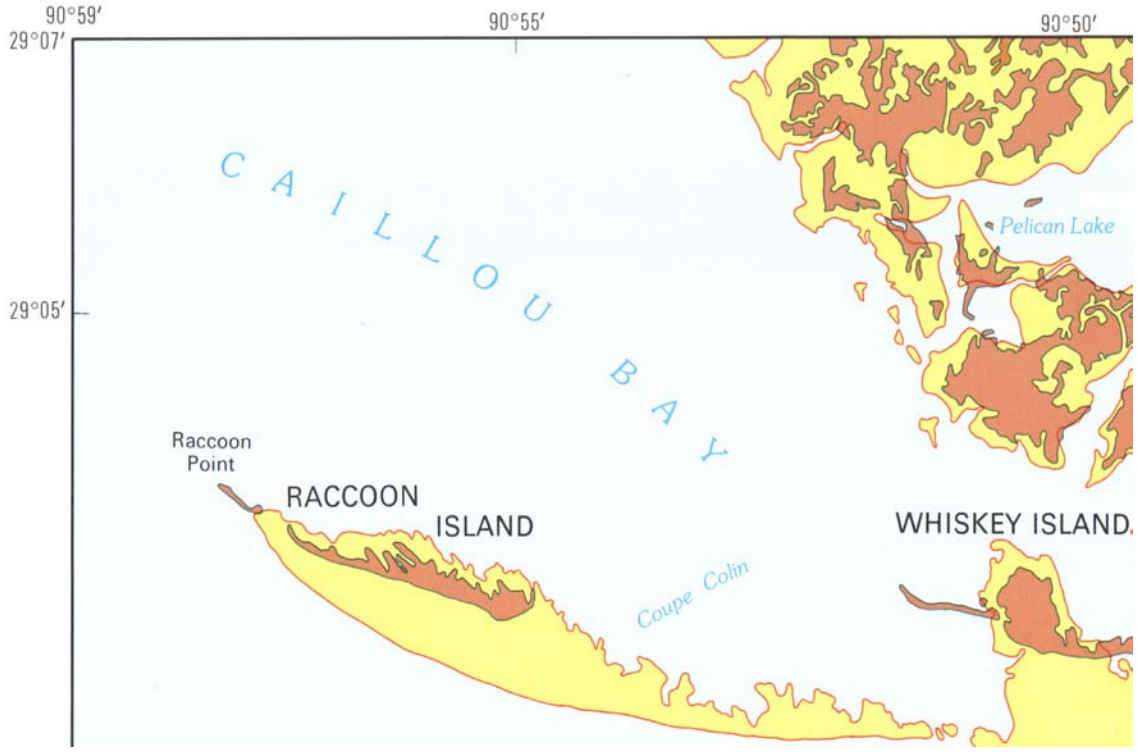

Figure 71. Historical shoreline change at Raccoon Island from the 1880s to 1990 (modified from McBride et al., 1992).

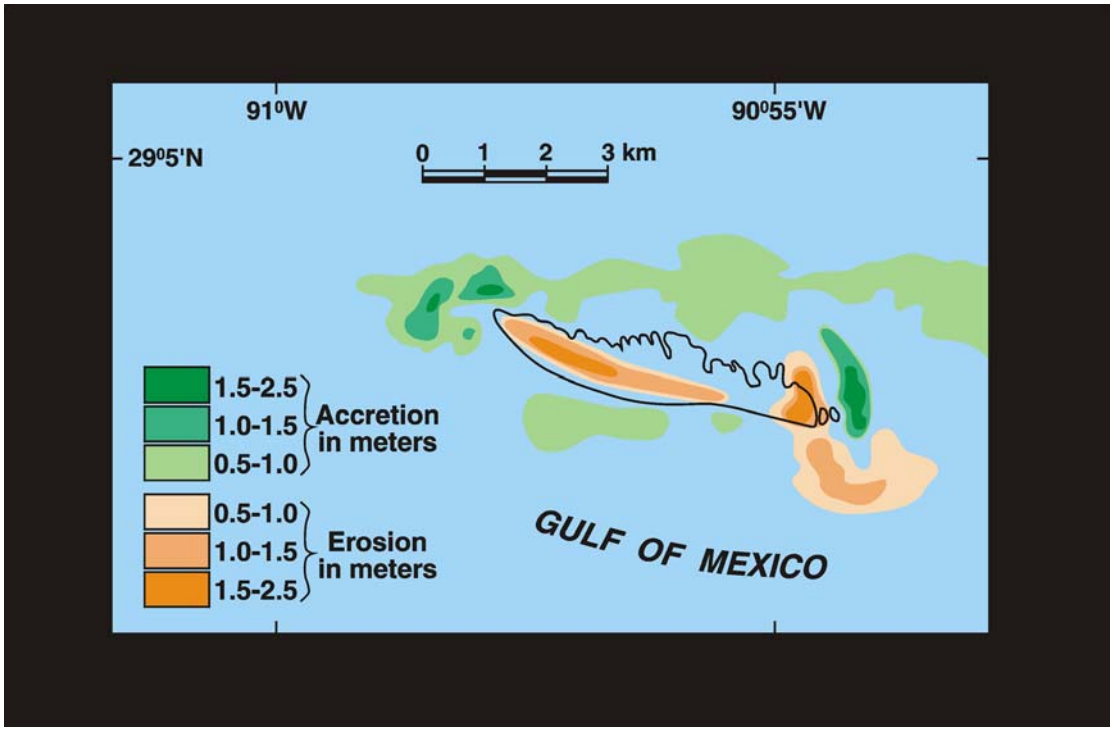

Figure 72. Bathymetric comparison from the 1940s through 1980s modified from List (1994).

The water column did not appear to be completely saturated since the upper sensor recorded concentrations of 1,000 g/l (8.35 lb/gal) and less during both events. Therefore, the suspended sediment concentrations indicated that a considerable amount of resuspension of sand was actively taking place during cold front events. A net flux of sediment was also measured in the onshore (cross-shore) direction and this will be elaborated on in answering Question 4.

A second line of evidence which points to the function of the shoal as an immediate source for sand deposited around the breakwaters is granulometric trends. Sediment is identical in size at both locations varying between fine and very fine sand. It is also very well sorted at both locations and fines from east to west. The coarsest material is found in the vicinity of breakwaters 0-3 and offshore on the upper shoreface. Sediment is very well sorted in the vicinity of the breakwaters and offshore on the shoal. To the west, along Raccoon Island and away from the structures, sorting becomes moderate with patches of very poorly sorted sediment evident in a few locations.

Question 3: What is the volume of sediment that comprises the source and what is the projected longevity and availability to nearshore processes of this source?

Using a sand thickness of 2.85 m (9.35 ft) obtained from vibracore RIC-1, an approximate volume of sand comprising the shoal fronting the breakwaters of 1.22 million cubic meters (1.6 million cubic yards) was calculated. This is somewhat of a conservative estimate in that the 1.83 m (6 ft) isobath was used to delineate the shoal. Sand in deeper water is likely part of this source but extended beyond the survey area. Since the time of construction of the breakwaters, to May 2002, we calculated that approximately 97,098 cubic meters (127,000 cubic yards) of deposition occurred behind the structures. Therefore, if all sand were removed from behind the breakwaters during a major storm, then conceivably the system could recover some 12 to 13 times and attain the same volume assuming the source continues to be viable. Complete removal of sand behind these structures has not occurred since construction. During TS Isidore and H Lili, for example, some 12,233 cubic meters (16,000 cubic yards) of material were removed. (The response and post-storm adjustment of the area is the subject of an ongoing study being conducted by the project investigators.) The short-term data obtained over the 2000-2002 period indicate a net decrease in sand volume of 9,000 cubic meters (12,000 cubic yards). This occurred mostly in 2001 and 2002 and equates to an annual loss rate of 6,000 cubic meters (8000 cubic yards). If this rate persists, then the project would return to pre-construction conditions in approximately 16 years. The statistics provided above do not take into account the effects of Isidore and Lili on the life span of the project.

Question 4: What are the precise roles of longshore and cross-shore sediment transport at the site?

The data indicate that the cross-shore distribution of sediment transport on the shoal shows a net flux onshore throughout much of the time series; during a few events offshore transport was measured for short durations. The longshore distribution is more symmetrical than the cross-shore, however, a net flux to the west is generally apparent. In order to investigate phase coupling of both cross-shore and longshore transport with

storm phase, significant wave height was correlated to transport rates. As wave height increases to a maximum, sediment transport is onshore. Since these conditions occur during pre-frontal stages during winter storms, winds are from the south. During the post-frontal phase when wind direction becomes northerly, waves are quickly attenuated resulting in a brief duration of sediment transport offshore. It was also noted that as waves begin to increase in height when winds veer to the south, sediment transport is onshore towards the breakwaters. In many instances, onshore transport continues even when winds veer to the north as the post-frontal phase of the event occurs and wave energy decreases. Onshore flux is evident until waves are attenuated almost completely during subsequent wind veering events and winds blow from the north. As wave energy decreases and fair-weather waves prevail the significantly reduced flux of sediment is still predominantly onshore. The longshore flux of sediment is predominantly westward during these events although some pronounced periods of eastward transport do occur during the increasing wave energy phase as southerly winds veer to the north. The data provide a convincing mechanism for dominant onshore transport and further support the hypothesis that the shoal fronting the breakwaters is the primary source of sand. Since their construction, this has permitted rapid deposition behind, between and seaward of the breakwaters.

It is evident that the cross-shore mechanism is important in the translation of Raccoon Island's Gulf shoreline landward through overwash processes over short time scales such as TS Isidore and H Lili (Figure 54) and over longer time scale (Figures 71 and 72). The longer time scales (decades to century scale) suggest that the shoreface is retreating at a rate less than the shoreline along Raccoon Island. Therefore, while sediment flux is onshore, wave conditions in the nearshore were not conducive to deposition and shoreline stability until the breakwaters were constructed. While construction of the structures provided nearshore conditions that were conducive to deposition, this has not been the case at other locations along the Louisiana coast where structures have not been effective over time in preventing shoreline retreat. Examples include East Timbalier Island and Holly Beach. The important difference between these

examples is that at the Raccoon Island breakwaters, the structures are fronted by a shoal which is serving as a sand source.

An extremely unique data set was obtained during both TS Isidore and H Lili in 2002 which revealed some important information regarding the shoals response to highly energetic events. The data show that net sediment flux was to the north for virtually all of the 6 day period during Isidore reaching a maximum of near 100 kg/m^2/s (20.48 lb/ft^2/s) during the earlier part of the storm. Some 30 kg/m^2/s (6.14 lb/ft^2/s) were measured moving offshore as the system moved onshore and currents were directed southward. With the exception of a short duration at the end of the storm, net longshore flux was westward during Isidore and reached a maximum of 160 kg/m^2/s (32.77 lb/ft^2/s). Eastward transport approached 50 kg/m^2/s (10.24 lb/ft^2/s). Net flux was considerably less during Lili but again, a net westward flux was evident in the data with a maximum of 100 kg/m^2/s (20.48 lb/ft^2/s) being attained. A short lived pulse of sediment flux to the east occurred towards the end of the storm approximating 20 kg/m^2/s (4.10 lb/ft^2/s). While sediment was transported onshore from the shoal during both events, a net volume loss of approximately 12,233 cubic meters (16,000 cubic yards) was experienced after Isidore and Lili in 2002.

Question 5: How is the beach west of the structures responding to breakwater construction?

By 2001, a downdrift (west) erosional shadow was becoming evident along Raccoon Island that would appear to be attributable to construction of the breakwaters. The shadow extends from transect 18, immediately west of breakwater 7, to transect 22, a distance of 548.64 m (1,800 ft). Based on the 2000-2002 data, the shoreline retreated at rates ranging between 14.83 to 22.97 m/yr (48.67 to 75.35 ft/yr) along this 548.64 m (1,800 ft) zone. Historically the same area eroded at rates ranging between 7.88 to 8.75 m/yr (25.86 to 28.72 ft/yr). While the short-term rates are considerably higher than those derived from the longer term data set (1880s-1990), and consequently some of the difference can be attributed to that, the morphological evidence of a downdrift landward

offset is convincing. West of this erosional shadow short and long term erosion rates decrease.

Question 6: Can the design criteria used to construct the breakwaters be refined to maximize sediment accumulation at this and other prospective sites?

The data presented in this report will provide considerable information regarding design criteria for future restoration efforts along this stretch of coast in addition to the response of beach and nearshore environments to breakwater construction given similar physical and hydrodynamic conditions at other sites. In particular, data presented here have provided new insight into the linkages between sediment flux in the littoral zone, proximal sediment sources and anticipated responses along adjacent coasts where structures may be built. The data indicate that the functional design of detached breakwaters should include an assessment of the availability of sediment immediately offshore. Given that the structures apparently disrupt the cross-shore wave propagation path, the possibility of cross-shore sand trapping should be addressed in the design of future projects, even for the largely non-permeable segmented structures. Neglecting the potential infusion from offshore explains the lack of agreement between the measured morphological response at Raccoon Island and the anticipated response according to the criteria established by Pope and Dean (1986). Based on data from several sites in the U.S. Pope and Dean (1986) examined the relationship between nearshore morphological response and two dimensionless parameters, ratio of offshore distance and water depth of the structure (X/ds) and ratio of structure length and gap width (Ls/Lg). According to the Pope and Dean (1986) graph shown here in Figure 70, the Raccoon Island breakwaters (with X/ds ≈ 60 to 90 and Ls/Lg ≈ 1) fall into the "no-sinuosity" range, i.e., negligible salient development. The first year response, including the growth of both the shoreline and Reverse Salients, do not agree with their prediction. The fact that the Raccoon Island breakwaters were constructed on the landward edge of a dynamic shoal resulted in an abnormally large value of X/ds. The data presented in the current report show conclusively that this shoal played a critical role in supplying a significant amount of

sediment, resulting in growth of the Reverse Salients. It is important to note that this response is likely an anomaly.

Data presented here will also be beneficial in potentially tweaking the engineering design of the current breakwater configuration. This includes increasing the potential for sand retention behind the eastern two breakwaters (0 and 1) and a reduction in shoreline retreat by the construction of an additional structure perpendicular to breakwater 0 and attachment to the beach at Raccoon Island. Engineering analysis and design will be required to further test the feasibility of this undertaking.

The recent loss of sand from behind the structures is being monitored and may be a function of the system being in a condition of dynamic equilibrium, although the equilibration time scale is not yet known. Continual monitoring of the site is necessary to quantify this phase.

Question 7: Are the trends that have been established for the first 12 months of monitoring likely short or longer-term?

Trends established in the first 12 months of monitoring showed rapid and persistent salient growth, the subsequent coalescence of salients and beach formation seaward of the structures. Calculations suggest that a maximum of approximately 97,098.47 cubic meters (127,000 cubic yards) of sediment were deposited behind the structures. From November 2000 to May 2002, some 9,174.66 cubic meters (12,000 cubic yards) of sand have been eroded from behind the structures, although some of that sediment appears to have been deposited immediately seaward of the gaps between the structures (see Figures 64 and 65). Approximately 126,916 cum (166,000 cuy) was lost from the offshore site. An additional 12,233 cubic meters (16,000 cubic yards) was eroded from behind the structures during Ts Isidore and H Lili in 2002, which accounts for a net loss of approximately 13% of the pre-storm volume. Therefore, even if the cyclone impacts of 2002 are ignored, the previous surveys conducted in 2000 through May 2002 indicate an erosional trend behind the structures. This appears to be occurring in the gaps between the breakwaters and behind breakwaters 0-2. Ongoing monitoring

will help determine if the beach in the vicinity of the breakwaters is in a condition of quasi steady state equilibrium or if the erosional trend is longer term. Barring a significant increase in storminess, it is anticipated that the volume of sediment should not decrease significantly since an abundance of sand exists on the shoal and the profile has not deepened beyond effective wave base. This statement, however, pertains to short time scales (years to a few decades). Over longer time scales, the rapidly subsiding coast on which these breakwaters have been constructed will cause shoreface retreat and a threshold will be reached when the sand shoal fronting the structures will become exhausted as a source. This phenomenon of shoal abandonment on the inner shelf along the Louisiana coast is well known on a larger scale, an example being Ship Shoal. In areas where structures are not fronted by a shoal, for example East Timbalier Island, rapid nearshore-beach translation landward is apparent.

REFERENCES

Armbruster, C.K., 1999. Monitoring Progress Report: Raccoon Island Breakwaters (TE-29). Monitoring Series No. TE-29-MSPR-0899-1. Louisiana Department of Natural Resources, Coastal Restoration Division, Baton Rouge. 32pp.

Davies, A. G., Soulsby, R. L., and King, H. L., 1988. A numerical model of the combined wave and current bottom boundary layer. *Journal of Geophysical Research 93, 491-508*.

Earle, M. D., McGehee, D., and Tubman, M., 1995. Field wave gaging program, wave data analysis standard. U.S. Army Corps of Engineers Waterways Experiment Station, Instruction Report CERC-95-1. Vicsburg, Mississippi.

Folk, R.L. and Ward, W.C., 1957. Brazos River bar: a study in the significance of grain size parameters. *Journal of Sedimentary Petrology, 27: 3-26*.

List, J.H., Jaffe, B.E., Sallenger, A.H., Jr., Williams, S.J., McBride, R.A., and Penland, S., 1994. Louisnana barrier island erosion study: Atlas of sea-floor changes from 1878 to 1989. U.S. Geological Survey Miscellaneous Investigation Series I-2150-B.

McBride, R.A., Penland, P.S., Jaffe, B., Williams, S.J., Sallenger, A.H., Jr., and Westphal, K.A., 1991. Shoreline changes of the Isles Dernieres barrier island arc, Louisiana, from 1853 to 1989: Scale 1:75,000, Investigative Map Series, Map I-2186 (1 sheet @ 42×52″), US Geological Survey.

McBride, R.A., Penland, S., Hiland, M.W., Williams, S.J., Westphal, K.A., Jaffe, B.E., and Sallenger, A.H., Jr., 1992. Analysis of barrier shoreline change in Louisiana from 1853 to 1989. In: Williams, S.J., Penland, S., and Sallenger, A.H., Jr. (Editors), Atlas of shoreline changes in Louisiana from 1853 to 1989. U.S. Geological Survey Miscellaneous Investigations Series I-2150-A.

McBride, R.A. and Byrnes, M.R., 1997. Regional variations in shore response along barrier island systems of the Mississippi River delta plain: historical change and future prediction. *Journal of Coastal Research, 13: 628-655*.

Pepper, D.A., and Stone, G.W., 2002. Atmospheric forcing of fine-sand transport on low-energy iner shelf: south-central Louisiana, USA. *Geo-Marine Letters, 22: 33-41*.

Pope, J. and Dean, J.L., 1986. Development of design criteria for segmented breakwaters. Proc. 20thth Coastal Eng. Conf., ASCE, 2144-2158.

Stone, G. W. and Xu, J., 1996. Wave Climate Modeling and Evaluation Relative to Sand Mining on Ship Shoal. Coastal Studies Institute, Louisiana State University, MMS 96-0059.

Stone, G. W., Grymes, J. M. I., Dingler, J. R., and Pepper, D. A., 1997. Overview and Significance of Hurricanes on the Louisiana Coast, U.S.A. Journal of Coastal Research 13[3], 656-669.

Stone, G.W. and McBride, R.A., 1998. Louisiana barrier islands and their importance in wetland protection: forecasting shoreline change and subsequent response of wave climate. Journal of Coastal Research, 14(3): 900-915.

Stone, G.W., Wang, P., Zhang, X., 1998a. Wave height measurements at the Raccoon Island breakwaters demonstration project (TE-29): Report on March 1998 field deployment. Coastal Studies Institute, Louisiana State University, Baton Rouge, La.

Stone, G.W., Wang, P., Zhang, X., 1998b. Wave height measurements at the Raccoon Island breakwaters demonstration project (TE-29): Report on July 1998 field deployment. Coastal Studies Institute, Louisiana State University, Baton Rouge, La.

Stone, G.W., Wang, P., Zhang, X., 1998c. Wave height measurements at the Raccoon Island breakwaters demonstration project (TE-29): Report on September 1998 field deployment and review of 12-month monitoring program. Coastal Studies Institute, Louisiana State University, Baton Rouge, La.

Stone, G.W., Wang, P., and Armbruster, C.K., 1999. Unanticipated response to detached, segmented breakwaters along Raccoon Island, Louisiana. Coastal Sediments ′99, Proceedings of the Conference, 2057-2072.

Stone, G.W., 2000. Wave climate and bottom boundary layer dynamics with implications for offshore sand mining and barrier island replenishment in south-central Louisiana. U.S. Department of the Interior, MMS, Gulf of Mexico OCS Region.

Stone, G.W., Sheremet, A., Zhang, X., He, Q., and Liu, B., 2003. Landfall of two tropical systems seven days apart along southcentral Louisiana. Coastal Sediments ′03, Book of Abstracts, 333-334.

Welch, P. D., 1967. The use of fast Fourier transformation for the estimation of power spectra: a method based on time averaging over short, modified periodogram. AU-15, 70-73. IEEE Transactions on Audio and Electroacoustics.

Wright, L. D., Sherwood, C. R., and Sternberg, R. W., 1997. Field measurements of fair weather bottom boundary layer processes and sediment suspension on the Louisiana inner continental shelf. *Marine Geology 140, 329-345*.

APPENDICES

APPENDIX I

WADMAS OBS Sensor Calibration

Since intensity of the backscattered signal is a function of grain size, the OBS was calibrated for the range of 0 - 6 g/l with a bulk surface sediment sample collected at the study site, Raccoon Island, LA.

A calibration of the turbidity sensors on the WADMAS instrument package was conducted at:

Coastal Studies Institute
Louisiana State University
Field Support Group Building
South Stadium Dr.
Baton Rouge, LA. 70803.

The turbidity sensor is of a type: Analite 195
Manufactured by:

McVan Instruments
58 Gedded Street
P.O. Box 298, Mulgrave
Victoria, Australia, 3170
Tel: (+61-3) 9582-7333

The calibration standard is of a type: Formazin Turbidity Standard 4000 NTU
Manufactured by:

Hach Company
P.O. Box 389
Loveland, CO. 80539
Tel: 970-669-3050
Lot: A2242
Expiration: August 2004

The instruments report their readings as a voltage proportional to the NTU optical reading. The relationship for voltage to NTU for the sensors is 1 volt to 400 NTU. The instrument was set up in the lab and solutions for a four-point calibration were prepared. The standard values selected for this calibration were 0, 100, 250, 400. The solutions were prepared using a laboratory sample jar with a ratio of distilled water and Formazin solution mixed to form the standard values of NTU.

The calibrations were preformed by mixing the solution in the sample jar on a magnetic mixing plate, stopping the mixing, and placing the probe in the solution for a reading. This was preformed three times for each solution standard and each probe. The results in voltages are as follows:

NTU Std. = 0

	Run 1	Run 2	Run 3
Probe 1	0	0	0
Probe 2	0	0	0
Probe 3	0	0	0

NTU Std. = 100

	Run 1	Run 2	Run 3
Probe 1	0.186	0.186	0.186
Probe 2	0.218	0.218	0.266
Probe 3	0.268	0.266	0.266

NTU Std. = 250

	Run 1	Run 2	Run 3
Probe 1	0.456	0.471	0.467
Probe 2	0.549	0.560	0.552
Probe 3	0.664	0.664	0.664

NTU Std. = 400

	Run 1	Run 2	Run 3
Probe 1	0.765	0.708	0.708
Probe 2	0.853	0.843	0.853
Probe 3	1.016	1.016	1.016

Voltage vs. NTU standard

400 NTU = 1.000 volts
250 NTU = 0.652 volts
100 NTU = 0.250 volts
0 NTU = 0.000 volts

Resultant NTU values from calibration

Probe	400 NTU	250 NTU	100 NTU	0 NTU
Probe 1	283.2	186.8	74.4	0.0
Probe 2	341.2	220.8	90.4	0.0
Probe 3	406.4	265.6	106.4	0.0

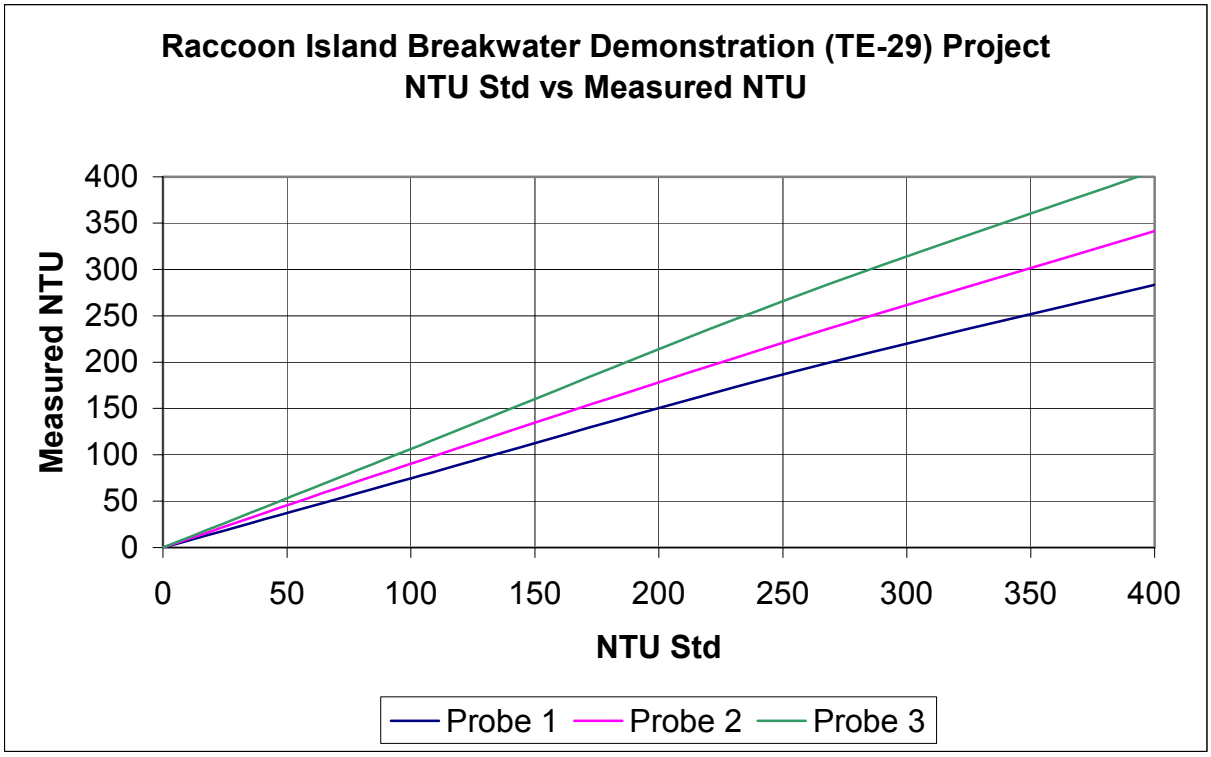

Correction Factors Calculated:

Correction factors were calculated to give best fit over the 0 to 400 NTU range

Probe 1 = 1.38
Probe 2 = 1.14
Probe 3 = 0.96

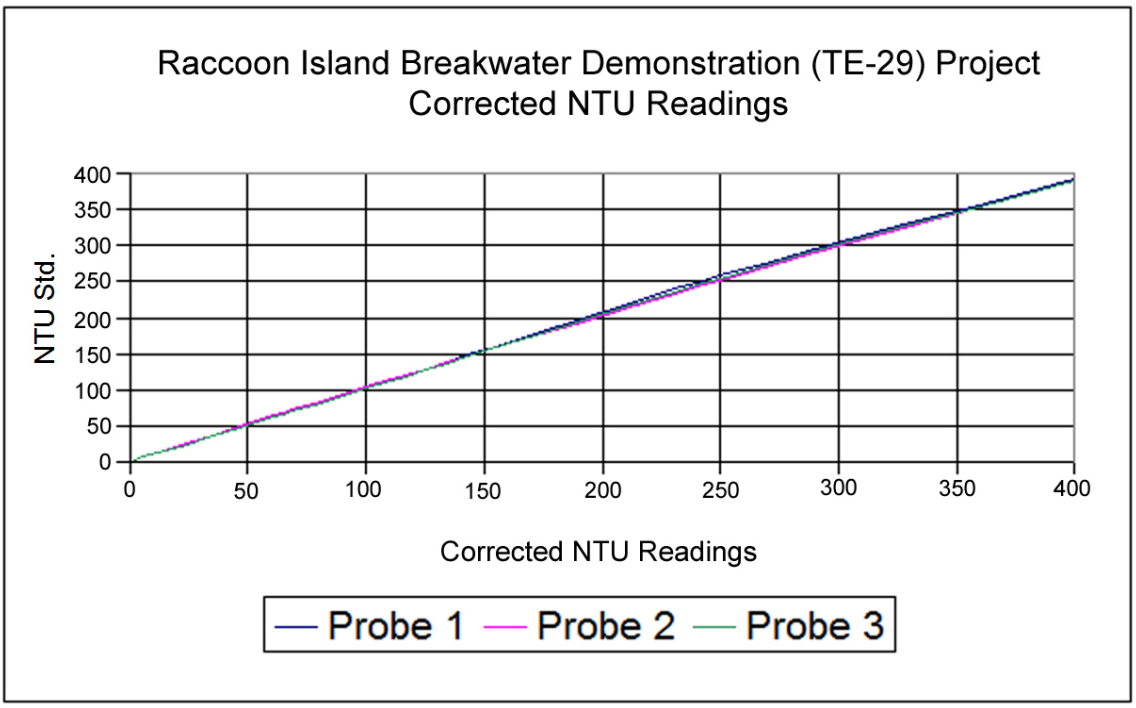

Sediment sample taken at Raccoon Island, LA On August 08, 2002 was mixed with 0.8 liters of water to obtain the following mixtures. These mixtures were then measures with Probe 3 to determine a relationship of NTU to sediment concentration for this particular sample.

Concentration (g/l)	Voltage Reading	Resultant NTU Reading
0.090875	0.011	4.4
0.206125	0.033	13.2
0.408125	0.066	26.4
0.601875	0.076	30.4
0.807875	0.148	59.2
0.990625	0.132	52.8
1.503500	0.235	94.0
2.017125	0.320	128.0
3.043375	0.410	164.0
4.010125	0.620	248.0
5.205250	0.850	340.0
6.051250	0.895	358.0